

# Dark Sectors and New, Light, Weakly-Coupled Particles

**Conveners:** Rouven Essig,<sup>1,\*</sup> John A. Jaros,<sup>2,†</sup> William Wester,<sup>3,‡</sup>

P. Hansson Adrian,<sup>2</sup> S. Andreas,<sup>4</sup> T. Averett,<sup>5</sup> O. Baker,<sup>6</sup> B. Batell,<sup>7</sup> M. Battaglieri,<sup>8</sup>  
 J. Beacham,<sup>9</sup> T. Beranek,<sup>10</sup> J. D. Bjorken,<sup>2</sup> F. Bossi,<sup>11</sup> J. R. Boyce,<sup>12,5</sup> G. D. Cates,<sup>13</sup>  
 A. Celentano,<sup>8,14</sup> A. S. Chou,<sup>3</sup> R. Cowan,<sup>15</sup> F. Curciarello,<sup>16,17</sup> H. Davoudiasl,<sup>18</sup> Patrick  
 deNiverville,<sup>19</sup> R. De Vita,<sup>17</sup> A. Denig,<sup>10</sup> R. Dharmapalan,<sup>20</sup> B. Döbrich,<sup>4</sup> B. Echenard,<sup>21</sup>  
 D. Espriu,<sup>22</sup> S. Fegan,<sup>8</sup> P. Fisher,<sup>15</sup> G. B. Franklin,<sup>23</sup> A. Gasparian,<sup>24</sup> Y. Gershtein,<sup>25</sup>  
 M. Graham,<sup>2</sup> A. Haas,<sup>9</sup> A. Hatzikoutelis,<sup>26</sup> M. Holtrop,<sup>27</sup> I. Irastorza,<sup>28</sup> E. Izaguirre,<sup>29</sup>  
 J. Jaeckel,<sup>30</sup> Y. Kahn,<sup>31</sup> N. Kalantarians,<sup>32</sup> G. Krnjaic,<sup>29</sup> V. Kubarovsky,<sup>12</sup> H-S. Lee,<sup>18,5,12</sup>  
 A. Lindner,<sup>4</sup> W. J. Marciano,<sup>18</sup> D. J. E. Marsh,<sup>29</sup> T. Maruyama,<sup>2</sup> D. McKeen,<sup>19</sup>  
 H. Merkel,<sup>10</sup> K. Moffeit,<sup>2</sup> G. Mueller,<sup>33</sup> T. K. Nelson,<sup>2</sup> M. Oriunno,<sup>2</sup> Z. Pavlovic,<sup>34</sup>  
 S. K. Phillips,<sup>27</sup> M. J. Pivovarov,<sup>35</sup> R. Poltis,<sup>36</sup> M. Pospelov,<sup>29</sup> S. Rajendran,<sup>37</sup>  
 J. Redondo,<sup>38,39</sup> A. Ringwald,<sup>4</sup> A. Ritz,<sup>19</sup> J. Ruz,<sup>35</sup> K. Saenboonruang,<sup>40</sup> P. Schuster,<sup>29</sup>  
 M. Shinn,<sup>12</sup> T. R. Slatyer,<sup>41</sup> J. H. Steffen,<sup>42</sup> S. Stepanyan,<sup>12</sup> D. B. Tanner,<sup>33</sup> J. Thaler,<sup>31</sup>  
 M. E. Tobar,<sup>43</sup> N. Toro,<sup>29</sup> A. Upadye,<sup>44,45</sup> R. Van de Water,<sup>34</sup> B. Vlahovic,<sup>46</sup> J. K. Vogel,<sup>35</sup>  
 D. Walker,<sup>2</sup> A. Weltman,<sup>36</sup> B. Wojtsekhowski,<sup>12</sup> S. Zhang,<sup>12</sup> and K. Zioutas<sup>47,48</sup>

<sup>1</sup>*C.N. Yang Inst. for Theoretical Physics, Stony Brook University, NY*

<sup>2</sup>*SLAC National Accelerator Laboratory, Menlo Park, CA*

<sup>3</sup>*Fermi National Accelerator Laboratory, Batavia, IL*

<sup>4</sup>*Deutsches Elektronen-Synchrotron DESY, Hamburg, Germany*

<sup>5</sup>*College of William and Mary, Williamsburg, VA*

<sup>6</sup>*Yale University, New Haven, CT*

<sup>7</sup>*University of Chicago, Chicago, IL*

<sup>8</sup>*Istituto Nazionale di Fisica Nucleare, Sezione di Genova, Italy*

<sup>9</sup>*New York University, NY*

<sup>10</sup>*Johannes Gutenberg University Mainz, Mainz, Germany*

<sup>11</sup>*Laboratori Nazionali di Frascati dell'INFN, Frascati, Italy*

<sup>12</sup>*Thomas Jefferson National Accelerator Facility, VA*

<sup>13</sup>*Department of Physics, University of Virginia, Virginia*

<sup>14</sup>*Dipartimento di Fisica, Universita' di Genova, Genova, Italy*

<sup>15</sup>*Laboratory for Nuclear Science, Massachusetts Inst. of Technology, MA*

<sup>16</sup>*Dipartimento di Fisica e di Scienze della Terra, Universit di Messina, Italy*

- 33 <sup>17</sup>*Istituto Nazionale di Fisica Nucleare, Sezione Catania, Italy*
- 34 <sup>18</sup>*Brookhaven National Laboratory, Upton, NY*
- 35 <sup>19</sup>*Dept. of Physics and Astronomy, University of Victoria, Canada*
- 36 <sup>20</sup>*The University of Alabama, Tuscaloosa, AL*
- 37 <sup>21</sup>*California Institute of Technology, CA*
- 38 <sup>22</sup>*Universitat de Barcelona, Spain*
- 39 <sup>23</sup>*Department of Physics, Carnegie Mellon University, PA*
- 40 <sup>24</sup>*North Carolina A&T State University, NC*
- 41 <sup>25</sup>*Rutgers University, NJ*
- 42 <sup>26</sup>*University of Tennessee, Knoxville, TN*
- 43 <sup>27</sup>*University of New Hampshire, NH*
- 44 <sup>28</sup>*Universidad de Zaragoza, Spain*
- 45 <sup>29</sup>*Perimeter Inst. for Theoretical Physics, Waterloo, Canada*
- 46 <sup>30</sup>*Institut für theoretische Physik, Universität Heidelberg, Germany*
- 47 <sup>31</sup>*Center for Theoretical Physics, Massachusetts Inst. of Technology, MA*
- 48 <sup>32</sup>*Department of Physics, Hampton University, MA*
- 49 <sup>33</sup>*University of Florida, Gainesville, FL*
- 50 <sup>34</sup>*Los Alamos National Laboratory, Los Alamos, NM*
- 51 <sup>35</sup>*Lawrence Livermore National Laboratory, CA*
- 52 <sup>36</sup>*University of Cape Town, Cape Town, South Africa*
- 53 <sup>37</sup>*Department of Physics, Stanford University, Stanford, CA*
- 54 <sup>38</sup>*Max Planck Institute für Physik, München, Germany*
- 55 <sup>39</sup>*Arnold Sommerfeld Center, Ludwig-Maximilians-University, München, Germany*
- 56 <sup>40</sup>*Kasetsart University, Chatuchak, Bangkok, Thailand*
- 57 <sup>41</sup>*Center for Theoretical Physics, Massachusetts Institute of Technology, MA*
- 58 <sup>42</sup>*Northwestern University, IL*
- 59 <sup>43</sup>*School of Physics, University of Western Australia, WA, Australia*
- 60 <sup>44</sup>*Argonne National Laboratory, IL*
- 61 <sup>45</sup>*Institute for the Early Universe, Ewha University, Seoul, Korea*
- 62 <sup>46</sup>*North Carolina Central University, Durham, NC*
- 63 <sup>47</sup>*University of Patras, Greece*
- 64 <sup>48</sup>*CERN, Geneva, Switzerland*

## Abstract

65

66 Dark sectors, consisting of new, light, weakly-coupled particles that do not interact with the  
67 known strong, weak, or electromagnetic forces, are a particularly compelling possibility for new  
68 physics. Nature may contain numerous dark sectors, each with their own beautiful structure,  
69 distinct particles, and forces. This review summarizes the physics motivation for dark sectors  
70 and the exciting opportunities for experimental exploration. It is the summary of the Intensity  
71 Frontier subgroup “New, Light, Weakly-coupled Particles” of the Community Summer Study 2013  
72 (“Snowmass on the Mississippi”). We discuss axions, which solve the strong CP problem and  
73 are an excellent dark matter candidate, and their generalization to axion-like particles. We also  
74 review dark photons and other dark-sector particles, including sub-GeV dark matter, which are  
75 theoretically natural, provide for dark matter candidates or new dark matter interactions, and could  
76 resolve outstanding puzzles in particle and astro-particle physics. In many cases, the exploration  
77 of dark sectors can proceed with existing facilities and comparatively modest experiments. A rich,  
78 diverse, and low-cost experimental program has been identified that has the potential for one or  
79 more game-changing discoveries. These physics opportunities should be vigorously pursued in the  
80 US and elsewhere.

---

\* rouven.essig@stonybrook.edu

† john@slac.stanford.edu

‡ wester@fnal.gov

**CONTENTS**

82	1. Overview	5
83	2. Axions and Axion-Like Particles	7
84	2.1. Theory & Theory Motivation	7
85	2.2. Phenomenological Motivation and Current Constraints	8
86	2.2.1. Dark Matter	8
87	2.2.2. Hints from astrophysics	10
88	2.3. Status and Plans for Terrestrial experiments	11
89	2.3.1. Laser Experiments	11
90	2.3.2. Microwave Cavities (Haloscopes)	15
91	2.3.3. Oscillating Moments	16
92	2.3.4. Helioscopes	17
93	2.3.5. Beam Dumps and Colliders	19
94	3. Dark Photons	19
95	3.1. Theory & Theory Motivation	19
96	3.2. Phenomenological Motivation and Current Constraints	22
97	3.2.1. Hints for MeV-GeV mass Dark Photons from Dark Matter	23
98	3.2.2. Ultra-light Dark Photons	27
99	3.3. Experimental Searches for Dark Photons: Status and Plans	27
100	3.3.1. Electron Beam Dump Experiments	28
101	3.3.2. Fixed-Target Experiments	29
102	3.3.3. Proton Beam Dump Experiments	31
103	3.3.4. Electron-Positron Colliders	31
104	3.3.5. Proton Colliders	33
105	3.3.6. Photon Regeneration Experiments (ultra-light dark photons)	34
106	3.3.7. Helioscopes (ultra-light dark photons)	35
107	3.3.8. Cold DM searches (ultra-light dark photons)	35
108	3.4. Opportunities for Future Experiments: New Ideas, Technologies, & Accelerators	36
109	3.4.1. Future Fixed Target Experiments	36
110	3.4.2. Searches at Future $e^+e^-$ Colliding Beam Facilities	38
111	3.4.3. Future Searches at the LHC	39
112	4. Light Dark-Sector States (incl. Sub-GeV Dark Matter)	39

113	4.1. Theory & Theory Motivation	39
114	4.1.1. Light Dark Matter	40
115	4.1.2. Light Dark-Sector States	41
116	4.1.3. Millicharged Particles	41
117	4.2. Phenomenological Motivation and Current Constraints	41
118	4.2.1. Constraints on Light Dark Matter and Dark Sectors	41
119	4.2.2. Additional constraints on Millicharged Particles	44
120	4.3. Proposed and Future Searches	46
121	4.3.1. Proton-fixed Target	46
122	4.3.2. B-factories	47
123	4.3.3. Electron fixed target	47
124	5. Chameleons	48
125	5.1. Theory & Motivation	48
126	5.2. Current laboratory constraints	51
127	5.3. Forecasts for Terrestrial experiments	51
128	5.4. Tests of the Chameleon Mechanism by Astrophysical Observation	53
129	5.5. Space tests of Gravity	55
130	6. Conclusions	55
131	References	57

## 132 1. OVERVIEW

133 The Standard Model (SM) of particle physics has achieved remarkable success as a result  
134 of several decades of *exploration*, of constantly pushing the boundaries of our knowledge  
135 of theory, experiment, and technology. However, while the SM provides a theoretically  
136 consistent description of all known particles and their interactions (ignoring gravity) up to  
137 the Planck scale, it is clearly incomplete as it does not address several pieces of evidence for  
138 new physics beyond the SM.

139 One particularly powerful piece of evidence for new physics comes from the existence of  
140 dark matter (DM). DM dominates the matter density in our Universe, but very little is known  
141 about it. Its existence provides a strong hint that there may be a *dark sector*, consisting of  
142 particles that do not interact with the known strong, weak, or electromagnetic forces. Given

143 the intricate structure of the SM, which describes only a subdominant component of the  
 144 Universe, it would not be too surprising if the dark sector contains a rich structure itself,  
 145 with DM making up only a part of it. Indeed, many dark sectors could exist, each with  
 146 its own beautiful structure, distinct particles, and forces. These dark sectors (or “hidden  
 147 sectors”) may contain *new light weakly-coupled particles* (NLWCPs), particles well below the  
 148 Weak-scale that interact only feebly with ordinary matter. Such particles could easily have  
 149 escaped past experimental searches, but a rich experimental program has now been devised  
 150 to look for several well-motivated possibilities.

151 Dark sectors are motivated also by bottom-up and top-down theoretical considerations.  
 152 They arise in many theoretical extensions to the SM, such as moduli that are present in  
 153 string theory or new (pseudo-)scalars that appear naturally when symmetries are broken at  
 154 high energy scales. Other powerful motivations include the strong CP problem, and vari-  
 155 ous experimental findings, including the discrepancy between the calculated and measured  
 156 anomalous magnetic moment of the muon and puzzling results from astrophysics. Besides  
 157 gravity, there are a few well-motivated interactions allowed by SM symmetries that provide  
 158 a “portal” from the SM sector into the dark sector. These portals include:

Portal	Particles	Operator(s)
“Vector”	Dark photons	$-\frac{\epsilon}{2\cos\theta_W} B_{\mu\nu} F'^{\mu\nu}$
“Axion”	Pseudoscalars	$\frac{a}{f_a} F_{\mu\nu} \tilde{F}^{\mu\nu}, \frac{a}{f_a} G_{i\mu\nu} \tilde{G}_i^{\mu\nu}, \frac{\partial_\mu a}{f_a} \bar{\psi} \gamma^\mu \gamma^5 \psi$
“Higgs”	Dark scalars	$(\mu S + \lambda S^2) H^\dagger H$
“Neutrino”	Sterile neutrinos	$y_N L H N$

160 The Higgs and neutrino portal are best explored at high-energy colliders and neutrino fa-  
 161 cilities, respectively. Our focus here will be on the vector and axion portals, which are  
 162 particularly well-motivated possibilities and can be explored with low-cost, high-impact ex-  
 163 periments.

164 This paper is a summary of the physics motivation and experimental opportunities of  
 165 the Intensity Frontier subgroup “New, Light, Weakly-coupled Particles” of the Community  
 166 Summer Study 2013 (“Snowmass on the Mississippi”). This paper updates and expounds  
 167 upon the summary included in the Fundamental Physics and the Intensity Frontier workshop  
 168 report [1]. This topic has also been studied in the context of the European strategy [2].

169 The outline of the remainder of this summary is as follows. §2 discusses the (QCD) axion  
 170 and more general “axion-like” particles (ALPs). §3 reviews dark photons, focusing on sub-  
 171 MeV and MeV-GeV masses. §4 describes sub-GeV DM, milli-charged particles, and other

172 hidden-sector particles. §5 focuses on chameleons. In all cases, we describe the theoretical  
173 motivation, the phenomenological motivation, the current constraints, and the current and  
174 future experimental opportunities. §6 contains our conclusions.

## 175 2. AXIONS AND AXION-LIKE PARTICLES

### 176 2.1. Theory & Theory Motivation

177 One of the unresolved puzzles in the SM is the lack of any observed  $CP$  violation in the strong  
178 interactions described by Quantum Chromodynamics (QCD). While the weak interactions  
179 are known to violate  $CP$ , the strong interactions also contain a  $CP$ -violating term in the  
180 Lagrangian,  $\frac{\Theta}{32\pi^2} G_{\mu\nu} \tilde{G}^{\mu\nu}$ , where  $G^{\mu\nu}$  is the gluon field strength. For non-zero quark masses,  
181 this term leads to (unobserved)  $CP$ -violating effects of the strong interactions. This so-  
182 called “strong  $CP$  problem” is often exemplified by the lack of observation of a neutron  
183 electric dipole moment down to a present experimental upper limit 10 orders of magnitude  
184 smaller than what is expected from a  $CP$ -violating QCD.

185 Solutions to this problem are scarce. Perhaps the most popular suggestion is the so-called  
186 Peccei-Quinn (PQ)  $U(1)$  approximate global symmetry, which is spontaneously broken at a  
187 scale  $f_a$ . The axion is a hypothetical particle that arises as the pseudo-Nambu-Goldstone  
188 boson (PNGB) of this symmetry breaking [3–5].

189 The axion mass is  $m_a \sim 6 \text{ meV} (10^9 \text{ GeV}/f_a)$ . Its coupling to ordinary matter is  
190 proportional to  $1/f_a$  and can be calculated in specific models. It couples generically to  
191 quarks (or hadrons at low energies) with coupling constants that are uncertain by  $\mathcal{O}(1)$   
192 model-dependent factors. The coupling to photons is also generic and has the form  $\mathcal{L} \supset$   
193  $-\frac{1}{4} g_{a\gamma\gamma} a F_{\mu\nu} \tilde{F}^{\mu\nu}$ , where the coupling constant  $g_{a\gamma\gamma} \sim 10^{-13} \text{ GeV}^{-1} (10^{10} \text{ GeV}/f_a)$  [6] has  
194 only a  $\mathcal{O}(1)$  model-dependency. The couplings to leptons are not guaranteed but appear in  
195 many theoretical realizations of the axion, particularly in models of grand unification. All  
196 of these interactions can play a role in searches for the axion, and allow the axion to be  
197 produced or detected in the laboratory and emitted by the sun or other stars.

198 The basic physical mechanism that leads to the axion — the spontaneous breaking at a  
199 high energy scale of a  $U(1)$  approximate global symmetry, generating a light PNGB — also  
200 allows for other axion-like particles (ALPs). Unlike axions, which are linked to the strong  
201 interactions and whose masses and couplings are determined by a single new parameter  $f_a$ ,  
202 ALPs are much less constrained, and their masses and couplings to photons are independent  
203 parameters. Searches for ALPs should not therefore be limited to the parameter space of

204 the axion itself. Both ALPs and axions are generic in string theory [7–13], with the natural  
 205 size of their decay constant  $f_a$  being the string scale, varying typically between  $10^9$  and  
 206  $10^{17}$  GeV.

## 207 **2.2. Phenomenological Motivation and Current Constraints**

208 Fig. 1 (top) shows the allowed axion parameter space as a function of  $f_a$  or, equivalently,  $m_a$ .  
 209 Direct searches for such particles and calculations of their effect on the cooling of stars and  
 210 on the supernova SN1987A exclude most values of  $f_a < 10^9$  GeV. Some of these constrain  
 211 only the axion coupling to photons ( $g_{a\gamma\gamma}$ ), while others constrain the axion coupling to  
 212 electrons ( $g_{ae}$ ). Recent and future laboratory tests (the latter shown in light green) can  
 213 probe  $f_a \lesssim 10^9$  GeV or  $f_a \gtrsim 10^{12}$  GeV (possibly higher) but intermediate values are more  
 214 challenging.

215 The parameter space for ALPs is shown in Fig. 1 (bottom). The axion parameter space  
 216 lies within an order of magnitude from the line labeled “KSVZ axion,” which represents  
 217 a particular QCD axion model. Experimentally excluded regions (dark green), constraints  
 218 from astronomical observations (gray) or from astrophysical, or cosmological arguments  
 219 (blue) are shown. Sensitivities of a few planned experiments are shown in light green.

### 220 **2.2.1. Dark Matter**

221 ALPs (including the QCD axion) can naturally serve as the Universe’s DM, meaning that the  
 222 galactic halo may be formed partly or entirely from these particles. They can be produced  
 223 thermally or non-thermally in the early Universe. Thermally produced axions are disfavored  
 224 by observations of the Universe’s large scale structure [20], but thermally produced ALP  
 225 DM is still allowed in sizable parts of parameter space ( $m_a \gtrsim 154$  eV,  $g_{a\gamma\gamma} \sim \mathcal{O}(10^{-17} -$   
 226  $10^{-13})$  GeV $^{-1}$ ) [21]. Non-thermal production can occur through the “vacuum misalignment  
 227 mechanism” or the decay of axionic strings and domain walls. Axions with large  $f_a$  do not  
 228 thermalize in the early Universe and their abundance today is set by the initial state set  
 229 during the Peccei-Quinn phase transition. There are two scenarios depending on whether the  
 230 PQ transition took place after or before inflation. In the first case, the dominant contribution  
 231 arises from the decay of cosmic strings and domain walls into axions. This scenario suggests  
 232 values of  $m_a \sim 80 - 400$   $\mu$ eV with large uncertainties arising from extrapolating the numerical  
 233 result for the string and domain wall decays [22, 23]. In the second scenario, inflation  
 234 homogenizes the initial axion field value in our observable Universe and the DM density



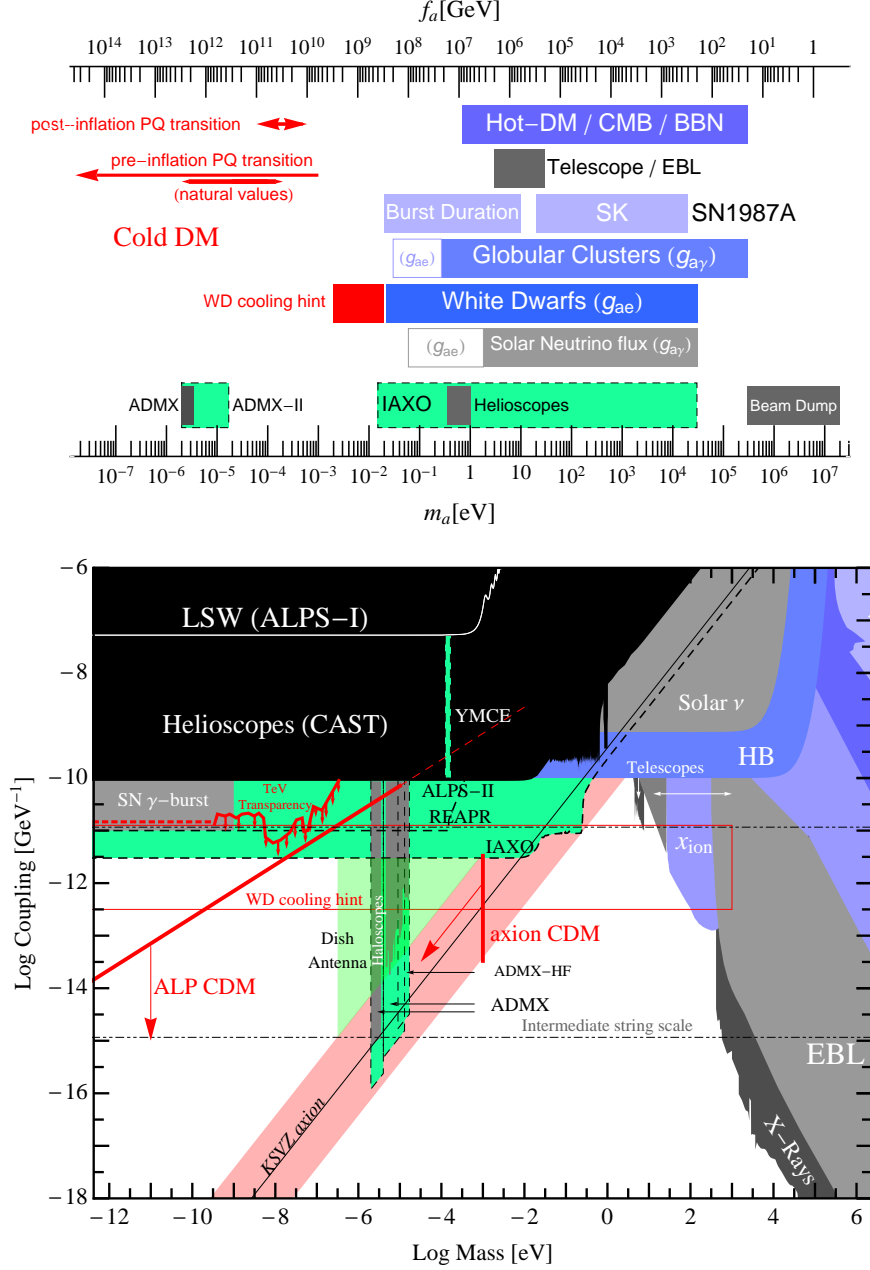


FIG. 1. Parameter space for axions (top) and axion-like particles (ALPs) (bottom). In the bottom plot, the QCD axion models lie within an order of magnitude from the explicitly shown “KSVZ” axion line (red band). Colored regions are: experimentally excluded regions (dark green), constraints from astronomical observations (gray) or from astrophysical or cosmological arguments (blue), and sensitivity of planned and suggested experiments (light green) (ADMX [14], ALPS-II [15], IAXO [16–18], Dish antenna [19]). Shown in red are boundaries where ALPs can account for all the dark matter produced either thermally in the big bang or non-thermally by the misalignment mechanism.

235 depends on this value. For values  $a_{\text{initial}} \sim f_a$  the observed DM density arises for  $m_a \sim$   
 236  $12 \mu\text{eV}$ . Smaller values of the mass are possible when  $a_{\text{initial}} \ll f_a$  and somewhat larger  
 237 masses (perhaps up to  $\text{meV}$  [24]) can be achieved by tuning towards  $a_{\text{initial}} = \pi f_a$ .

238 All in all, the natural values  $m_a \sim 10^{-5} - 10^{-4} \text{ eV}$  present a clear experimental target.  
 239 The Axion DM eXperiment (ADMX) will soon probe part of this preferred parameter space.  
 240 Extending these arguments to ALPs, a much larger parameter space needs to be explored  
 241 as indicated in Fig. 1; see also *e.g.*, [25].

242 One important constraint on axion (or ALP) DM is the generation of isocurvature tem-  
 243 perature fluctuations in the cosmic microwave background if the axion/ALP exists dur-  
 244 ing inflation. Cosmic microwave background (CMB) probes like the Planck satellite con-  
 245 strain these fluctuations, setting very strong constraints on the Hubble scale during inflation,  
 246  $H_I \lesssim O(10^6) \text{ GeV}$ . Observing tensor modes in the CMB allows one to determine  $H_I$ , pro-  
 247 viding a crucial test of axion/ALP DM.

248 It is noteworthy that axion or ALP DM may also form a Bose-Einstein condensate [26],  
 249 which may lead to caustic rings in spiral galaxies, which may already have been observed.  
 250 This also has detectable consequences in terrestrial direct detection experiments like ADMX.

251 Ultra-light ALPs with masses in the  $10^{-33} - 10^{-18} \text{ eV}$  range can also contribute to the DM  
 252 in the Universe, affecting structure formation in a manner distinct from cold DM (CDM).  
 253 The distinction arises due to a scale dependent sound speed in the ultra-light ALPs fluid [27–  
 254 29]. Large scale structure and the CMB thus allow one to constrain the fraction of DM that  
 255 can be made up of such ultra-light ALPs. Future surveys such as Euclid stand to improve  
 256 constraints with specific improvements at the lowest masses and with discerning differences  
 257 between ultra-light ALPs and thermal neutrinos of  $\text{eV}$  mass [30, 31]. The effect of these  
 258 ALPs on the CMB and weak lensing tomography has been explored in detail in [30, 32].  
 259 Furthermore, if these ultra-light ALPs are fundamental fields present during inflation they  
 260 carry isocurvature perturbations. This allows to do consistency checks but also test models  
 261 of inflation [32, 33].

### 262 **2.2.2. Hints from astrophysics**

263 In the last few years some astrophysical anomalies have found plausible explanations in  
 264 terms of axion/ALPs suggesting target areas in parameter space reachable by near-future  
 265 experiments. We refer here to the apparent non-standard energy loss of white dwarf stars,  
 266 *e.g.*, [34–38] (see however [39]) and the anomalous transparency of the Universe for TeV  
 267 gamma rays, *e.g.*, [40–45]. The required coupling strengths seem within reach in controlled

laboratory experiments at the intensity frontier, and can serve as useful benchmarks, c.f. Fig. 1.

In the mass range  $10^{-24} \text{ eV} \leq m_a \lesssim 10^{-20} \text{ eV}$ , large scale structure formation of ultra-light ALPs is analogous to warm DM (WDM), and is thus relevant to problems with CDM structure formation, such as the cusp-core, missing-satellites, and too-big-to-fail problems [28]. The virtue of ultra-light ALPs is that they avoid the so-called ‘Catch 22’ of WDM [46]. The relevance of ultra-light ALPs to these problems in large scale structure is explored in [47].

### 2.3. Status and Plans for Terrestrial experiments

#### 2.3.1. Laser Experiments

The simplest and most unambiguous purely laboratory experiment to look for axions (or light scalars or pseudoscalars more generally) is photon regeneration [48] (“shining light through the wall” [49]). A laser beam traverses a magnetic field, and the field stimulates a small fraction of photons to convert to axions of the same energy. A material barrier easily blocks the primary laser beam; in contrast, the axion component of the beam travels through the wall unimpeded and enters a second magnet. There, with the same probability, the axions are converted back to photons. Because the photon-regeneration rate goes as  $g_{a\gamma\gamma}^4$ , the sensitivity of the experiment is poor in its basic form, improved only by increasing the laser intensity, the magnetic field strength, or the length of the interaction regions. As initially suggested by Hoogeveen and Ziegenhagen [50] and recently discussed in detail [51–54] very large gains may be realized in both the photon-regeneration rate and in the resulting limits on  $g_{a\gamma\gamma}$  by introducing matched optical resonators in both the axion production and the photon regeneration regions.

Detailed designs for such an experiment exist, including the scheme for locking two matched high-finesse optical resonators, the signal detection method, and the ultimate noise limits [15, 52, 53]. Such experiments would improve on present limits on  $g_{a\gamma\gamma}$  by at least a factor of 10. We note also that these experiments, although challenging, are feasible using well-established technologies developed for example for laser interferometer gravitational-wave detectors [55, 56]. No new technology is needed. Two developed designs exist: the Resonantly Enhanced Axion-Photon Regeneration (REAPR) experiment, a Florida-Fermilab collaboration, and the Any Light Particle Search II (ALPS II) being mounted at DESY.

Figure 2(a) shows the photon regeneration experiment as usually conceived. If  $E_0$  is the amplitude of the laser field propagating to the right, the amplitude of the axion field

traversing the wall is  $E_0\sqrt{P}$  where  $P$  is the conversion probability in the magnet on the LHS of Fig. 2a. Let  $P'$  be the conversion probability in the magnet on the RHS. The field generated on that side is then  $E_S = E_0\sqrt{P'P}$  and the number of regenerated photons is  $N_S = P'PN_0$  where  $N_0$  is the number of photons in the initial laser beam.

It can be shown [48, 57, 58] that the photon to axion conversion probability  $P$  in a region of length  $L$  permeated by a constant magnetic field  $B_0$  transverse to the direction of propagation, is given by ( $\hbar = c = 1$ )

$$P = \frac{1}{4}(g_{a\gamma\gamma}B_0L)^2. \quad (1)$$

This equation is written for the effect in vacuum and for the case where the difference between the axion and photon momenta  $q = m_a^2/2\omega$  is small compared to  $1/L$ . The axion to photon conversion probability in this same region is also equal to  $P$ .

A number of photon regeneration experiments have reported results [59–66], with the best limits [66] being  $g_{a\gamma\gamma} < 6.5 \times 10^{-8} \text{ GeV}^{-1}$ . None of these experiments used cavities on the photon regeneration side of the optical barrier; recycling on the production side has been used in two [59, 65].

Photon regeneration is enhanced by employing matched Fabry-Perot optical cavities, Fig. 2(b), one within the axion generation magnet and the second within the photon regeneration magnet [50–52]. The first cavity, the axion generation cavity, serves to build up the electric field on the input (left) side of the experiment. It is easy to see that when the cavity is resonant to the laser wavelength, the laser power in the high-field region is increased by a factor of  $\mathcal{F}_a/\pi$  where  $\mathcal{F}_a = 4\pi T_{1a}/(T_{1a} + V_a)^2$  is the finesse of the cavity,  $T_{1a}$  is the transmittance of the input mirror, and  $V_a$  is the roundtrip loss of the cavity due to absorption of the coatings, scattering from defects, diffraction from the finite mirror size, and transmission through the end mirror. The increase in the laser power increases the number of created axions by a factor of  $\mathcal{F}_a/\pi$ . These axions propagate through the “wall” and reconvert into photons in the regeneration cavity on the right side. The intra-cavity photon field builds up under the conditions that the second cavity is resonant at the laser wavelength and that the spatial overlap integral  $\eta$  between the axion mode and the electric field mode is good. This overlap condition requires that the spatial eigenmodes of the two cavities are extensions of each other, e.g., when the Gaussian eigenmode in one cavity propagated to the other cavity is identical to the Gaussian eigenmode of that cavity.

To detect the regenerated field, a small part is allowed to transmit through one of the

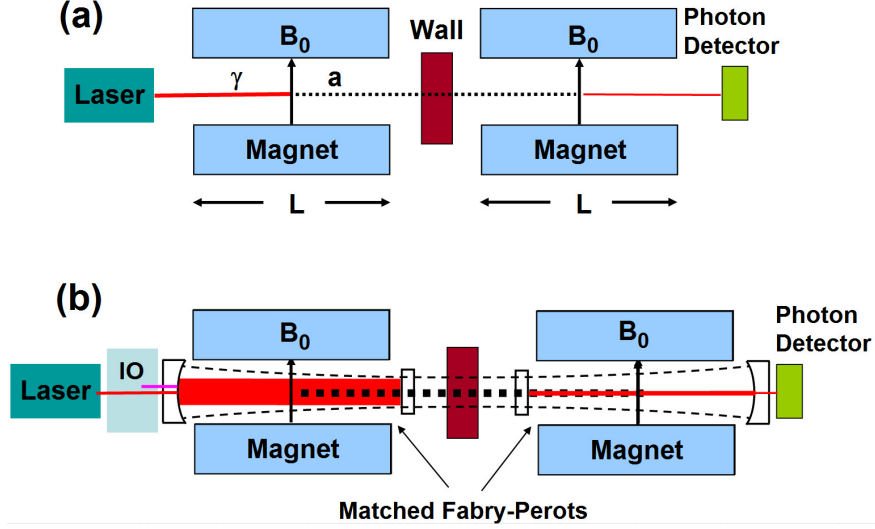


FIG. 2. (a) Simple photon regeneration to produce axions or axion-like particles. (b) Resonant photon regeneration, employing matched Fabry-Perot cavities. The overall envelope schematically shown by the thin dashed lines indicates the important condition that the axion wave, and thus the Fabry-Perot mode, in the photon regeneration cavity must follow that of the hypothetically unimpeded photon wave from the Fabry-Perot mode in the axion generation magnet. Between the laser and the cavity are optics (IO) that manage mode matching of the laser to the cavity, imposes RF sidebands for reflection locking of the laser to the cavity, and provides isolation for the laser. The detection system is also fed by matching and beam-steering optics. Not shown is the second laser for locking the regeneration cavity and for heterodyne readout.

331 cavity mirrors. The number of detected photons behind the regeneration cavity is [50–52]

$$N_S = \eta^2 \frac{\mathcal{F}_\gamma}{\pi} \frac{\mathcal{F}_a}{\pi} P^2 N_{in}. \quad (2)$$

332 Note that resonant regeneration gives an enhancement factor of  $\sim (\mathcal{F}/\pi)^2$  over simple pho-  
 333 ton regeneration. This factor may feasibly be  $10^{10}$ , corresponding to an improvement in  
 334 sensitivity to  $g_{a\gamma\gamma}$  of  $\approx 300$ .

335 The resonantly-enhanced photon regeneration experiment, involving the design and active  
 336 locking of high-finesse Fabry-Perot resonators and the heterodyne detection of weak signals  
 337 at the shot-noise limit, is well supported by the laser and optics technology developed  
 338 for LIGO [55]. We mention briefly REAPR and ALP=II and then discuss the expected  
 339 sensitivities of these experiments.

340 For a baseline of 36-m, 5 T, magnets, an input power of 10 W, a cavity finesse of  $\mathcal{F} \sim$   
 341  $\pi \times 10^5$  ( $T = 10$  ppm =  $V$ ) for both cavities, and 10 days of operation, we find at signal-to-

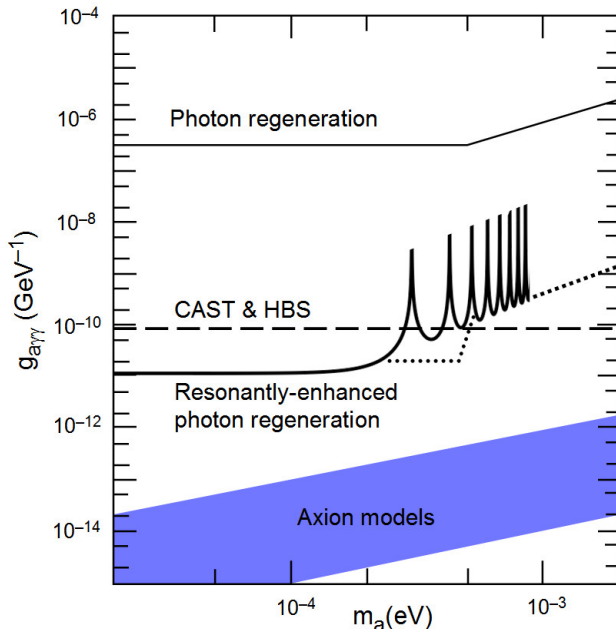


FIG. 3. Exclusion plot of mass and photon coupling ( $m_a, g_{a\gamma\gamma}$ ) for the axion, and the 95% CL exclusion limit for the resonantly enhanced photon regeneration (REPR) experiment. The existing exclusion limits indicated on the plot include the best direct solar axion search (CAST collaboration) [71], the Horizontal Branch Star limit [72], and previous laser experiments [62, 65].

342 noise ratio of unity,

$$g_{a\gamma\gamma}^{min} = \frac{2 \times 10^{-11}}{\text{GeV}} \left[ \frac{0.95}{\eta} \right] \left[ \frac{180 \text{ Tm}}{BL} \right] \left[ \frac{3 \times 10^5}{\mathcal{F}} \right]^{1/2} \left[ \frac{10 \text{ W}}{P_{in}} \right]^{1/4} \left[ \frac{10 \text{ days}}{\tau} \right]^{1/4}. \quad (3)$$

343 The experiment yields a 95% exclusion limit ( $3\sigma$ ) for axions or generalized pseudoscalars with  
 344  $g_{a\gamma\gamma}^{min} < 2.0 \times 10^{-11} \text{ GeV}^{-1}$  after 90 days cumulative running, well into territory unexplored by  
 345 stellar evolution bounds or direct solar searches. Note that the exclusion sensitivity follows  
 346 the inverse of  $\text{sinc}(qL/2)$ ; for REAPR the first null sensitivity occurs at  $2.8 \times 10^{-4} \text{ eV}$  and  
 347 for ALPS-II at about half this value. The momentum mismatch between a massless photon  
 348 and a massive axion defines the oscillation length of the process to be  $L_{osc} = 2\pi/q$ . (As  
 349 pointed out in [48] however, there is a practical strategy to extend the mass range upwards  
 350 if the total magnetic length  $L$  is comprised of a string of  $N$  individual identical dipoles of  
 351 length  $l$ . In this case, one may configure the magnet string as a “wiggler” to cover higher  
 352 regions of mass, up to values corresponding to the oscillation length determined by a single  
 353 dipole.) The sensitivity of both nonresonant and resonant regeneration experiments, as well  
 354 as other relevant limits, are shown in Fig. 3.

355 The optical prototypes being developed for the resonant regeneration experiment will

356 also have sensitivity to photon-light dark photon oscillations [73, 74] driven by the kinetic  
 357 mixing and the dark photon mass. Unlike the case of photon-axion oscillations, photon-  
 358 paraphoton oscillations do not require the presence of an external magnetic field, and so  
 359 can be performed with just the prototype optics and data acquisition system. On account  
 360 of the gain from the resonant cavities, a search with a REAPR or ALPS-II prototype with  
 361 meter-length cavities supersede the LIPSS limit [75] in less than 1 second of running. With  
 362 a 10-day run, the sensitivity will be improved by a factor of 300, reaching mixing angles  
 363  $\chi \approx 10^{-9}$  [76]. While not the primary goal of the project, a physics result on paraphotons  
 364 will come for free during the development phase of a resonantly-enhanced axion-photon  
 365 regeneration experiment.

366 Light shining through walls can also be done with "light" in the microwave regime [77–  
 367 81]. Allowing for highly sensitive resonant searches for axion-like particles as well as light  
 368 dark photons.

### 369 **2.3.2. Microwave Cavities (Haloscopes)**

370 Soon after the axion was realized to be a natural DM candidate, a detection concept was  
 371 proposed that relies on the resonant conversion of DM axions into photons via the Primakoff  
 372 effect [82]. Though the axion mass is unknown, various production mechanisms in the early  
 373 Universe point to a mass scale of a few to tens of  $\mu\text{eV}$  if the axion is the dominant form  
 374 of DM. The detection concept relies on DM axions passing through a microwave cavity  
 375 in the presence of a strong magnetic field where they can resonantly convert into photons  
 376 when the cavity frequency matches the axion mass. A  $4.13 \mu\text{eV}$  axion would convert into  
 377 a 1 GHz photon, which can be detected with an ultra-sensitive receiver. Axions in the DM  
 378 halo are predicted to have virial velocities of  $10^{-3} c$ , leading to a spread in axion energies of  
 379  $\Delta E_a/E_a \sim 10^{-6}$  (or 1 kHz for our 1 GHz axion example).

380 Initial experiments run at Brookhaven National Laboratory [83] and the University of  
 381 Florida [84] came within an order of magnitude of the sensitivity needed to reach plausible  
 382 axion couplings. ADMX [85] was assembled at Lawrence Livermore National Laboratory and  
 383 consists of a large, 8 T superconducting solenoid magnet with a 0.5 m diameter, 1 m long,  
 384 open bore. Copper-plated stainless steel microwave cavities are used and have  $Q_C \sim 10^5$ ,  
 385 low enough to be insensitive to the expected spread in axion energies. The  $\text{TM}_{010}$  mode  
 386 has the largest cavity form factor and is moved to scan axion masses by translating vertical  
 387 copper or dielectric tuning rods inside the cavity from the edge to the center. TE and TEM  
 388 modes do not couple to the pseudoscalar axion.

Using the ADMX setup and an estimated local DM density of  $\rho_{DM} = 0.45 \text{ GeV/cm}^3$  [86], an axion conversion power  $P_a \sim 10^{-24} \text{ W}$  is expected for plausible DM axions, with the possibility of scanning an appreciable frequency space (hundreds of MHz) in just a few years. Initial data runs were cooled with pumped LHe to achieve physical temperatures of  $< 2 \text{ K}$  and used SQUID amplifiers to reach plausible DM axion couplings [87]. Recently the ADMX experiment has been moved to the University of Washington where it will be outfitted with a dilution refrigerator that will increase sensitivity and scan rate. A second ADMX site, dubbed ADMX-HF, is being constructed at Yale and will allow access to  $> 2 \text{ GHz}$  while ADMX scans from  $0.4 - 2 \text{ GHz}$ . To achieve a greater mass reach, near-quantum limited X-band amplifiers and large volume resonant cavities will have to be developed.

As shown in Fig. 1, ADMX and ADMX-HF are sensitive to axion and ALP DM in the range of a few to tens of  $\mu\text{eV}$ . The experiments also have exceptional sensitivity to hidden photons in the same mass region, as shown in Fig. 7. The Yale Microwave Cavity Experiment (YMCE) is an additional current microwave cavity effort [88].

### 2.3.3. Oscillating Moments

Ultra-light particles such as axions and ALPs can be DM only if they have a large number density, making it possible to describe the DM axion (and ALP) as oscillating classical fields whose energy density is given by the DM density. In addition to single particle scattering that is often used to detect DM (such as WIMP DM), a classical field can give rise to energy and phase shifts. Measurements of such phase shifts can be used to search for the classical DM axion field. This is similar to searches for gravitational waves where the detection is not based on the unobservably small rate at of graviton scattering but rather on the phase shifts caused by the classical gravitational wave field.

Axion DM causes a time-varying nucleon electric dipole moment which produces oscillating CP-odd nuclear moments [89, 90]. In analogy with nuclear magnetic resonance, these moments cause precession of nucleon spins in the presence of a background electric field. The nucleon spin precession can be measured through precision magnetometry in a material sample [91]. With current techniques, this experiment has sensitivity to axion masses  $m_a \lesssim 10^{-9} \text{ eV}$ , corresponding to theoretically well-motivated axion decay constants  $f_a \gtrsim 10^{16} \text{ GeV}$ . With improved magnetometry, this experiment could ultimately cover the entire range of masses  $m_a \lesssim 10^{-6} \text{ eV}$ , complementing the region accessible to current axion searches.

Similarly, ALP DM can give rise to precession of nucleon spins that are not aligned



422 with the direction of the local momentum of the DM [90]. Such a precession can also  
423 be detected with the nuclear magnetic resonance and precision magnetometry techniques  
424 described in [91].

#### 425 **2.3.4. Helioscopes**

426 Axions could be produced from blackbody photons in the solar core via the Primakoff ef-  
427 fect [92] in the presence of strong electromagnetic fields in the plasma. Since the interaction  
428 of these axions with ordinary matter is extraordinarily weak, they can escape the solar  
429 interior, stream undisturbed to Earth and reconvert in a strong laboratory transverse mag-  
430 netic field via the inverse Primakoff effect [93–95]. The minimum requirements for such a  
431 helioscope experiment of high sensitivity are a powerful magnet of large volume and an ap-  
432 propriate X-ray sensor covering the exit of the magnet bore. Ideally, the magnet is equipped  
433 with a mechanical system enabling it to follow the Sun and thus increasing exposure time.  
434 Sensitivity can be further enhanced by the use of X-ray optics to focus the putative signal  
435 and therefore reducing detector size and background levels.

436 The first axion helioscope search was carried out at Brookhaven National Laboratory in  
437 1992 with a static dipole magnet [96]. A second-generation experiment, the Tokyo Axion  
438 Helioscope, uses a more powerful magnet and dynamic tracking of the Sun [97–99]. The  
439 CERN Axion Solar Telescope (CAST), a helioscope of the third generation and the most  
440 sensitive solar axion search to date, began data collection in 2003. It employs an LHC dipole  
441 test magnet of 10 m length and 10 T field strength [100] with an elaborate elevation and  
442 azimuth drive to track the Sun. CAST is the first solar axion search exploiting X-ray optics  
443 to improve the signal to background ratio (a factor of 150 in the case of CAST) [101]. For  
444  $m_a < 0.02$  eV, CAST has set an upper limit of  $g_{a\gamma} < 8.8 \times 10^{-11}$  GeV $^{-1}$  and a slightly larger  
445 value of  $g_{a\gamma}$  for higher axion masses [102–106]. The exclusion plots are shown in Fig. 4.  
446 CAST has also established the first helioscope limits for non-hadronic axion models [109].

448 So far each subsequent generation of axion helioscopes has resulted in an improvement in  
449 sensitivity to the axion-photon coupling constant  $g_{a\gamma}$  of about a factor 6 over its predeces-  
450 sors. To date, all axion helioscopes have used “recycled” magnets built for other purposes.  
451 The IAXO collaboration has recently shown [110] that a further substantial step beyond  
452 the current state-of-the-art represented by CAST is possible with a new fourth-generation  
453 axion helioscope, dubbed the International AXion Observatory (IAXO). The concept relies  
454 on a purpose-built ATLAS-like magnet capable of tracking the sun for about 10 hours each  
455 day, focusing X-ray optics to minimize detector area, and low background X-ray detectors

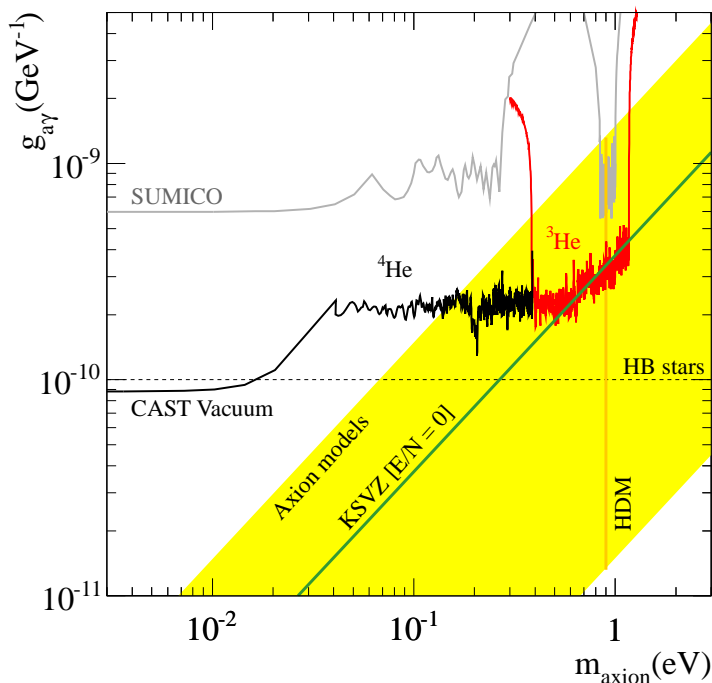


FIG. 4. Exclusion regions for axions and axion-like particles in the  $m_a - g_{a\gamma\gamma}$  plane achieved by CAST in the vacuum [102, 103],  $^4\text{He}$  [104], and  $^3\text{He}$  phase [105, 106]. We also show constraints from the Tokyo helioscope, horizontal branch (HB) stars [107], and the hot dark matter (HDM) bound [108]. The yellow band labeled “Axion models” represents typical theoretical models with  $|E/N - 1.95| = 0.07 - 7$ . The green solid line inside the band is for  $E/N = 0$  (KSVZ model).

456 optimized for operation in the 0.5 – 10 keV energy band. Pushing the current helioscope  
 457 boundaries to explore the range in  $g_{a\gamma}$  down to a few  $10^{-12}$   $\text{GeV}^{-1}$  (see Fig. 5), with sensi-  
 458 tivity to QCD axion models down to the meV scale and to ALPs at lower masses, is highly  
 459 motivated as was shown in previous sections. Lowering X-ray detector thresholds to 0.1 keV  
 460 would allow IAXO to test whether solar processes can create chameleons [111] and further  
 461 constrain standard axion-electron models. More speculative, but of tremendous potential  
 462 scientific gain, would be the operation of microwave cavities inside IAXO’s magnet, to allow  
 463 a simultaneous search for solar and DM axions [*e.g.*, [112]]. Searches for solar axions and  
 464 chameleons that exploit naturally occurring magnetic fields are described in [112–114] and  
 465 reviewed in [115]. IAXO can carry out this task as one of the main experimental pathways  
 466 in the next decade for the axion community. A detection with IAXO would have profound  
 467 implications for particle physics, with clear evidence of physics beyond the SM.

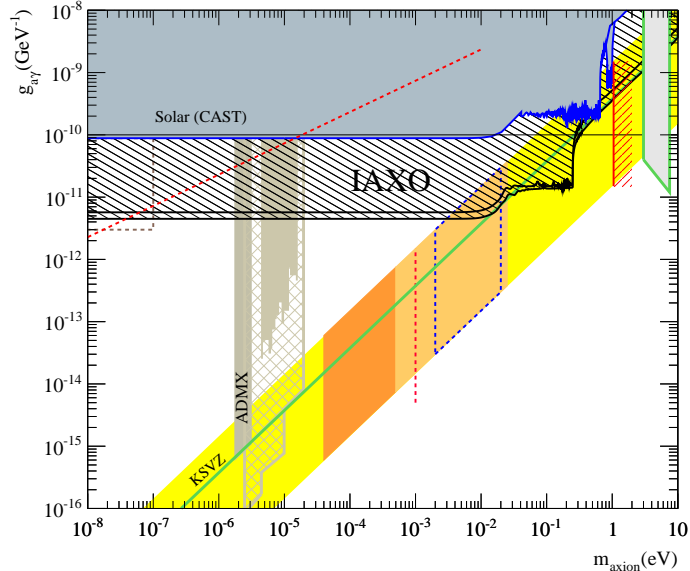


FIG. 5. Expected sensitivity of IAXO compared with current bounds from CAST and ADMX. Also future prospects of ADMX are shown (dashed brown region).

### 2.3.5. Beam Dumps and Colliders

Axions and ALPs can also be searched for in beam-dump and collider experiments. We describe these type of experiments in greater detail in the next section, although we do not discuss their sensitivity to axions and ALPs. See e.g. [116] and references therein.

## 3. DARK PHOTONS

### 3.1. Theory & Theory Motivation

This section describes the theory and motivation for new forces mediated by new abelian  $U(1)$  gauge bosons  $A'$  that couple very weakly to electrically charged particles through “kinetic mixing” with the photon [117, 118]. We will usually refer to the  $A'$  as a “dark photon”, but it is also often called a “U-boson”, “hidden-sector,” “heavy,” “dark,” “para-,” or “secluded” photon. Generalizations to other types of couplings beyond those generated by kinetic mixing exist, but our main focus will here be on this particularly simple type.

Kinetic mixing produces an effective parity-conserving interaction  $\epsilon e A'_\mu J_{EM}^\mu$  of the  $A'$  to the electromagnetic current  $J_{EM}^\mu$ , suppressed relative to the electron charge  $e$  by the parameter  $\epsilon$ , which theoretically is not required to be small. In fact,  $\epsilon$  can theoretically be  $\mathcal{O}(1)$ , as the vector portal is a dimension-four operator and unsuppressed by any high mass scale. In particular models, however,  $\epsilon$  can be calculated and can be naturally small (we

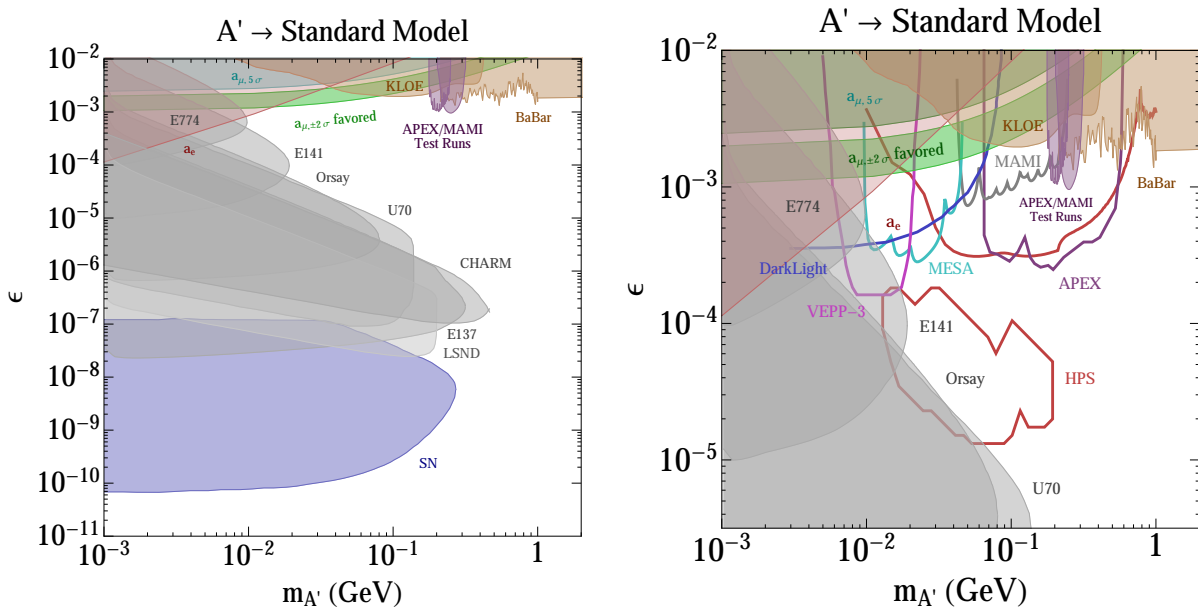


FIG. 6. Parameter space for dark photons ( $A'$ ) with mass  $m_{A'} > 1$  MeV (see Fig. 7 for  $m_{A'} < 1$  MeV). Shown are existing 90% confidence level limits from the SLAC and Fermilab beam dump experiments E137, E141, and E774 [119–122] the electron and muon anomalous magnetic moment  $a_\mu$  [123–125], KLOE [126] (see also [126, 127]), the test run results reported by APEX [128] and MAMI [129], an estimate using a BaBar result [119, 130, 131], and a constraint from supernova cooling [119, 132, 133]. In the green band, the  $A'$  can explain the observed discrepancy between the calculated and measured muon anomalous magnetic moment [123] at 90% confidence level. On the right, we show in more detail the parameter space for larger values of  $\epsilon$ . This parameter space can be probed by several proposed experiments, including APEX [134], HPS [135], DarkLight [136], VEPP-3 [137, 138], MAMI, and MESA [139]. Existing and future  $e^+e^-$  colliders such as *BABAR*, *BELLE*, *KLOE*, *SuperB*, *BELLE-2*, and *KLOE-2* can also probe large parts of the parameter space for  $\epsilon > 10^{-4} - 10^{-3}$ ; their reach is not explicitly shown.

485 often write the coupling strength as  $\alpha' \equiv \epsilon^2 \alpha$  where  $\alpha = e^2/4\pi \simeq 1/137$ ). In particular,  
 486 if the value of  $\epsilon$  at very high energies is zero, then  $\epsilon$  can be generated by perturbative  
 487 or non-perturbative effects. Perturbative contributions can include heavy messengers that  
 488 carry both hypercharge and the new  $U(1)$  charge, and quantum loops of various order can  
 489 generate  $\epsilon \sim 10^{-8} - 10^{-2}$  [140]. Non-perturbative and large-volume effects common in string  
 490 theory constructions can generate much smaller  $\epsilon$ . While there is no clear minimum for  $\epsilon$ ,  
 491 values in the  $10^{-12} - 10^{-3}$  range have been predicted in the literature [141–144].

492 A dark sector consisting of particles that do not couple to any of the known forces  
 493 and containing an  $A'$  is generic in many new physics scenarios. Such hidden sectors can

494 have a rich structure, consisting of, for example, fermions and many other gauge bosons.  
 495 The photon coupling to the  $A'$  could provide the only non-gravitational window into their  
 496 existence. Hidden sectors are generic, for example, in string theory constructions [145–148].  
 497 and recent studies have drawn a very clear picture of the different possibilities obtainable in  
 498 type-II compactifications (see dotted contours in Fig. 7). Several portals beyond the kinetic  
 499 mixing portal are possible, many of which can be investigated at the intensity frontier.

500 Masses for the  $A'$  can arise via the Higgs mechanism and can take on a large range of  
 501 values.  $A'$  masses in the MeV–GeV range arise in the models of [149–152] (these models  
 502 often involve supersymmetry). However, much smaller (sub-eV) masses are also possible.  
 503 Masses can also be generated via the Stückelberg mechanism, which is especially relevant  
 504 in the case of large volume string compactifications with branes [142]. In this case, the  
 505 mass and size of the kinetic mixing are typically linked through one scale, the string scale  
 506  $M_s$ , and therefore related to each other. In Fig. 7, various theoretically motivated regions  
 507 are shown [142, 143]. The  $A'$  mass can be as small as  $M_s^2/M_{\text{Pl}}$ , i.e.  $m_{A'} \sim \text{meV}$  (GeV)  
 508 for  $M_s \sim \text{TeV}$  ( $10^{10}$  GeV). Note that particles charged under a *massive*  $A'$  do not have an  
 509 electromagnetic millicharge, but a *massless*  $A'$  can lead to millicharged particles (see §4.1.3).

510 The previous discussion focused on kinetic mixing between the hypercharge  $U(1)_Y$  and the  
 511 dark  $U(1)$  gauge bosons, parametrized by  $\epsilon$ . As we mentioned above, many generalizations  
 512 exist. One generalization is obtained by allowing for the possibility of mass matrix mixing,  
 513 parametrized by  $\epsilon_Z$ , between the dark photon and the heavy  $Z$  boson of the SM [153].  
 514 Because of its expanded properties, the dark  $U(1)$  vector boson has been dubbed the “dark  
 515  $Z$ ” and labeled  $Z_d$  in such a picture, in order to emphasize its  $Z$ -like properties [153]. Overall,  
 516 the  $Z_d$  couples to both the electromagnetic ( $J_\mu^{\text{EM}}$ ) and the weak neutral ( $J_\mu^{\text{NC}}$ ) currents of  
 517 the SM, via [153]

$$\mathcal{L}_{\text{int}} = - \left( \epsilon e J_\mu^{\text{EM}} + \epsilon_Z \frac{g}{2 \cos \theta_W} J_\mu^{\text{NC}} \right) Z_d^\mu. \quad (4)$$

518 The additional interactions involving  $\epsilon_Z$  violate parity and current conservation. Conse-  
 519 quently, new phenomena such as “Dark Parity Violation” in atoms and polarized electron  
 520 scattering can occur [153, 154]. Enhancements in rare “dark” decays of the Higgs as well  
 521 as  $K$  and  $B$  mesons into  $Z_d$  particles can also occur, suggesting new experimental areas of  
 522 discovery [124, 153, 155]. Note however that for small  $m_{A'}$ ,  $\epsilon_Z$  is suppressed by  $(m_{A'}/m_Z)^2$   
 523 (if it originates exclusively from kinetic mixing) and these effects are extremely small.

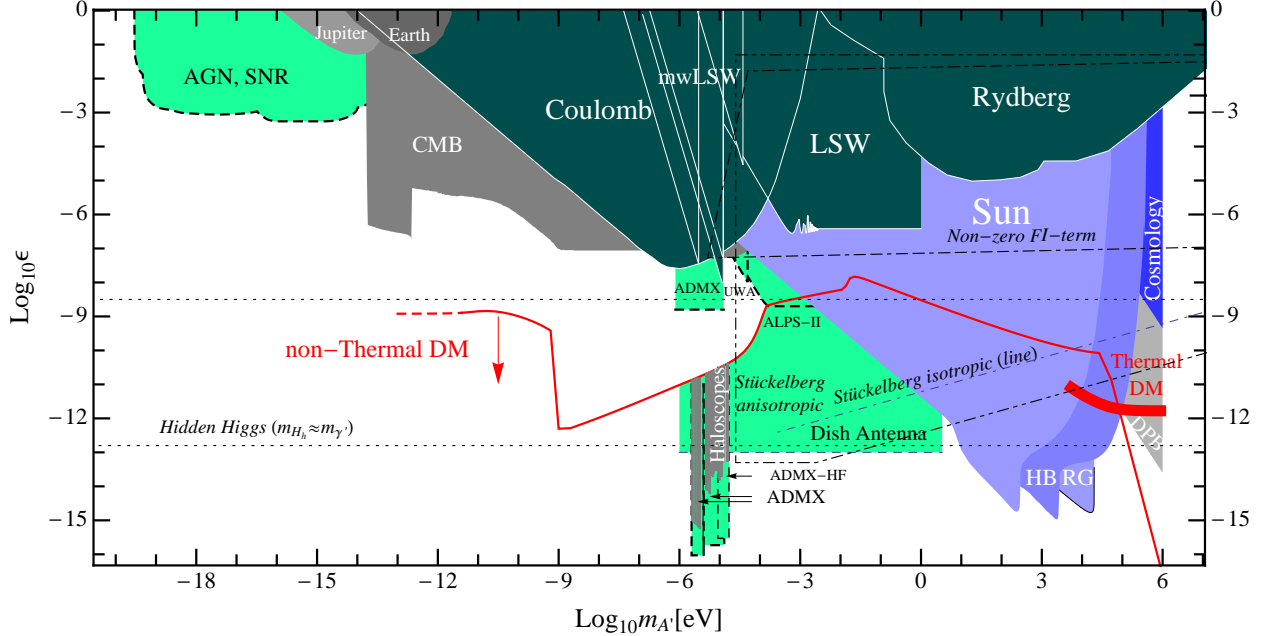


FIG. 7. Parameter space for hidden-photons ( $A'$ ) with mass  $m_{A'} < 1$  MeV (see Fig. 6 for  $m_{A'} > 1$  MeV). Colored regions are: experimentally excluded regions (dark green), constraints from astronomical observations (gray) or from astrophysical, or cosmological arguments (blue), and sensitivity of planned and suggested experiments (light green) (ADMX [14], ALPS-II [15], Dish antenna [19], AGN/SNR [168]). Shown in red are boundaries where the  $A'$  would account for all the DM produced either thermally in the Big Bang or non-thermally by the misalignment mechanism (the corresponding line is an upper bound). Regions bounded by dotted lines show predictions from string theory corresponding to different possibilities for the nature of the  $A'$  mass: Hidden-Higgs, a Fayet-Iliopoulos term, or the Stückelberg mechanism. Predictions are uncertain by  $\mathcal{O}(1)$ -factors.

### 3.2. Phenomenological Motivation and Current Constraints

A natural dividing line is  $m_{A'} \sim 2m_e \sim 1$  MeV. For  $m_{A'} > 1$  MeV, an  $A'$  can decay to electrically charged particles (*e.g.*,  $e^+e^-$ ,  $\mu^+\mu^-$ , or  $\pi^+\pi^-$ ) or to light hidden-sector particles (if available), which can in turn decay to ordinary matter. Such an  $A'$  can be efficiently produced in electron or proton fixed-target experiments [116, 119, 128, 129, 134–137, 156] and at  $e^+e^-$  and hadron colliders [126, 127, 130, 140, 150, 157–165], see §3.3. Hidden-sector particles could be directly produced through an off-shell  $A'$  and decay to ordinary matter. An  $A'$  in this mass range is motivated by the theoretical considerations discussed above, by anomalies related to DM [166, 167], and by the discrepancy between the measured and

533 calculated value of the anomalous magnetic moment of the muon [123].

534 Fig. 6 shows existing constraints for  $m_{A'} > 1$  MeV [119] and the sensitivity of several  
535 planned experiments that will explore part of the remaining allowed parameter space. These  
536 include the future fixed-target experiments APEX [128, 134], HPS [135], DarkLight [136] at  
537 Jefferson Laboratory, an experiment using VEPP-3 [137, 138], and experiments using the  
538 MAMI and MESA [139] at the University of Mainz. Existing and future  $e^+e^-$  colliders can  
539 also probe large parts of the parameter space for  $\epsilon > 10^{-4} - 10^{-3}$ , and include *BABAR*, Belle,  
540 KLOE, Super*B*, Belle II, and KLOE-2 (Fig. 6 only shows existing constraints, and no future  
541 sensitivity, for these experiments). Proton colliders such as the LHC and Tevatron can also  
542 see remarkable signatures for light hidden-sectors [157]. This rich experimental program is  
543 discussed in more detail in §3.3.

544 For  $m_{A'} < 1$  MeV, the  $A'$  decay to  $e^+e^-$  is kinematically forbidden, and only a much  
545 slower decay to three photons is allowed. For the most part of the parameter space shown  
546 in Fig. 7, the  $A'$  lifetime is longer than the age of the Universe. This figure shows the  
547 constraints, theoretically and phenomenologically motivated regions, and some soon-to-be  
548 probed parameter space. At these low masses, the mixing of  $A'$  with the photon can reveal  
549 itself in the phenomenon of photon  $\leftrightarrow A'$  oscillations [73]. This happens in general when  
550 the propagation and the interaction eigenstates are misaligned, the most famous case being  
551 neutrino flavor oscillations. Oscillatory patterns decohere very fast with increasing mass and  
552 are typically not relevant for  $m_{A'} > 1$  MeV. Photons emitted from a source can transform  
553 to an  $A'$ , which, being weakly interacting, might leave no trace. The effective photon  
554 disappearance is frequency dependent and distorts continuous spectra with a characteristic  
555 sinusoidal pattern in photon wavelength.

556 As axions or ALPs,  $A'$  bosons can also be DM through the vacuum-misalignment mech-  
557 anism [25, 169]. This intriguing possibility can be realized in a wide range of values for  $m_{A'}$   
558 and  $\epsilon$ , see Fig. 7. Experiments such as ADMX, looking for axion DM, is sensitive to  $A'$ 's  
559 as well. In this case, the use of magnetic fields to trigger the  $A' \rightarrow$  photon conversion is  
560 not required. This is another example, where the same experimental apparatus can often  
561 look for several kinds of particles. A few experimental searches are planned and discussed  
562 in §3.3.6, but a large parameter space still remains to be experimentally explored.

### 563 **3.2.1. Hints for MeV-GeV mass Dark Photons from Dark Matter**

564 Couplings between DM and dark photons at the MeV-GeV scale can drastically modify the  
565 phenomenology of DM. In direct detection experiments, the scattering cross section can be

566 increased due to the light mediator, or alternatively the kinematics of the scattering can be  
 567 altered if the mediator couples to nearly-degenerate states. In indirect searches, the self-  
 568 annihilation and self-scattering rates for the DM can both be enhanced at low velocities;  
 569 the former can lead to striking signals in cosmic rays, photons, and neutrinos, while the  
 570 latter can significantly modify the internal structure of DM halos. While the search for dark  
 571 photons has strong motivations entirely independent from their possible link to DM, their  
 572 detection could potentially provide an entirely new window on the dark sector.

573 **Cosmic rays:**

574 In 2008, the PAMELA experiment reported an unexpected rise in the ratio of cosmic-  
 575 ray (CR) positrons to CR electrons, beginning at  $\sim 10$  GeV and extending to above 100  
 576 GeV [170]. This result was later confirmed by the Fermi Gamma-Ray Space Telescope [171]  
 577 and most recently by AMS-02 [172]. The (largely model-independent) expectation from  
 578 standard CR propagation models is that the positron fraction should fall with increasing  
 579 energy. While there are proposals for generating the positron excess by modifications to CR  
 580 propagation, they require non-trivial changes to the usual propagation paradigm, e.g. that  
 581 the positrons do not suffer significant radiative losses over kpc distances [173], or that the  
 582 positron production by proton scattering occurs primarily within the original CR accelera-  
 583 tion site [174, 175]. Complementary measurements of the total  $e^+e^-$  spectrum by the Fermi  
 584 Gamma-Ray Space Telescope [176] are consistent with a new source of  $e^+e^-$  pairs in the  
 585 10-1000 GeV energy range.

586 The annihilation of weak-scale DM provides an attractive hypothesis for the origin of  
 587 this signal, but there are several difficulties with the conventional WIMP interpretation,  
 588 e.g. [177]. (Non-DM explanations involving a new  $e^+e^-$  source have also been advanced,  
 589 with the most popular being a population of pulsars; see e.g. [178, 179].) DM annihilating  
 590 to a dark photon which subsequently decays, however, naturally yields (i) an enhanced  
 591 signal (by up to 2-3 orders of magnitude) and (ii) a sufficiently hard positron spectrum  
 592 to match the observations, as well as forbidding the production of antiprotons, if the dark  
 593 photon is lighter than twice the proton mass (an antiproton excess was searched for, and  
 594 not observed) [166, 167]. Benchmark models of this type were computed for  $m_{A'} \sim 200 -$   
 595  $900$  MeV in [180], and found to provide a good fit to the data.

596 The AMS-02 data, with their much smaller uncertainties, prefer a somewhat softer spec-  
 597 trum of positrons than PAMELA. In turn, this favors dark photon models where the dark  
 598 photon is heavy enough to decay to muons and charged pions, or possibly multi-particle final  
 599 states (e.g. via decays through the dark sector); the spectrum due to dark photon decay to



600 an  $e^+e^-$  pair is (as the sole channel) somewhat harder than preferred by the data [181].  
 601 Direct leptophilic annihilation to SM particles no longer appears to provide a good expla-  
 602 nation for the signal: the softer spectrum favors  $\tau^+\tau^-$  final states, which are constrained by  
 603 searches for gamma-rays from dwarf galaxies [182].

604 There are also gamma-ray bounds on  $\mu^+\mu^-$ ,  $\pi^+\pi^-$ , and  $e^+e^-$  final states, but gamma-ray  
 605 production in these decays is small, and so the bounds are generally much weaker (unless  
 606 upscattering of ambient starlight by electrons is included, but this contribution also depends  
 607 on the electron propagation). Constraints from the inner Galaxy are dependent on the slope  
 608 of the DM density profile, which is not well-constrained by the data or theory; constraints  
 609 from the outer halo and extragalactic gamma-ray background depend sensitively on the  
 610 amount of small-scale substructure present, which is also poorly known. There is tension  
 611 between gamma-ray observations and the predictions from models fitting the PAMELA  
 612 signal, e.g. [183–185], but stronger statements are limited by the astrophysical uncertainties.

613 A more robust constraint arises from measurements of the CMB. DM annihilation during  
 614 the epoch of recombination can inject electrons and photons, which modify the ionization  
 615 history of the Universe; this in turn modifies the scattering of CMB photons at late times  
 616 and perturbs the observed anisotropy spectrum [186]. The current constraints probe relevant  
 617 regions of parameter space [187, 188], and the Planck polarization data should improve the  
 618 sensitivity by another factor of two, e.g. [187, 189]. The constraints are weaker if the local  
 619 DM density is higher by a factor of  $\sim \sqrt{2}$ , or by permitting an  $\mathcal{O}(1)$  contribution to the  
 620 signal from local clumps of DM. This second option is particularly attractive for lighter  
 621 dark photons ( $m_{A'} \ll 1$  GeV), where the annihilation cross section continues to grow at  
 622 velocities smaller than that of the main Milky-Way halo, and so the constraints from the  
 623 CMB (originating from an epoch when the DM was extremely slow-moving) grow even  
 624 stronger; this conclusion can be evaded if the excess observed by AMS-02 largely originates  
 625 from DM clumps with small internal velocity dispersions [190].

626 The constraints discussed above do not apply if the signal originates from decaying DM  
 627 (e.g. [191]). In this case the size of the signal is not a difficulty, but the lack of antiprotons  
 628 and the hard spectrum still motivate scenarios with decay through dark photons.

### 629 **Light DM:**

630 There have been several experimental results that might hint at the presence of  $\mathcal{O}(1-10)$   
 631 GeV DM. The CDMS experiment has recently reported three events in their signal region  
 632 [192], with the best fit WIMP hypothesis being favored over the background-only hypothesis  
 633 at 99.8% confidence. The best-fit WIMP mass is 8.6 GeV/cm<sup>2</sup>, with a 68% confidence

634 contour extending from 6.5 – 20 GeV. This region is in good agreement with earlier hints  
 635 of a signal from CoGeNT [193]; it appears in tension with limits from XENON100, but the  
 636 comparison does depend on the response of xenon to low-energy nuclear recoils and on the  
 637 DM velocity distribution [194].

638 The preferred DM-nucleon scattering cross section for the CDMS events,  $\sigma \approx 2 \times 10^{-41}$   
 639  $\text{cm}^2$ , is quite large. The two SM particles which might be expected to mediate such a  
 640 scattering are the  $Z$  boson and the Higgs, both of which are constrained (for light DM) by  
 641 bounds on the invisible decay width of the  $Z$  and the Higgs; the cross section preferred by  
 642 CDMS seems clearly ruled out for Higgs portal DM [195], and barely consistent for scattering  
 643 through the  $Z$  [196]. This observation motivates the existence of a new mediator particle, in  
 644 the event that the signal is indeed due to DM, e.g. [197]. A dark photon mediator naturally  
 645 enhances the cross section; if the mass of the dark photon is inherited from the weak scale,  
 646 the relation  $m_{A'} \sim \sqrt{\epsilon} m_Z$  naturally predicts a DM-nucleon cross section comparable to that  
 647 mediated by the  $Z$ , but the constraints on invisible decays no longer apply.

648 There have also been hints of possible annihilation signals from  $\sim 10$  GeV DM in the  
 649 Galactic Center and inner Galaxy [198–201]; these signals can be accommodated by light  
 650 DM annihilation to dark photons which subsequently decay to SM particles [202].

### 651 **Self-interacting DM:**

652 Any coupling between MeV-GeV dark photons and DM will also give rise to a long-range  
 653 self-interaction for the DM. This in turn can modify DM structure formation, flattening the  
 654 cusps at the centers of halos [203] and reducing the concentration of subhalos [204]. These are  
 655 two areas in which there are marked disagreements between the predictions of collisionless  
 656 cold DM simulations and observations of galaxies, and the effect of self-interaction is to  
 657 bring the two into closer agreement.

658 Recent work on the cross section required to achieve agreement has pointed to a low-  
 659 velocity cross section in the range of  $\sigma/m_{\text{DM}} \sim 0.1 - 1 \text{ cm}^2/\text{g}$  [205]. In dark-photon scenarios  
 660 where the potential due to self-interaction can be approximated as a Yukawa potential, the  
 661 maximum transfer cross section (in the classical regime, see [206]) is given by  $\sigma_T \approx 22.7/m_{A'}^2$   
 662 (e.g. [204]). Setting  $\sigma_T/m_{\text{DM}} \simeq 1 \text{ cm}^2/\text{g}$ , we require  $m_{A'} \approx 70 \text{ MeV} \times \sqrt{\text{GeV}/m_{\text{DM}}}$ , in  
 663 agreement with similar estimates in [190]. It is remarkable that this entirely independent  
 664 line of enquiry suggests a mass scale in the range accessible by dark photon searches.

### 3.2.2. Ultra-light Dark Photons

In recent years, fits to cosmological data including large-scale structure and the CMB anisotropies (WMAP and Planck) have suggested the existence of dark radiation, i.e. a relic population of relativistic particles decoupled from ordinary matter.  $A'$ s with meV mass and  $\epsilon \sim \mathcal{O}(10^{-6})$  would be produced in the early Universe in the right amount to account for this tendency [76] but a recent examination of the stellar evolution constraints showed that this region is ruled out [207]. If dark radiation exists and it is due to  $A'$ s the relic abundance has to be produced by decays or annihilation of dark-sector particles. Constraints on this scenario are very mild so there is motivation to explore a large range of masses and  $\epsilon$ .

More interesting is the possibility that light  $A'$ s constitute the DM of the Universe. There are two possibilities depending on the origin of the relic density of  $A'$ s. If  $m_{A'} \sim 100$  keV and  $\epsilon \sim 10^{-12}$  (thick red band labelled “Thermal DM” in Fig. 7) the right amount of DM  $A'$ s is produced by oscillations from the photon thermal bath before big bang nucleosynthesis [208]. This hypothesis can be tested in direct DM detection experiments or indirectly through the  $A'$  decay into three photons, which could be observed above the astrophysical diffuse X-ray backgrounds [208, 209]. In this case, DM  $A'$ s have larger velocities than standard “cold” DM qualifying as “warm” DM. This possibility is very appealing in the light of the unresolved issues with structure formation present in the cold DM paradigm mentioned in Sec. 2.2.2.

Alternatively, a CDM relic of  $A'$  can be produced by the “misalignment mechanism” in a way analogous to axions and ALPs [25, 169]. In this case, a small part of the DM  $A'$ s possibly oscillates into photons in the early Universe leaving a fingerprint in cosmological observables like the CMB spectrum, abundances of light elements created during BBN, and the isotropic diffuse photon background [25]. The region above the line labelled “non-Thermal DM” in Fig. 7) is free from any of such constraints and thus perfectly viable for CDM  $A'$ .

### 3.3. Experimental Searches for Dark Photons: Status and Plans

For  $m_{A'} > 1$  MeV, our discussion here focuses on the case where the dark photon can only decay into SM matter, with  $\epsilon$ -suppressed decay width. Another possibility is that the dark photon has  $\epsilon$ -unsuppressed couplings to some new species “ $\chi$ ” of fermions or bosons (dark-sector matter), which are neutral under the SM gauge group, and in particular are electrically neutral. The latter will be discussed in detail in §4. We also comment on searches for ultralight  $A'$ , i.e.  $m_{A'} < 1$  MeV.

### 3.3.1. Electron Beam Dump Experiments

In electron beam dump experiments, a high-intensity electron beam dumped onto a fixed target provides the large luminosities needed to probe the weak couplings of dark photons. When the electrons from the beam scatter in the target, the dark photons can be emitted in a process similar to ordinary bremsstrahlung because of the kinetic mixing. The dark photons are highly boosted carrying most of the initial beam energy and get emitted at small angles in the forward direction. The detector is placed behind a sufficiently long shield to suppress the SM background. Dark photons can traverse this shielding due to their weak interactions with the SM and can then be detected through their decay into leptons (mostly  $e^+e^-$  for the mass range of interest). Therefore, a decay length of  $\mathcal{O}(\text{cm} - \text{m})$  is needed in order for the dark photons to be observable by decaying behind the shield and before the detector. This is possible for dark photons with masses larger than  $2m_e$  up to  $\mathcal{O}(100)$  MeV and small values of  $\epsilon$  (roughly  $10^{-7} \lesssim \epsilon \lesssim 10^{-3}$ ). Electron beam dump experiments are thus well suited to probe this region of the parameter space.

Depending on the specific experimental set-up with respect to the decay length of the dark photon, the possible reach of an experiment is determined not only by the collected luminosity but also by the choice of the beam energy, the length of the shield, and the distance to the detector. Large values  $\epsilon$  for which the lifetime is very short are not accessible, since the dark photon decays within the shield. At very small values of  $\epsilon$ , the sensitivity of these experiments is limited by statistics as there are very few dark photons that will be produced and that decay before the detector. The total number of events expected in such experiments from decays of dark photons has been determined in [119, 210].

Several electron beam dump experiments were operated in the last decades to search for light metastable pseudoscalar or scalar particles (e.g. axion-like particles or Higgs-like particles). Examples are the experiments E141 [121] and E137 [120] at SLAC, the E774 [122] experiment at Fermilab, an experiment at KEK [211] and an experiment in Orsay [212]. The measurements performed by the experiments at SLAC and Fermilab have been reanalysed in [119] to derive constraints on the dark photon mass and coupling. Updated limits for all experiments were presented in [210], where the acceptances obtained with Monte Carlo simulations for each experimental set-up have been included. These limits are shown in Fig. 6 together with all current constraints. Electron beam dump experiments cover the lower left corner of the parameter space in which the lifetime of the dark photon is sufficiently large to be observed behind the shield. In order to extend these limits with future experiments to smaller values of  $\epsilon$  large luminosities and/or a long distance to the detector are needed,

730 since the lower limit of an experiment’s reach scales only with the fourth root of those two  
731 parameters.

### 732 3.3.2. Fixed-Target Experiments

733 Fixed-target experiments using high-current electron beams are an excellent place to search  
734 for  $A'$ s with masses  $2m_e < m_{A'} < \text{GeV}$  and couplings down to  $\epsilon^2 \equiv \alpha'/\alpha > 10^{-10}$ . In  
735 these experiments, the  $A'$  is radiated off electrons that scatter on target nuclei. Radiative  
736 and Bethe-Heitler trident production give rise to large backgrounds. Generally speaking,  
737 three experimental approaches have been proposed: dual-arm spectrometers, forward ver-  
738 texing spectrometers, and full final-state reconstruction. In most cases, the detectors are  
739 optimized to detect the  $e^+e^-$  daughters of the  $A'$ . The complementary approaches map out  
740 different regions in the mass-coupling parameter space. General strategies for  $A'$  searches  
741 with electron fixed-target experiments were laid out in [119]. The reach for recently proposed  
742 dark photon searches is shown in Fig. 6.

743 Several experiments have been proposed to search for dark photons: APEX, HPS, and  
744 DarkLight at Jefferson Lab (JLab), and A1 using MAMI and MESA at Mainz.

745 Existing dual-arm spectrometers at Hall A at JLab and MAMI at Mainz have already  
746 been used to search for dark photons. Two groups, the  $A'$  Experiment (APEX) collaboration  
747 at JLab and the A1 collaboration at Mainz, have performed short test runs (few days of  
748 data taking) and published search results with sensitivity down to  $\alpha'/\alpha > 10^{-6}$  over narrow  
749 mass ranges [128, 129]. These results clearly demonstrate the high sensitivity that can be  
750 reached in fixed-target experiments. These experiments use high-current beams ( $\sim 100 \mu\text{A}$ )  
751 on relatively thick targets (radiation length  $X_0 \sim 1\text{-}10\%$ ) to overcome the low geometric  
752 acceptance of the detectors ( $\sim 10^{-3}$ ). Beam energy and spectrometer angles are varied to  
753 cover overlapping regions of invariant mass. Searches for  $A'$  involve looking for a bump  
754 in the  $e^+e^-$  invariant mass distribution over the large trident background, which requires  
755 excellent mass resolution.

756 APEX has been approved for a month-long run, tentatively in 2016. Using high-current  
757 beams ( $\sim 100\mu\text{A}$ ) at four different beam energies on relatively thick targets (1-10% of a  
758 radiation length), the proposed full APEX experiment will probe  $A'$  masses from 65 to 550  
759 MeV for couplings  $\alpha'/\alpha > 10^{-7}$  [134].

760 A1 has already taken some more data, with the expectation that they will probe  $A'$  masses  
761 in the range 50 – 120 MeV with a sensitivity in  $\alpha'/\alpha$  similar to the test run published in  
762 2011. Furthermore, A1 is developing a new experiment to search for dark photon decay

763 vertices displaced from the target by approximately 10 mm. They hope to cover the  $A'$   
764 mass range  $40 < m_{A'} < 130$  MeV with a sensitivity in  $\alpha'/\alpha$  from  $10^{-9}$  down to  $10^{-11}$ .

765 The Heavy Photon Search (HPS) collaboration [135] has proposed an experiment for  
766 Hall B at JLab using a Si-strip based vertex tracker inside a magnet to measure the invariant  
767 mass and decay point of  $e^+e^-$  pairs and a  $\text{PbWO}_4$  crystal calorimeter to trigger. HPS uses  
768 lower beam currents and thinner targets than the dual arm spectrometers, but compensates  
769 with large ( $\sim 20\%$ ) forward acceptance. HPS has high-rate data acquisition and triggering  
770 to handle copious beam backgrounds and high-rate trident production. Because it can  
771 discriminate  $A'$  decays displaced more than a few millimeters from the large, prompt, trident  
772 background, HPS has enhanced sensitivity to small couplings, roughly  $10^{-7} > \alpha'/\alpha > 10^{-10}$   
773 for masses  $30 < m_{A'} < 500$  MeV. For prompt decays, HPS will simultaneously explore  
774 couplings  $\alpha'/\alpha > 10^{-7}$  over the same mass range. HPS has conducted a successful test run  
775 at JLab during the spring of 2012, which demonstrated technical feasibility and confirmed  
776 simulations of the background rates. The proposal for “full” HPS was approved and funded  
777 by DOE in Summer, 2013. JLab has scheduled commissioning and running during 2014 and  
778 2015. HPS is being constructed during 2013-2014, will be installed at JLab in September,  
779 2014, and will begin running thereafter at the upgraded CEBAF accelerator.

780 The DarkLight detector is a compact, magnetic spectrometer designed to search for decays  
781 to lepton pairs of a dark photon  $A'$  in the mass range  $10 \text{ MeV} < m_{A'} < 90 \text{ MeV}$  at coupling  
782 strengths of  $10^{-7} < \alpha'/\alpha < 10^{-4}$ . The experiment will use the 100 MeV beam of the JLaB  
783 FEL incident on a hydrogen gas target at the center of a solenoidal detector, comprising  
784 silicon detectors (for the recoil proton), a low mass tracker (for the leptons), and shower  
785 counters (for photon detection). By measuring all the final state particles, Darklight can  
786 provide full kinematic reconstruction. The available information also permits searching for  
787 invisible  $A'$  decays via a missing mass measurement. A series of beam tests in summer 2012  
788 verified that sustained, high-power transmission of the FEL beam through millimeter-size  
789 apertures is feasible [213, 214]. JLab has approved Darklight. A full technical design is  
790 underway and funding is being sought. The goal is to begin data taking in 2016.

791 The MESA accelerator [215], which recently has been approved for funding within the  
792 PRISMA cluster of excellence at the University of Mainz, hopes to cover a mass range  
793 comparable to that covered by Darklight. The MESA accelerator (155 MeV beam energy)  
794 will be operated in the energy recovering linac mode with one recirculating arc as well as  
795 a windowless gas jet target. The Mainz group is considering to use two compact high-  
796 resolution spectrometers rather than a high-acceptance tracking detector. The project is

797 several years off.

### 798 3.3.3. Proton Beam Dump Experiments

799 Proton beam dump experiments can also search for dark photons which decay to visible  
800 channels. Several reinterpretations of past experimental analyses from LSND [116, 156, 216],  
801  $\nu$ -Cal I [217–219], NOMAD [220, 221], PS191 [220, 222], and CHARM [223, 224] have re-  
802 sulted in limits on dark photons that are complementary to those coming from electron fixed  
803 target experiments, precision QED, and B-factories. One can take advantage of the large  
804 sample of pseudoscalar mesons (*e.g.*,  $\pi^0$ ,  $\eta$ ) produced in the proton-target collisions, which  
805 will decay to  $\gamma A'$  with a branching ratio proportional to  $\epsilon^2$  if kinematically allowed [156].  
806 These experiments probe a similar region in  $A'$  mass and coupling parameter space as past  
807 electron beam dumps discussed in Section 3.3.1, but do have unique sensitivity in certain  
808 cases. It remains to be investigated whether future proton beam dump experiments can  
809 cover new regions of  $A'$  parameter space.

810 Proton beam dump experiments also have significant sensitivity to invisible decays of  $A'$ ,  
811 particularly when the decay products are stable and can re-scatter in the detector, (*e.g.*, as  
812 in the case of  $A'$  decaying to dark matter). In fact, there is a proposal to do a dedicated  
813 beam dump mode run at MiniBooNE to search for light dark matter [225]. This subject is  
814 discussed in more detail in §4.

### 815 3.3.4. Electron-Positron Colliders

816 During the past 15 years, high luminosity  $e^+e^-$  flavor factories have been producing an  
817 enormous amount of data at different center-of-mass energies. In Frascati (Italy), the KLOE  
818 experiment running at the DAΦNE collider, has acquired about  $2.5 \text{ fb}^{-1}$  of data at the  
819  $\phi(1020)$  peak. B-factories at PEP-II (USA) and KEK-B (Japan) have delivered an integrated  
820 luminosity of  $0.5\text{--}1 \text{ ab}^{-1}$  to *BABAR* and *Belle*, respectively. In China, the Beijing BEPC  
821 collider is currently running at various energies near the charm threshold and has already  
822 delivered several inverse femtobarn of data to the BESIII experiment.

823 These large datasets have been exploited to search for dark photon production in the  
824 following processes:

- 825 • The radiative production of a dark photon ( $A'$ ) followed by its decay into a charged  
826 lepton or photon pair,  $e^+e^- \rightarrow \gamma A'$ ,  $A' \rightarrow l^+l^-$ ,  $\gamma\gamma$  ( $l = e, \mu$ ) [149].
- 827 • The associated production of a dark photon with a new light scalar particle, generally

828 dubbed as  $h'$ . The existence of the latter is postulated in models where the hidden  
 829 symmetry is broken by some Higgs mechanism [160]. Similarly to the SM Higgs,  
 830 the mass of the  $h'$  is not predictable by first principles and could be at the  $\sim$  GeV  
 831 scale as well. The phenomenology is driven by the mass hierarchy. While scalar  
 832 bosons heavier than two dark photons decay promptly, giving rise to events of the  
 833 type  $e^+e^- \rightarrow A'h' \rightarrow 3A', A' \rightarrow l^+l^-, \pi^+\pi^-$ , their lifetime becomes large enough to  
 834 escape undetected for  $m_{h'} < m_{A'}$ , resulting in  $e^+e^- \rightarrow A'h' \rightarrow l^+l^- + \text{missing energy}$   
 835 events.

- 836 • Radiative meson decays, which could also produce a dark photon with a branching  
 837 ratio suppressed by a factor  $\epsilon^2$  [130].

838 The search for a light CP-odd Higgs ( $A^0$ ) in  $\Upsilon(2S, 3S) \rightarrow \gamma A^0, A^0 \rightarrow \mu^+\mu^-$  conducted by  
 839 *BABAR* [131] has been reinterpreted in terms of constraints on dark photon production [119,  
 840 130, 134], as its signature is identical to that of  $e^+e^- \rightarrow \gamma A', A' \rightarrow \mu^+\mu^-$ . Limits on the  
 841 coupling  $\epsilon^2$  at the level of  $10^{-5}$  have been set. Future analyses based on the full *BABAR* and  
 842 Belle datasets are expected to increase the sensitivity by an order of magnitude.

843 A search for a dark photon and an associated scalar boson has been performed at *BABAR*  
 844 in the range  $0.8 < m_{h'} < 10.0$  GeV and  $0.25 < m_{A'} < 3.0$  GeV, with the constraint  
 845  $m_{h'} > 2m_{A'}$  [164]. The signal is either fully reconstructed into three lepton or pion pairs, or  
 846 partially reconstructed as two dileptonic resonances, assigning the remaining dark photon  
 847 to the recoiling system. No significant signal is observed, and upper limits on the product  
 848  $\alpha_D \epsilon^2$  are set at the level  $10^{-10} - 10^{-8}$ . These bounds are translated into constraints on the  
 849 mixing strength in the range  $10^{-4} - 10^{-3}$ , assuming  $\alpha_D = \alpha \simeq 1/137$ . A similar search  
 850 currently performed by Belle should improve these limits by a factor of two.

851 KLOE has searched for  $\phi(1020) \rightarrow \eta A', A' \rightarrow e^+e^-$  decays, in which the  $\eta$  was tagged  
 852 with either the  $3\pi^0$  or the  $\pi^+\pi^-\pi^0$  final states [126, 127]. The  $A' \rightarrow \mu^+\mu^-, \pi^+\pi^-$  channels  
 853 were not included due to a higher background level. After subtraction of the  $\phi$  Dalitz  
 854 decay background, no evident peak is observed, and the following limits are set at 90% CL:  
 855  $\epsilon^2 < 1.5 \times 10^{-5}$  for  $30 < m_{A'} < 420$  MeV,  $\epsilon^2 < 5 \times 10^{-6}$  for  $60 < m_{A'} < 190$  MeV.

856 The BESIII Collaboration has published a search for invisible decays of the  $\eta$  and  $\eta'$   
 857 mesons, motivated by the possible existence of light neutral dark matter particles [226].  
 858 Events are selected from  $J/\psi \rightarrow \phi\eta(\eta')$  decays, where the  $\phi$  is tagged by its charged kaon  
 859 decay mode. No significant signal is observed, and 90% CL limits on the branching ratio  
 860  $BR(\eta \rightarrow \text{invisible}) < 1.0 \times 10^{-4}$  and  $BR(\eta' \rightarrow \text{invisible}) < 5.3 \times 10^{-4}$  are set. These bounds



861 constrain the invisible dark photon decay through  $\eta(\eta') \rightarrow A'A', A' \rightarrow \textit{invisible}$ .

### 862 **Future Searches using Current Datasets**

863 Current datasets have not been fully exploited to search for signatures of a dark sector.  
864 Current studies of the  $e^+e^- \rightarrow \gamma A', A' \rightarrow l^+l^-, \pi^+\pi^-$  based on the full *BABAR* and Belle  
865 datasets are expected to probe values of the coupling  $\epsilon^2$  down to  $\sim 10^{-6}$ , and extend the  
866 coverage down to  $\sim 20$  MeV, covering the full region favored by the  $g - 2$  discrepancy.  
867 KLOE is expected to probe values of  $\epsilon^2$  between  $\sim 10^{-5}$  and  $\sim 7 \times 10^{-7}$  in the range  
868  $500 < m_{A'} < 1000$  MeV using the  $e^+e^- \rightarrow \mu^+\mu^-\gamma$  sample selected for the study of the  
869 hadronic contribution to the muon magnetic anomaly. Similarly, invisible dark photon  
870 decays could be studied in the  $e^+e^- \rightarrow \gamma + \textit{invisible}$  final state, using data collected at  
871 *BABAR* with a specific single-photon trigger (see also §4). This search could probe dark  
872 photon masses  $0 < m_{A'} < 5$  GeV, significantly extending the parameter space covered by  
873 proposed searches in neutrino experiments [225]. The calorimeter hermeticity and energy  
874 resolution play a crucial role for this study, as well as the amount of accidental background.  
875 Similar considerations apply to searches for purely neutral dark photon decays.

876 A search for a light  $h'$ , pair produced with a dark photon is being performed at KLOE  
877 using  $e^+e^- \rightarrow A'h' \rightarrow l^+l^- + \textit{missing energy}$  events. This search fully complements the  
878 analysis performed by *BABAR* covering a totally different parameter space. Extensions to  
879 non-Abelian model could easily be probed using current datasets. The simplest scenario  
880 include four gauge bosons, one dark photon and three additional dark bosons, generically  
881 denoted  $W'$ . A search for di-boson production has been performed at *BABAR* in the four  
882 lepton final state,  $e^+e^- \rightarrow W'W', W' \rightarrow l^+l^-$  ( $l = e, \mu$ ), assuming both bosons have similar  
883 masses [227]. More generic setups could easily be investigated.

884 The existence of a dark scalar or pseudo-scalar particle can also be investigated in  $B \rightarrow$   
885  $K^{(*)}l^+l^-$  decays. The sensitivity of *BABAR* and Belle searches to the SM Higgs–dark scalar  
886 mixing angle and pseudo-scalar couplings constants are projected to be at the level of  $10^{-4}$ –  
887  $10^{-3}$  and  $10^3$  TeV, respectively [228].

### 888 **3.3.5. Proton Colliders**

889 Proton colliders have the ability to reach high center-of-mass energy, making it possible to  
890 produce  $Z$  bosons, Higgs bosons, and perhaps other new, heavy particles (such as supersym-  
891 metric particles,  $W'/Z'$  states, or hidden-sector particles) directly. As pointed out in many  
892 theoretical studies [151, 157, 165, 230, 231], if new states are produced, they could decay to  
893  $A'$  bosons and other hidden-sector states with very large branching ratios. For GeV-scale

894  $A'$  masses, the  $A'$  would be highly boosted when produced in such decays and its decay  
895 products would form collimated jets, mostly composed of leptons (“lepton-jets” [151]).

896 The general-purpose proton collider experiments at the Tevatron and LHC have all pre-  
897 sented first searches for lepton-jets in heavy-particle decays [162, 163, 232–234]. The searches  
898 usually employ a specialized lepton-jet identification algorithm to distinguish them from the  
899 large multi-jet background. Events with additional large missing transverse energy (from  
900 other escaping hidden-sector particles) or a particular di-lepton mass (corresponding to the  
901  $A'$  mass) have also been searched for [235]. Results have often been interpreted in super-  
902 symmetric scenarios; the updated ATLAS analysis using 7 TeV pp data from 2011 excludes  
903 di-squark production with a squark mass up to about 1000 GeV or a weakly-produced state  
904 with mass up to about 400 GeV, decaying through cascades to two lepton-jets [236]. Current  
905 searches have mostly focused on  $A'$  bosons heavy enough to decay to muon pairs, since this  
906 offers a cleaner signal than electron pairs, but good sensitivity has also been seen down to  
907  $\sim 50$  MeV (limited by photon conversions to  $e^+e^-$  pairs).

908 ATLAS has recently searched for decays of the Higgs boson to electron lepton-jets, ex-  
909 cluding a branching ratio of about 50% [237]. Searches have mostly focused so far on prompt  
910 decays of dark photons, but ATLAS has now searched for decays of the Higgs boson to long-  
911 lived  $A'$  bosons decaying to muons in the muon chambers, constraining the branching ratio  
912 to be less than 10% for a proper lifetime between 10 and 100 mm [238].

### 913 **3.3.6. Photon Regeneration Experiments (ultra-light dark photons)**

914 Light dark photons ( $\sim$  meV) may be searched for in photon regeneration experiments.  
915 Experiments using laser light as REAPR and ALPS-II have already been explained in §2.3.1.  
916 The sensitivity of ALPS-II (in its final phase) is shown in Fig. 7 (REAPR would be similar).  
917 It reaches the region where meV mass  $A'$  can be cold DM. This region is motivated by type-II  
918 string models, in particular anisotropic compactifications (with one very large dimension),  
919 where the  $A'$  arises via the Stuckelberg mechanism.

920 Photon regeneration experiments have been performed in the microwave range ( $\mu$ eV  
921  $A'$  masses) by attempting the transfer of power between isolated microwave cavities in  
922 tune following the concept of [77, 78] (dark green sharp triangles labelled “mwLSW”). The  
923 current constraints correspond to proof-of-concept experiments by groups in the University  
924 of Western Australia (UWA) [79] and ADMX [80] and a more mature experiment performed  
925 at CERN [81]. The axion-sensitivity improvements expected by ADMX (see 2.3.2) will also  
926 allow a much more sensitive parasitic search of  $A'$ s, see curve labelled ADMX in Fig. 7 [80].

### 927 **3.3.7. Helioscopes (ultra-light dark photons)**

928 Helioscopes looking for solar axions can detect transversely polarized  $A'$ s emitted from the  
929 solar interior [239]. If the  $A'$  mass is due to the Stuckelberg mechanism, the region in which  
930 they are sensitive is already excluded by our knowledge of the Sun [207] (the emission of  
931 longitudinally polarized  $A'$ s would require a too high solar core temperature to be compatible  
932 with the measured solar neutrino fluxes [240]). If the  $A'$  mass comes from a Higgs mechanism,  
933 the situation is different and is currently being explored [241]. The SHIPS helioscope in the  
934 Hamburg Sternwarte [242] is currently looking for this possibility but more theoretical input  
935 is required to assess the impact of its measurements and future directions.

936 A more promising endeavor is to detect the solar flux of longitudinally polarized  $A'$ s,  
937 which dominates for  $m_{A'} \lesssim 10$  eV. These  $A'$ s have typical energies 10-300 eV and produce  
938 ionization in DM detectors such as XENON10 [241]. The first rough analysis of [241] shows  
939 a very promising venue to search for Stuckelberg  $A'$ s near the solar limit. This line shall  
940 benefit of future experiments with more exposure and more detailed analysis of the low  
941 energy single-electron ionization events. The parameter-space regions that can be explored  
942 are motivated from string theory and from DM.

### 943 **3.3.8. Cold DM searches (ultra-light dark photons)**

944 If DM comprises cold  $A'$ s produced by the misalignment mechanism it will produce a signal  
945 in Haloscopes looking for axion DM if they are tuned to the  $A'$  mass [25]. The signal has two  
946 characteristics that make it different from an axion signal. First, it is not proportional to the  
947 magnetic field and thus survives when this is switched off (which could lead one to think it is  
948 a systematic). Second, the  $A'$  polarization vector changes its orientation with respect to the  
949 cavity eigenmodes producing an oscillation of the effectiveness of the DM-cavity coupling  
950 and thus of the power output. If the  $A'$  polarization is homogeneously aligned in the DM  
951 halo only a daily modulation is expected, but if this is not the case, more complicated  
952 patterns are to be expected. The sensitivity of the next phases of ADMX to axion DM can  
953 be directly translated into sensitivity to  $A'$  DM (green regions labelled ADMX and ADMX-  
954 HF in the low- $\epsilon$  regime of Fig. 7). The sensitivity of these experiments is impressive, as  
955 a moderate coverage of the axion line in axion searches implies orders of magnitude in  $\epsilon$   
956 of pristine unexplored parameter space. The Yale search of 0.1 meV ALP DM [243] is a  
957 good example. With its sensitivity goal of  $g_{a\gamma\gamma} \sim \mathcal{O}(10^{-10})$  GeV $^{-1}$  it can barely surpass the  
958 strong astrophysical constraints on ALPs but its sensitivity to  $A'$ s is  $\chi \simeq 10^{-12}$ , two orders

959 of magnitude deep into unexplored territory.

960 The vast amount of parameter space to be explored has inspired new DM *broadband*  
961 experiments. The idea is avoid the time-consuming (and technology dependent) mode-  
962 tuning of resonant cavities and employ a dish antenna (which triggers  $A'$  DM conversion  
963 into light of frequency given by the  $A'$  mass) and a broadband receiver [244, 245]. With  
964 this setup one can study the 3-D momentum distribution of DM in the halo [244]. One can  
965 also search for axion/ALP DM by embedding it in a strong magnetic field parallel to the  
966 dish surface [244]. Currently there are no experiments of this type being planned but a few  
967 groups in Hamburg (DESY), CERN, and University of Zaragoza have expressed interest.

### 968 **3.4. Opportunities for Future Experiments: New Ideas, Technologies, & Ac-** 969 **celerators**

970 The physics motivations for dark photons, as outlined in §3.1, easily motivate extending  
971 searches far beyond the present generation of experiments. Large parts of the mass-coupling  
972 parameter space, shown in Fig. 6, will remain uncovered after the experiments at JLab and  
973 Mainz have run, and after data from the B- and  $\Phi$ -factories will have been fully analyzed. If  
974 something is found in the present generation of experiments, it will be incumbent on future  
975 experiments to confirm the findings, explore the detailed properties of the new particle, and  
976 to seek any cousins. That exercise will demand experiments with improved performance and  
977 reach. If nothing is found in the present searches, there remains a vast and viable region of  
978 parameter space to explore. Specific models for dark photons have been advanced, which  
979 populate the virgin territory, and general considerations from theory and phenomenology do  
980 so as well. So extending searches for dark photons throughout the whole of the parameter  
981 space is a high priority in either case.

982 Future experiments can improve upon coverage of the dark photon parameter space sig-  
983 nificantly. Future fixed target electro-production experiments and future  $e^+e^-$  colliding  
984 beam facilities can extend the search for visible dark photon decays, and future beam dump  
985 experiments, discussed below in §4, will extend the search for invisible decays, ultralight  
986 dark photons, and millicharged particles.

#### 987 **3.4.1. Future Fixed Target Experiments**

988 At fixed target machines, several generic improvements look possible which can expand  
989 the reach significantly. First, in HPS-like experiments, it should be possible to boost the

990 integrated luminosity by at least one order of magnitude by boosting the product of the  
991 current on target and the run time. Boosting the current on target will require tracking  
992 detectors that avoid the highest occupancy/radiation damage environments yet preserve  
993 most of the acceptance, or new pixellated and rad hard detectors that can tolerate the higher  
994 rates. Second, studies have shown that catching the recoil electron in addition to the  $A'$   
995 decay products, will boost the mass resolution by a factor  $\sim 2$ , and will reduce Bethe-Heitler  
996 backgrounds by as much as a factor of 2 to 3, improving the significance. Third, triggering  
997 on pions and muons can boost the sensitivity for  $A'$ s for masses beyond the dimuon mass  
998 by large factors where the  $\rho$  dominates the  $A'$  decays, and will help significantly for higher  
999 masses too. Fourth, using low- $Z$  nuclear targets and maximal beam energies improves the  
1000 reach in the 300 – 1000 MeV range too, since the radiative  $A'$  cross section increases with  
1001 higher beam energies and form-factor suppression will be mitigated by going to smaller,  
1002 lower- $Z$  nuclei. CEBAF12 at JLab will provide 12 GeV beams where these effects can boost  
1003 production by a factor of 5 or more. Fifth, since the sensitivity of bump hunt searches depend  
1004 inversely with the square root of the invariant mass resolution and directly with the square  
1005 root of the acceptance, and since vertex searches depend critically on the vertex resolution,  
1006 improving these parameters can lead to significant gains. It is not unreasonable to assume  
1007 a factor of 2 improvement in the acceptance and the mass resolution. The vertex resolution  
1008 can be improved by using thinner targets (with compensating higher currents), shorter  
1009 extrapolation distances from the first detector layer to the target, and thinner detectors,  
1010 yielding better impact parameter resolution. Taken together, future experiments may be  
1011 able to discriminate  $A'$  decays just a few mm from the target (vs 15 mm in the current  
1012 version of HPS). Finally, optimized analysis procedures and multivariate analyses may buy  
1013 factors of two improvement in sensitivity. An estimate [246] Snowmass of the reach of a  
1014 future experiment, which assumes a factor 4 improvement in mass resolution, a factor 2 in  
1015 vertex resolution, 30 times the luminosity, and higher energy running with particle ID, gives  
1016 Fig. 8. Note that this exercise exploits just one of the current approaches for fixed target  
1017 electroproduction.

1018 New approaches may be even more powerful [247]. While detailed performance estimates  
1019 for new experimental layouts are not yet available, several new ideas are being discussed  
1020 and the possibilities for improving the reach of dark photon searches significantly look very  
1021 real.

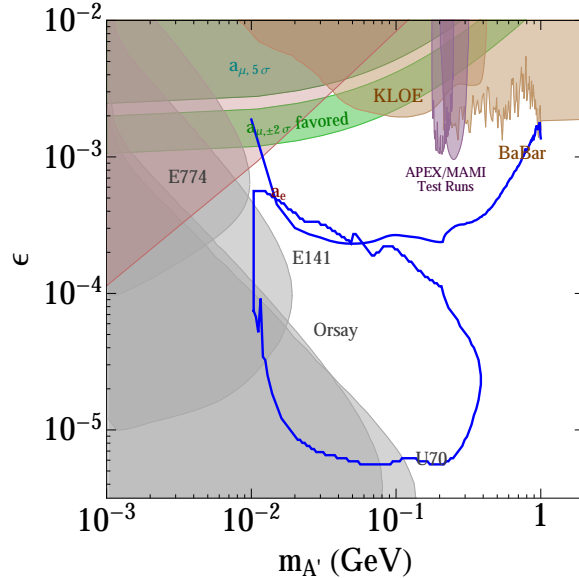


FIG. 8. Parameter space for hidden-photons ( $A'$ ) with mass  $m_{A'} > 1$  MeV (see Fig. 6 for present constraints and presently planned experiments), showing in blue a reach projection possible in a future HPS-style fixed target experiment. The projected reach here assumes a factor of two improvement in the vertex resolution, a factor of four improvement in mass resolution, a factor of 30 times more luminosity, and higher-energy running with improved particle ID.

### 3.4.2. Searches at Future $e^+e^-$ Colliding Beam Facilities

The  $e^+e^-$  colliding beam machines have conducted sensitive searches for dark photons over a wide range of masses. These searches, using existing data sets, are continuing. Since future facilities are already approved, it is comparatively straight-forward to extrapolate their performance for future searches. The coupling accessible by current datasets from  $e^+e^-$  colliders are at the level  $\epsilon^2 \sim 10^{-6} - 10^{-5}$  for dark photon masses below a few hundred MeV. This limitation comes essentially from the available statistics and thus the luminosity that can be delivered by the accelerators. The luminosity typically scales quadratically with their center of mass energy, basically compensating the inverse scaling of the relevant production cross-sections.

Current factories reach instantaneous luminosities of a few times  $10^{32}$  ( $10^{34}$ )  $\text{cm}^{-2}\text{s}^{-1}$  at 1 (10) GeV. Several next generation flavor factories have been proposed or are currently under construction. The upgraded KEK B-factory, SuperKEKB, is expected to start taking data in 2016 and should collect  $50 \text{ ab}^{-1}$  by 2022, about two orders of magnitude larger than the dataset collected by Belle. Several tau-charm factories operating between 2 – 5 GeV with instantaneous luminosities at the level of  $10^{35} - 10^{36} \text{ cm}^{-2}\text{s}^{-1}$  have been proposed, but

1038 remain to be funded at the time of this writing. Their expected sensitivity would roughly be  
 1039 at the level SuperKEKB should reach. At Frascati, KLOE-2 will install a new inner tracker,  
 1040 a cylindrical GEM detector, to improve the momentum resolution of charged particles while  
 1041 keeping the amount of material at a minimum. This approach will hopefully reduce the  
 1042 background from photon conversions produced in  $e^+e^- \rightarrow \gamma\gamma, \gamma \rightarrow e^+e^-$  events, allowing  
 1043 KLOE-2 to explore the very low mass region.

1044 An alternative approach has been proposed by the authors of [138], colliding a *single*  
 1045 intense positron beam on an internal target. Specifically, the VEPP-3 collaboration has  
 1046 proposed to use a 500 MeV positron beam of VEPP-3 on a hydrogen gas internal target.  
 1047 The search method is based on the study of the missing mass spectrum in the reaction  
 1048  $e^+e^- \rightarrow A'\gamma$ , which allows the observation of a dark photon independently of its decay  
 1049 modes and lifetime in the range  $m_{A'} = 5 - 20$  MeV, see Fig. 6.

1050 In summary, next generation flavor factories could probe values of the coupling  $\epsilon^2$  down  
 1051 to a level comparable to presently planned fixed target experiments for prompt decays, while  
 1052 extending their mass coverage to significantly higher masses. Should a signal be observed,  
 1053  $e^+e^-$  colliders will be ideally suited to investigate in detail the structure of a hidden sector,  
 1054 complementing dedicated experiments.

### 1055 3.4.3. Future Searches at the LHC

1056 The large datasets expected at the LHC in the near-term future ( $300 \text{ fb}^{-1}$  at 14 TeV) will  
 1057 contain billions of  $Z$  and millions of Higgs bosons, allowing branching ratios to lepton-jets  
 1058 as low as  $10^{-7}$  (or  $\epsilon \simeq 10^{-3}$ ) to be probed for  $Z$  decays and  $10^{-3}$  for Higgs decays. Strongly-  
 1059 produced SUSY particles with masses up to 1 (2.5) TeV are another potential source of  
 1060 lepton jets, if decays proceed through the hidden sector. In fact, the lepton jet signature  
 1061 could even be critical for their discovery. In the longer term with its very high luminosity  
 1062 option ( $3000 \text{ fb}^{-1}$ ), the LHC will allow ever more sensitive  $Z$  and Higgs decay searches, and  
 1063 extend the mass reach for SUSY production even higher.

## 1064 4. LIGHT DARK-SECTOR STATES (INCL. SUB-GEV DARK MATTER)

### 1065 4.1. Theory & Theory Motivation

1066 DM and neutrino mass provide strong empirical evidence for physics beyond the SM. Ar-  
 1067 guably, rather than suggesting any specific mass scale for new physics, they point to a hidden  
 1068 (or dark) sector, weakly-coupled to the SM. Dark sectors containing light stable degrees of

1069 freedom, with mass in the MeV-GeV range, are of particular interest as DM candidates as  
1070 this regime is poorly explored in comparison to the weak scale. Experiments at the intensity  
1071 frontier are ideally suited to explore this light dark-sector landscape, as discussed in this  
1072 section.

#### 1073 4.1.1. Light Dark Matter

1074 DM provides one of the strongest empirical motivations for new particle physics, with ev-  
1075 idence coming from various disparate sources in astrophysics and cosmology. While most  
1076 activity has focused on the possibility of weakly-interacting massive particles (WIMPs) with  
1077 a weak-scale mass, this is certainly not the only possibility. The lack of evidence for non-SM  
1078 physics at the weak scale from the LHC motivates a broader perspective on the physics of  
1079 DM, and new experimental strategies to detect its non-gravitational interactions are called  
1080 for. A wider theoretical view has also been motivated in recent years by anomalies in di-  
1081 rect and indirect detection [170, 248, 249], possible inconsistencies of the  $\Lambda$ CDM picture of  
1082 structure formation on galactic scales [250], and the advent of precision CMB tests of light  
1083 degrees of freedom during recombination.

1084 The mass range from the electron threshold  $\sim 0.5$  MeV up to multi-TeV characterizes the  
1085 favored range for DM candidates with non-negligible SM couplings (on the scale of terrestrial  
1086 particle physics experiments). The simple thermal relic framework, with abundance fixed  
1087 by freeze-out in the early Universe, allows DM in the MeV-GeV mass range if there are  
1088 light (dark-force) mediators which control the annihilation rate [251]. Related scenarios,  
1089 such as asymmetric DM, also require significant annihilation rates in the early Universe,  
1090 and thus light mediators are a rather robust prediction of models of MeV-GeV-scale DM  
1091 that achieves thermal equilibrium. Current direct detection experiments searching for elastic  
1092 nuclear recoils lose sensitivity rapidly once the mass drops below a few GeV, although several  
1093 ideas have been proposed to look for DM scattering off electrons or molecules [252, 253].  
1094 Experiments at the intensity frontier provide a natural alternative route to explore this light  
1095 MeV-GeV scale DM regime. Crucially, the light mediators required for DM annihilation to  
1096 the SM provide, by inversion, an accessible production channel for light DM that can be  
1097 exploited in high luminosity experiments.

1098 Models of sub-GeV DM are subject to a number of terrestrial and cosmological con-  
1099 straints, as discussed below. However, simple models interacting through one or more of the  
1100 portal couplings are viable over a large parameter range; e.g. an MeV-GeV mass complex  
1101 scalar charged under a massive dark photon can be thermal relic DM, with SM interactions



1102 mediated by the kinetic mixing portal.

### 1103 **4.1.2. Light Dark-Sector States**

1104 There is no compelling argument, beyond simplicity, for cold DM to be composed of a single  
1105 species, or even a small number of species. Light stable thermal relics require the presence  
1106 of additional light mediators as discussed above, and the dark sector may be quite complex.  
1107 Indeed, the annihilation channels required for (thermalized) DM in the early Universe could  
1108 occur within the dark sector itself if there are additional light states, subject to constraints  
1109 from cosmology on the number of relativistic degrees of freedom. Since SM neutrinos do  
1110 contribute a (highly sub-dominant) fraction of hot DM, we already know that in the broadest  
1111 sense DM must be comprised of multiple components. Thus care is required to assess the  
1112 experimental sensitivity according to the underlying assumptions about the stability of the  
1113 dark sector state in cosmological scales, and whether or not stable dark sector states under  
1114 study comprise some or all of DM.

### 1115 **4.1.3. Millicharged Particles**

1116 Particles with small un-quantized electric charge, often called mini- or milli-charged particles  
1117 (MCPs), also arise naturally in many extensions of the SM. MCPs are a natural consequence  
1118 of extra  $U(1)$ s and the kinetic mixing discussed in §3.1 for massless  $A'$  fields. In this case,  
1119 any matter charged (solely) under the hidden  $U(1)$  obtains a small electric charge. MCPs  
1120 can also arise in extra-dimensional scenarios or as hidden magnetic monopoles receiving  
1121 their mass from a magnetic mixing effect [254–256]. Milli-charged fermions are particularly  
1122 attractive because chiral symmetry protects their mass against quantum corrections, making  
1123 it more natural to have small or even vanishing masses. MCPs have also been suggested as  
1124 DM candidates [257–259].

1125 Terrestrial experiments as well as astrophysical and cosmological observations provide  
1126 interesting bounds on MCPs. These limits, in addition to comments on future prospects,  
1127 are summarized in §4.2.2.

## 1128 **4.2. Phenomenological Motivation and Current Constraints**

### 1129 **4.2.1. Constraints on Light Dark Matter and Dark Sectors**

1130 A variety of terrestrial, astrophysical and cosmological constraints exist on light DM and  
1131 dark sector states, which we now summarize. We focus on the scenario with dark sector

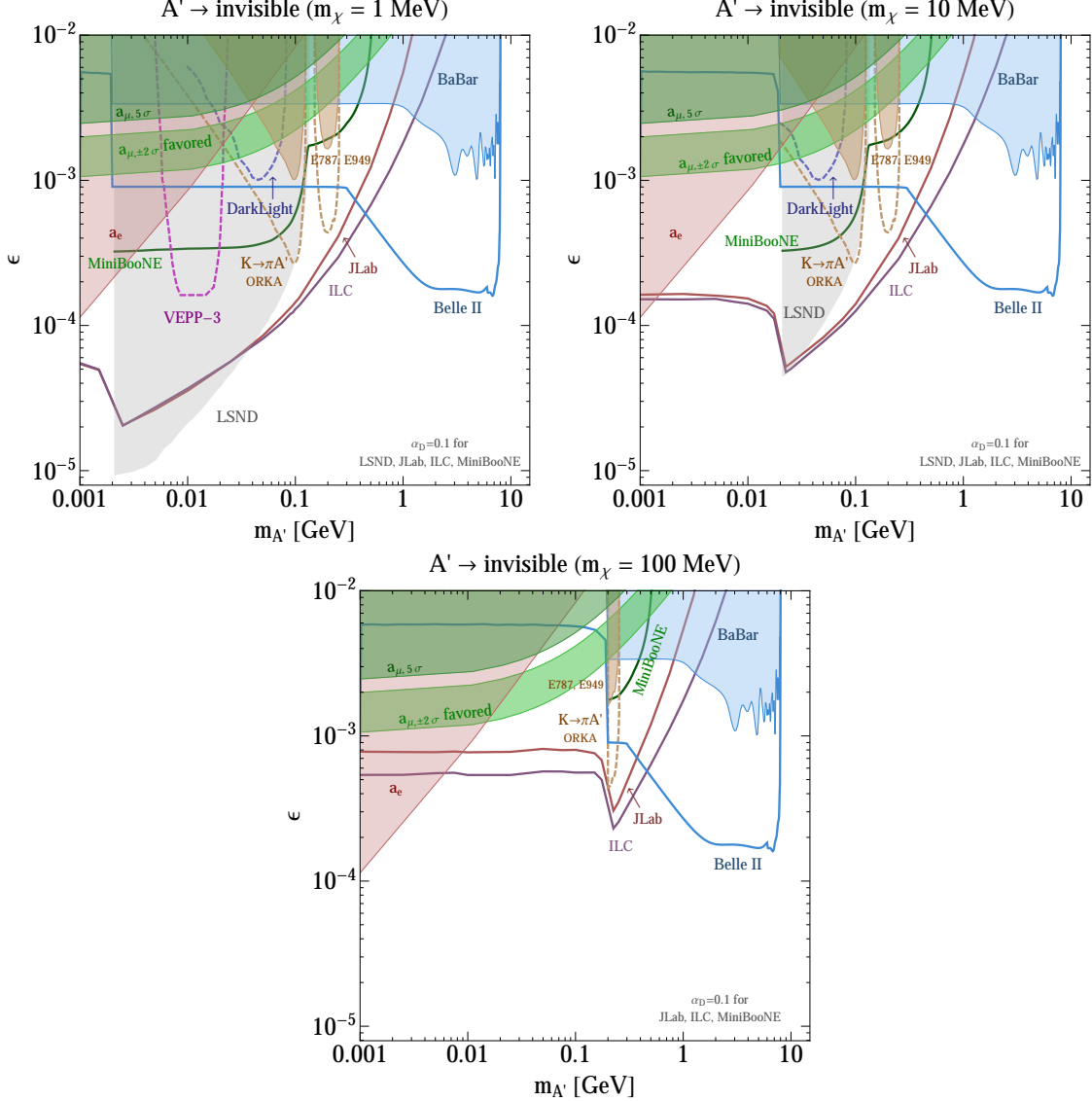


FIG. 9. Parameter space for dark photons decaying invisibly to dark-sector states  $\chi$  for various  $m_\chi$ . Constraints from precision QED tests of  $\alpha$  (red) and the muon anomalous magnetic moment (green) [123] are independent of the  $A'$  decay mode (these are the same as in Fig. 6). Constraints from (on-shell)  $A'$  decays to *any* invisible final state arise from the measured  $K^+ \rightarrow \pi^+ \nu \bar{\nu}$  branching ratio [123, 225, 260] (brown) and from a *BABAR* mono-photon search [261–263] (blue); significant improvements are possible with DarkLight [265] (dark blue dashed), VEPP-3 [137, 138] (magenta dashed), ORKA [262] (brown dashed), and BELLE II [262] (light blue solid). If the  $\chi$  are long-lived/stable and can re-scatter in a downstream detector, constraints arise also from LSND (gray) for  $m'_A < m_{\pi^0}$ ,  $m_\chi < m'_A/2$  [264]. Additional parameter space can then also be probed at existing/future proton beam-dump facilities like Project X, LSND etc., (the solid dark green line shows a proposed MiniBooNE beam-off-target-run [225]), and at electron-beam dumps at JLab (dark red), the ILC (purple), and other facilities like SLAC, SuperKEKB etc. (not shown) [263].

1132 states  $\chi$  (including DM) interacting with the SM through a dark photon, emphasizing the  
 1133 assumptions going into each limit. For example, the limits depend on the dark photon and  
 1134 light DM mass. We also note that generalizations to beyond the kinetic mixing portal,  
 1135 including for example leptophilic DM, can drastically alter the limits. The limits on dark  
 1136 photons that couple to light DM, along with prospects for various future experiments to be  
 1137 discussed below, are displayed in Fig. 9.

1138 Several constraints are common to both visibly (see §3) and invisibly decaying dark  
 1139 photons. In particular, precision QED measurements [123] and precision tests of the fine-  
 1140 structure constant  $\alpha$  (including the electron anomalous magnetic moment) constrain the  
 1141 kinetic mixing parameter  $\epsilon \lesssim 10^{-4}$  ( $10^{-2}$ ) for a dark photon mass  $m_{A'} \sim 1$  MeV (100 MeV).  
 1142 The muon anomalous magnetic moment provides a stronger constraint for heavier dark  
 1143 photons, with  $\epsilon \lesssim \text{few} \times 10^{-3}$  ( $10^{-2}$ ) for  $m_{A'} \sim 50$  MeV (300 MeV). Furthermore, model-  
 1144 independent constraints from the measurements of the  $Z$ -boson mass, precision electroweak  
 1145 observables, and  $e^+e^-$  reactions at a variety of c.o.m. energies constrain  $\epsilon \lesssim 3 \times 10^{-2}$   
 1146 independent of  $m_{A'}$  [266] (not shown).

1147 The next class of constraints relevant to this scenario relies on the assumption that the  
 1148 dark photon decays invisibly (but not necessarily to stable states like DM). Measurements  
 1149 of the  $K^+ \rightarrow \pi^+\nu\bar{\nu}$  branching ratio [260] place limits on  $\epsilon$  in the range  $10^{-2} - 10^{-3}$  if  
 1150 the decay  $K^+ \rightarrow \pi^+A'$  is kinematically allowed. Strong constraints on  $\epsilon$  exist in a narrow  
 1151 region  $m_{A'} \sim m_{J/\psi}$ , in which case the the decay  $J/\psi \rightarrow \text{invisible}$  is resonantly enhanced.  
 1152 Furthermore, a limit on the branching fraction  $\Upsilon(3S) \rightarrow \gamma + A^0$ ,  $A^0 \rightarrow \text{invisible}$  (with  $A^0$  a  
 1153 scalar [261]) can be recast as a limit on the continuum process  $e^+e^- \rightarrow \gamma A'$ ,  $A' \rightarrow \text{invisible}$ ,  
 1154 leading to  $\epsilon \lesssim \text{few} \times 10^{-3}$  [262, 263].

1155 If the dark sector states  $\chi$  are stable (e.g., if  $\chi$  is the DM), or at least metastable with  
 1156 lifetimes of  $O(100 \text{ m})$ , then proton- and electron-beam fixed target experiments are sensitive  
 1157 to the scattering of  $\chi$  with electrons or nuclei, with a rate that depends on  $\alpha_D$ . The LSND  
 1158 measurement of the electron-neutrino elastic scattering cross section [267] places a limit in  
 1159 the range  $\epsilon \lesssim 10^{-5} - 10^{-3}$  for  $\alpha_D = 0.1$ ,  $m'_A < m_{\pi^0}$ ,  $m_\chi < m'_A/2$  [264]. Furthermore,  
 1160 the SLAC MilliQ search for milli-charged particles [268] is sensitive to  $A'$ 's heavier than  $\pi^0$ ,  
 1161 and constrains values of  $\epsilon$  as low as  $10^{-3}$  [269] (not shown). Constraints from the SLAC  
 1162 beam-dump experiment E137 are also applicable [270] (not shown).

1163 Direct detection experiments can probe light DM  $\chi$  in the halo through its scattering with  
 1164 electrons [252, 253]. An analysis of the XENON10 dataset has placed limits on the  $\chi$ -electron  
 1165 scattering cross section  $\sigma_e < 10^{-37} \text{ cm}^2$  for  $\chi$  masses in the range 20 MeV - 1 GeV [253],

1166 and more recent direct detection experiments as well as dedicated future experiments could  
 1167 probe significant new parameter space.

1168 Late-time DM annihilation to charged particles can distort the CMB. Assuming  $\chi$  satu-  
 1169 rates the observed relic density and annihilates through an  $s$ -wave reaction, then the CMB es-  
 1170 sentially rules out this scenario [186–189]. These bounds are, however, model-dependent and  
 1171 may be avoided in several ways, for example: 1)  $\chi$  may annihilate through a  $p$ -wave process,  
 1172 e.g. scalar DM annihilating through an  $s$ -channel dark photon to SM fermion pairs [264], 2)  
 1173 the dark sector may contain new light states, opening up new annihilation modes for  $\chi$ , which  
 1174 do not end with electromagnetic final states, 3) the DM may be matter-asymmetric [271],  
 1175 and 4)  $\chi$  may comprise a sub-dominant component of the DM.

#### 1176 4.2.2. Additional constraints on Millicharged Particles

1177 Several portions of the charge-vs-mass ( $Q$ -vs- $m_{\text{MCP}}$ ) parameter space for MCPs can be  
 1178 excluded based upon available experimental results. Some of these bounds, e.g. direct mea-  
 1179 surements, rely on relatively few assumptions, while others are dependent on the accuracy  
 1180 of astrophysical and cosmological models. Fig. 10 illustrates the parameter space for MCPs  
 1181 and a brief summary of the most stringent bounds follows.

1182 Direct measurements cover large parts of the parameter space of MCPs for  $Q \sim e$ . The  
 1183 SLAC ASP (Anomalous Single Photon) search for  $e^+e^- \rightarrow \gamma X$  final states, where  $X$  is any  
 1184 weakly interacting particle, set a bound of  $Q > 0.08e$  for  $m_{\text{MCP}} \lesssim 10$  GeV [272, 273]. Data  
 1185 from a proton beam dump experiment, E613, at Fermilab excludes charges between  $10^{-1}e$   
 1186 and  $10^{-2}e$  for  $m_{\text{MCP}} < 200$  MeV [274]. A SLAC electron beam dump experiment looking  
 1187 for trident production  $e^- N \rightarrow e^- N Q^+ Q^-$  set a bound of  $Q > 0.03e$  for  $m_{\text{MCP}} < 1$  GeV  
 1188 [272]. Moreover, the SLAC MilliQ experiment set a bound of  $5.8 \times 10^{-4}e$  for  $m_{\text{MCP}} < 100$   
 1189 MeV [268]. In addition to these accelerator-based experiments, the results of a search for  
 1190 orthopositronium decays into invisible particles can be recast into bounds on MCPs. This  
 1191 measurement gives a bound of  $Q < 8.6 \times 10^{-5}e$  for  $m_{\text{MCP}} < 500$  keV [275]. Finally, the  
 1192 precise agreement between the measured and calculated values for the Lamb shift can be  
 1193 used to set a bound of  $Q < (1/9)e m_{\text{MCP}}$  for  $M \gtrsim 3$  keV [272, 276].

1194 Additional constraints can be placed on MCPs from indirect cosmology and astrophysics  
 1195 results (See [272] and references therein). Photons travelling in a plasma acquire an effective  
 1196 mass and can decay into MCPs. Therefore MCPs produced inside stars can contribute to  
 1197 their cooling. White dwarf and red giant stars bound MCPs for  $m_{\text{MCP}} \lesssim$  keV by requiring  
 1198 that the MCP production rate not exceed the rate of nuclear energy production.

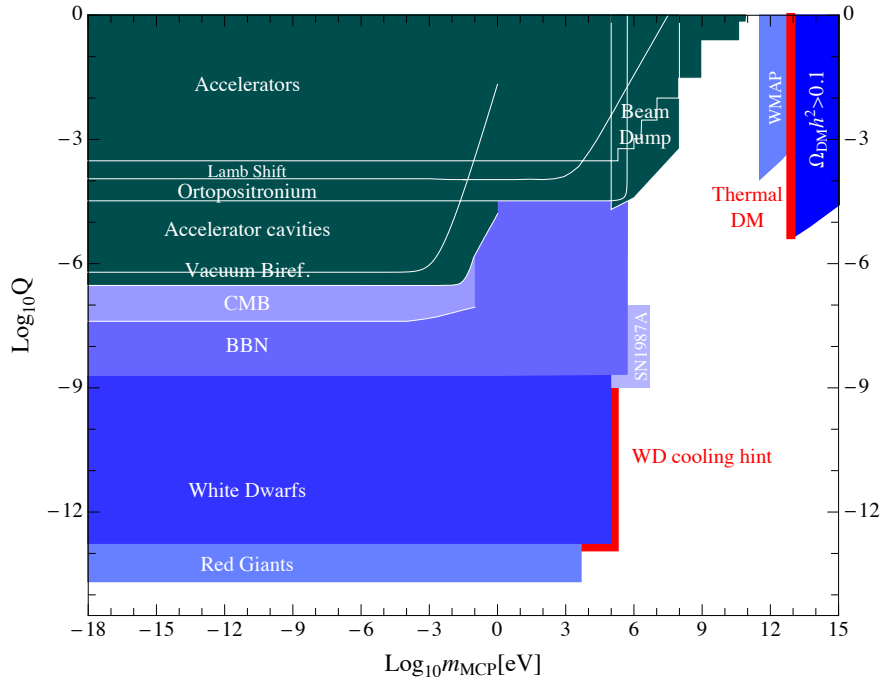


FIG. 10. Bounds on the millicharge  $Q$  vs mass  $m_{\text{MCP}}$  from astrophysics and various experiments.

1199 Constraints from cosmology include bounds from BBN on the effective relativistic degrees  
 1200 of freedom. CMB data from WMAP is also an indirect test ground for new invisible states  
 1201 that inject charged particles into the CMB. In addition, requiring that the MCPs relic density  
 1202 not over-close the Universe excludes  $m_{\text{MCP}} \sim \text{TeV}$  for  $Q \sim e$ . For sub-eV masses, light-  
 1203 shining-through-wall-type setups can even go below some cosmological constraints [277, 278].

1204 New electron and proton beam dump experiments, planned or proposed to search for  
 1205 light DM, could also cover new parameters space of MCPs, particularly the  $m_{\text{MCP}} \sim \text{GeV}$   
 1206 region. The primary modes of production are  $pN \rightarrow pNQ^+Q^-$  or  $pp \rightarrow Q^+Q^-$  at proton  
 1207 beam dump experiments, and  $e^-N \rightarrow e^-NQ^+Q^-$  at electron beam dump experiments.  
 1208 MCPs produced at the beam dump would then travel and scatter elastically off of nuclei at  
 1209 a detector situated downstream of the target and able to look for neutral current scattering  
 1210 events. The detection of MCPs relies on an experiment sensitive to low momentum recoil  
 1212 channels, such as electron recoils and/or coherent nuclear scattering, see §4.3.3.

### 1213 4.3. Proposed and Future Searches

#### 1214 4.3.1. Proton-fixed Target

1215 Proton-beam fixed target-detector setups have significant potential to search for light DM  
1216 and other long-lived dark sector states. An intense source of dark sector states can be pro-  
1217 duced in the primary proton-target collisions and detected through their scattering [156, 264,  
1218 279] or visible decays [116, 156] in a near detector. Of particular importance to this experi-  
1219 mental program are the existing and future Fermilab neutrino factories such as MiniBooNE,  
1220 MINOS, NO $\nu$ A, MicroBooNE, and LBNE, which have an unprecedented opportunity to  
1221 search for light DM. The studies in [156, 264, 279] demonstrate the existence of a large  
1222 DM signal in existing neutrino experiments for motivated regions of DM parameter space.  
1223 However, numerous experimental challenges remain to maximize the sensitivity to the DM  
1224 signal, foremost among them competing with the large neutrino neutral current background.

1225 A proposal for a dedicated search for light DM at MiniBooNE is described in [225].  
1226 DM particles  $\chi$ , interacting with the SM through a kinetically mixed dark photon, can  
1227 be produced through the decays of secondary pseudoscalar mesons,  $\pi^0, \eta \rightarrow \gamma A', A' \rightarrow$   
1228  $\chi\chi^*$ . Such DM particles can travel to the detector and scatter via  $A'$  exchange, leaving the  
1229 signature of a recoiling electron or nucleon. The MiniBooNE sensitivities to DM masses  
1230 of 1, 10, 100 MeV are represented by the green contours in Fig. 9. MiniBooNE can probe  
1231 motivated regions of DM parameter space in which the relic density is saturated and the  
1232 muon anomalous magnetic moment discrepancy is explained. The signal significance for  
1233 several operational modes is can be found in [225].

1234 In order to mitigate the neutrino background, [225] proposed to run in a beam-off target  
1235 configuration, in which the protons are steered past the target and onto either 1) the perma-  
1236 nent iron absorber located at the end of the 50 m decay volume, or 2) a deployed absorber  
1237 positioned 25 m from the target. A one week test run in the 50 m absorber configuration  
1238 measured a reduction of the neutrino flux by a factor of 42. Additional improvements in  
1239 distinguishing  $\chi$  signal from the neutrino background are possible by exploiting the fine  
1240 ns-level timing resolution between the detector and proton spill, since heavy  $O(100 \text{ MeV})$   
1241 DM particles will scatter out of time.

1242 The experimental approach to search for light DM employed by MiniBooNE is applicable  
1243 to other neutrino experiments and intense proton sources, such as MINOS, NO $\nu$ A, Micro-  
1244 BooNE, LBNE, and Project X. For instance, the MicroBooNE LAr detector can also perform  
1245 a search with comparable sensitivity to that outlined for MiniBooNE with a long enough

1246 beam-off-target run. More generally, the DM mass range that can be covered is governed by  
1247 the proton beam energy and the production mechanism, as well as the ability to overcome  
1248 the neutrino neutral current background. For instance with the FNAL Booster (8.9 GeV)  
1249 and Main Injector (120 GeV) as well as a future Project X, the accessible DM mass range is  
1250 a few MeV to a few GeV. Both LBNE [280] and Project X [281] have considered light DM  
1251 searches to expand the physics reach and help motivate the projects.

1252 The search for light DM provides an additional physics motivation for intense proton  
1253 beam facilities. Given the significant investment in existing and future infrastructure for  
1254 neutrino experiments, it is critical to take advantage of the unique opportunity afforded by  
1255 these experiments to probe the non-gravitational interactions of light DM and more generally  
1256 explore the possibility of of a dark sector with new, light, weakly-coupled states.

### 1257 **4.3.2. B-factories**

1258 B-factories like *BABAR* and Belle and future super-B factories like Belle 2 are powerful probes  
1259 of light DM with a light mediator. An existing mono-photon search by *BABAR* [261] already  
1260 places important constraints on this class of models [262, 263] (see also [140, 149, 282]), and  
1261 similar search at a future B-factory can probe significantly more parameter space [262].  
1262 Such searches are more powerful than searches at other collider or fixed-target facilities  
1263 for mediator and hidden-sector particle masses between a few hundred MeV to 10 GeV.  
1264 Mediators produced on-shell and decaying invisibly to hidden-sector particles such as DM can  
1265 be probed particularly well. Sensitivity to light DM produced through an off-shell mediator  
1266 is more limited, but may be improved with a better theoretical control of backgrounds,  
1267 allowing background subtraction and a search for kinematic edges. The implementation of  
1268 a mono-photon trigger at Belle II would be a necessary step towards providing this crucial  
1269 window into such light dark sectors.

### 1270 **4.3.3. Electron fixed target**

1271 Electron beam fixed target experiments enable powerful low-background searches for new  
1272 light weakly-coupled particles and can operate parasitically at several existing facilities  
1273 [263]. Electron-nucleus collisions feature a light dark-sector particle production rate com-  
1274 parable to that of neutrino factories, but the production mechanism is analogous to QED  
1275 bremsstrahlung. Importantly, beam related neutrino and neutron backgrounds are negligi-  
1276 ble. Electron beam production also features especially forward-peaked particle kinematics,

1277 so for multi-GeV beam energies, experimental baselines on a 10 m scale, and 1 m-scale detec-  
1278 tors, the signal acceptance is of order one for sub-GeV DM masses. This approach is sensitive  
1279 to any new physics that couples to leptonic currents and is limited only by cosmogenic back-  
1280 grounds, which are both beatable and systematically reducible; even a test implementation  
1281 with no cosmogenic neutron reduction offers sensitivity to well motivated regions of param-  
1282 eter space. Previous generations of electron beam experiments, such as the MilliQ or E137  
1283 experiment at SLAC have already demonstrated sensitivity to light DM [269, 270].

1284 The minimal setup requires a  $\mathcal{O}(\text{m}^3)$  fiducial volume (or smaller) detector sensitive to  
1285 neutral current scattering placed 10s of meters downstream of an existing electron beam  
1286 dump. At low momentum transfers, DM scattering predominantly yields elastic electron  
1287 and coherent nuclear recoils in the detector. At higher momentum transfers, inelastic hadro-  
1288 production and quasi-elastic nucleon ejection dominate the signal yield. The approach offers  
1289 comparable sensitivity using either continuous wave (CW) or pulsed electron beams, but  
1290 CW sensitivity is limited by cosmogenic background so background reduction strategies are  
1291 required to achieve optimal sensitivity; for pulsed beams, timing cuts render cosmogenic  
1292 backgrounds negligible. This approach can be realized parasitically at several existing elec-  
1293 tron fixed target facilities including SLAC, JLab, and Mainz. It may also be possible to  
1294 utilize pulsed beams at the SuperKEK linac beam and (in the future) at the ILC.

1295 Fig. 9 shows the sensitivity projections for a  $1 \text{ m}^3$  detector placed 20 m downstream of  
1296 an Aluminum beam dump. Two lines are shown, giving the 10-event sensitivity per  $5 \times 10^{22}$   
1297 electrons-on-target, for a hypothetical experiment at JLab using a 12 GeV beam (red) and at  
1298 ILC using a 125 GeV beam (purple). Excellent sensitivity is obtained for light dark photon  
1299 and light dark-matter masses.

## 1300 5. CHAMELEONS

### 1301 5.1. Theory & Motivation

1302 Cosmological observations are able to pinpoint with great precision details of the Universe  
1303 on the largest scales, while particle physics experiments probe the nature of matter on the  
1304 very smallest scales with equally astounding precision. However, these observations have left  
1305 us with some of the greatest unsolved problems of our time, most notably the remarkable  
1306 realisation that the most dominant contribution to the energy density of our Universe is also  
1307 the least well understood. Dark energy, credited with the observed accelerated expansion  
1308 of the Universe, makes up around 70% of the total matter budget in the Universe however



1309 there is no single convincing explanation for this observation nor is there a clear pathway to  
1310 distinguishing between different models through cosmological observations. If this accelera-  
1311 tion is not caused by a cosmological constant then the most convincing explanations come  
1312 in the form of scalar field models that are phenomenological but with the hope of being  
1313 effective field theories of ultra-violet physics. If a scalar field is indeed responsible for this  
1314 observed acceleration it would need to be very light  $m \sim H_0$  and evolving still today. These  
1315 light fields should couple to all forms of matter with a coupling constant set by  $G_N$ . A  
1316 coupling of this kind would cause an as yet unobserved fifth force and should be observable  
1317 in a plethora of settings from the early Universe through big bang nucleosynthesis, structure  
1318 formation and in all tests of gravity done today. Thus, we are left with a puzzle as to how  
1319 a scalar field can both be observable as dark energy and yet not be observed to date in all  
1320 other contexts.

1321

1322 A solution to this puzzle was presented in [283–285] with so-called chameleon fields.  
1323 Chameleon fields are a compelling dark energy candidate, as they couple to all SM particles  
1324 without violating any known laws or experiments of physics. Importantly, these fields are  
1325 testable in ways entirely complementary to the standard observational cosmology techniques,  
1326 and thus provide a new window into dark energy through an array of possible laboratory  
1327 and astrophysical tests and space tests of gravity. Such a coupling, if detected, could reveal  
1328 the nature of dark energy and may help lead the way to the development of a quantum  
1329 theory of gravity.

1330

1331 A canonical scalar field is the simplest dynamical extension of the SM that could ex-  
1332 plain dark energy. In the absence of a self interaction, this field’s couplings to matter —  
1333 which we would expect to exist unless a forbidden by some symmetry — would lead to a  
1334 new, fifth fundamental force whose effects have yet to be observed. However, scalar field  
1335 dark energy models typically require a self interaction, resulting in a nonlinear equation  
1336 of motion [286, 287]. Such a self interaction, in conjunction with a matter coupling, gives  
1337 the scalar field a large effective mass in regions of high matter density [283, 284]. A scalar  
1338 field that is massive locally mediates a short-range fifth force that is difficult to detect,  
1339 earning it the name “chameleon field.” Furthermore, the massive chameleon field is sourced  
1340 only by the thin shell of matter on the outer surface of a dense extended object. These  
1341 nonlinear effects serve to screen fifth forces, making them more difficult to detect in certain  
1342 environments.

1344 Current best theories treat chameleon dark energy as an effective field theory [285, 288]  
 1345 describing new particles and forces that might be seen in upcoming experiments, and whose  
 1346 detection would point the way to a more fundamental theory. The ultraviolet (UV) behav-  
 1347 ior of such theories and their connection to fundamental physics are not yet understood,  
 1348 although progress is being made [289–292].

1349 A chameleon field couples to DM and all matter types, in principle with independent  
 1350 strengths. At the classical level, a chameleon field is not required to couple to photons,  
 1351 though such a coupling is not forbidden. However, when quantum corrections are included,  
 1352 a photon coupling about three orders of magnitude smaller than the matter coupling is typi-  
 1353 cally generated [293]. The lowest order chameleon-photon interaction couples the chameleon  
 1354 field to the square of the photon field strength tensor, implying that in a background elec-  
 1355 tromagnetic field, photons and chameleon particles can interconvert through oscillations.  
 1356 The mass of chameleon fields produced will depend on the environmental energy density  
 1357 as well as the electromagnetic field strength. This opens the vista to an array of different  
 1358 tests for these fields on Earth, in space, and through astrophysical observations. Several  
 1359 astrophysical puzzles could also be explained by chameleons, *e.g.*, [294]. Their coupling  
 1360 to photons, combined with their light masses in certain environments, allows chameleons  
 1361 to be produced with intense beams of photons, electrons, or protons and detected with  
 1362 sensitive equipment. This makes them, by definition, targets for the intensity frontier. In  
 1363 fact chameleon particles are a natural bridge between the cosmic frontier and the intensity  
 1364 frontier; not only do they hold the possibility of being a dark energy candidate but they are  
 1365 testable through astrophysical and laboratory means.

1366

1367 The chameleon dark energy parameter space is considerably more complicated than that  
 1368 of axions, but constraints can be provided under some assumptions. With the caveat that all  
 1369 matter couplings are the same but not equal to the photon coupling, and the assumption of  
 1370 a specific chameleon potential,  $V(\phi) = M_\Lambda^4(1 + M_\Lambda^n/\phi^n)$  in which we set the scale  $M_\Lambda = 2.4 \times$   
 1371  $10^{-3}$  eV to the observed dark energy density and, for concreteness,  $n = 1$ , our constraints  
 1372 and forecasts are provided by Fig. 11. Current constraints (solid regions) and forecasts  
 1373 (curves) are discussed below.

## 1374 5.2. Current laboratory constraints

1375 Laboratory constraints on chameleon dark energy come from two different types of exper-  
1376 iments: fifth force searches, and photon coupling experiments, both of which are shown  
1377 as shaded regions in Figure 11. Gravitation-strength fifth forces can be measured directly  
1378 between two macroscopic objects, such as the source and test masses in a torsion pendulum.  
1379 Currently the shortest-range torsion pendulum constraints on gravitation-strength forces  
1380 come from the Eöt-Wash experiment [295]. The source and test masses in Eöt-Wash are  
1381 parallel metal disks a few centimeters in diameter with matched sets of surface features. As  
1382 the lower disk is rotated, gravity and any fifth forces induce torques in the upper disk so as to  
1383 align the surface features. The separation between the disks can be varied, and the torsional  
1384 oscillations in the upper disk can be compared with predictions. Another type of fifth force  
1385 experiment uses an ultracold gas of neutrons whose bouncing states in the gravitational field  
1386 of the Earth are quantized, with energy splittings  $\sim 1$  peV [296]. If the neutrons feel a fifth  
1387 force from the experimental apparatus comparable to the gravitational force of the Earth,  
1388 then the energy splittings will be altered. The Grenoble experiment measures these energy  
1389 splittings at the  $\sim 10\%$  level, excluding very strong matter couplings  $\beta_m \gtrsim 10^{11}$ .

1390 Dark energy may couple to the electroweak sector in addition to matter. Such a cou-  
1391 pling would allow photons propagating through a magnetic field to oscillate into particles of  
1392 dark energy, which can then be trapped inside a chamber if the dark energy effective mass  
1393 becomes large in the chamber walls. An “afterglow experiment” produces dark energy par-  
1394 ticles through oscillation and then switches off the photon source, allowing the population  
1395 of trapped dark energy particles to regenerate photons which may emerge from the chamber  
1396 as an afterglow. Current afterglow constraints from the CHASE experiment [297] exclude  
1397 photon couplings  $10^{11} \lesssim \beta_\gamma \lesssim 10^{16}$  for  $\beta_m \gtrsim 10^4$ , as shown in Fig. 11 for an inverse-power-  
1398 law chameleon potential [297–299]. At yet higher photon couplings the trapped dark energy  
1399 particles regenerate photons too quickly for CHASE to detect them. However, collider ex-  
1400 periments can exclude such models, by constraining chameleon loop corrections to precision  
1401 electroweak observables [300].

## 1402 5.3. Forecasts for Terrestrial experiments

1403 Proposed experiments promise to improve constraints on chameleon dark energy by orders  
1404 of magnitude over the next several years. Fig. 11 summarizes forecasts and preliminary  
1405 constraints, shown as solid lines. The next-generation Eöt-Wash experiment, currently under

Experiment	Type	Couplings excluded
Eöt-Wash	torsion pendulum	$0.01 \lesssim \beta \lesssim 10$
Lamoreaux	Casimir	$\beta \gtrsim 10^5$ ( $\phi^4$ )
Grenoble	bouncing neutron	$\beta \gtrsim 10^{11}$
GRANIT	bouncing neutron	forecast: $\beta \gtrsim 10^8$
NIST	neutron interferometry	forecast: $\beta \gtrsim 10^7$
CHASE	afterglow	$10^{11} \lesssim \beta_\gamma \lesssim 10^{16}$ subject to $10^4 \lesssim \beta_m \lesssim 10^{13}$ ,
ADMX	microwave cavity	$m_{\text{eff}} = 1.952 \mu\text{eV}$ , $10^9 \lesssim \beta_\gamma \lesssim 10^{15}$
CAST	helioscope	forecast: $\beta_m \lesssim 10^9$ , $\beta_\gamma > 10^{10}$

TABLE I. Laboratory tests of dark energy. Approximate constraints on chameleon models with potential  $V(\phi) = M_\Lambda^4(1 + M_\Lambda/\phi)$  and  $M_\Lambda = 2.4 \times 10^{-3}$  eV (unless otherwise noted).

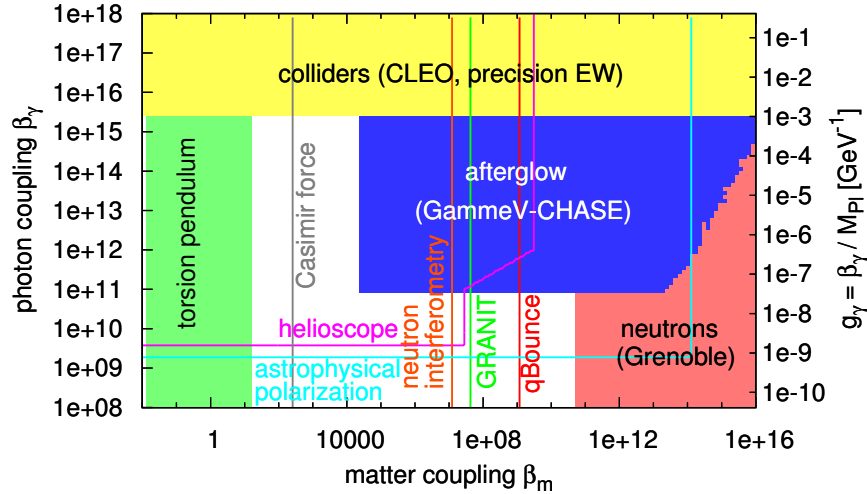


FIG. 11. Constraints on the matter and photons couplings for a chameleon dark energy model with  $V(\phi) = M_\Lambda^4(1 + M_\Lambda/\phi)$ . Current constraints are shown as shaded regions, while forecasts are shown as solid lines.

1406 way, will have an increased force sensitivity and probe smaller distances. This will allow  
1407 it to detect or exclude a large class of chameleon models with well-controlled quantum  
1408 corrections [301, 302]. Improvements to fifth force measurements using neutrons should  
1409 improve constraints on the chameleon-matter coupling considerably. Also proposed is a  
1410 neutron interferometry experiment at NIST, which should be competitive with the bouncing  
1411 neutron experiments. A neutron interferometer splits a neutron beam and sends the two

1412 through two different chambers, one containing a dense gas which suppresses chameleon  
1413 field perturbations, and the other a vacuum chamber in which scalar field gradients are  
1414 large. These gradients will retard the neutron beam passing through the vacuum chamber,  
1415 resulting in a phase shift which varies nonlinearly with the gas pressure. Potentially more  
1416 powerful are the next-generation Casimir force experiments [303]. However, these currently  
1417 suffer from systematic uncertainties including the proper calculation of thermal corrections  
1418 to the Casimir effect. The forecasts shown require that the total uncertainty in the Casimir  
1419 force be reduced below 1% at distances of  $5 - 10 \mu\text{m}$ .

1420 Other planned experiments search for photon-coupled chameleons. Afterglow experiments  
1421 have been proposed at JLab and the Tore Supra tokamak, while a microwave cavity-based  
1422 afterglow experiment is under way at Yale. Since forecasts for these experiments are not  
1423 available for the chameleon potential assumed in Fig. 11, we are unable to include them in  
1424 the figure. However, the JLab and Tore Supra experiments are expected to fill in some of the  
1425 gap between CHASE and torsion pendulum experiments, while the microwave cavity search  
1426 is a precision experiment capable of targeting a model with a specific mass in response to  
1427 hints from an afterglow experiment. Yet another type of experiment is the helioscope, which  
1428 uses a high magnetic field to regenerate photons from scalar particles produced in the Sun  
1429 [304]. Since such particles do not need to be trapped prior to detection, helioscope forecasts  
1430 extend down to arbitrarily low matter couplings. One proposed helioscope adds an X-ray  
1431 mirror to the CAST axion helioscope at CERN in order to increase its chameleon collecting  
1432 area; forecasts for this experiment are shown.

#### 1433 **5.4. Tests of the Chameleon Mechanism by Astrophysical Observation**

1434 Complimentary to detector based experiments, chameleons offer a rich phenomenology of  
1435 unique astrophysical signatures. Combining data from astrophysical observations with lab-  
1436 oratory experimental data will allow us to constrain chameleon models. Below we review  
1437 some of the more intriguing astrophysical signatures predicted in chameleon models. One  
1438 benefit of observational tests of chameleons is that these observations may be performed  
1439 complementarily with observations taken for reasons not related to chameleon gravity. Or-  
1440 dinary matter interacting via a low mass particle ( $m \sim H_0$ ) leading to a new fifth force  
1441 typically requires a very small coupling. Bounds on any additional fifth force have been set  
1442 by measuring the frequency shift of photons passing near the Sun from the Cassini satellite  
1443 on their way to Earth [305].

1444 The screening mechanism from chameleons has significant consequences for the forma-  
 1445 tion of structure. These modifications to structure formation include an earlier collapse  
 1446 of density perturbations compared to the prediction from  $\Lambda$ CDM and clumpier DM halos  
 1447 [306]. Another effect on structure formation in chameleon gravity is that the critical density  
 1448 required for collapse depends on the comoving size of the inhomogeneity itself [307]. Also,  
 1449 galactic satellite orbits become modified based on the size of the satellite itself due to a  
 1450 backreaction from the satellite causing a velocity difference of up to 10% near the thin shell  
 1451 [308].

1452 Due to the existence of the two-photon vertex ( $\mathcal{L}_{\phi\leftrightarrow\gamma} = F^{\mu\nu}F_{\mu\nu}\phi/4M$ ), chameleons mix  
 1453 with photons in the presence of a background magnetic field. This mixing is the result of the  
 1454 propagation eigenstates being different from the photon polarization-chameleon eigenstates.  
 1455 The result of this mixing is a non-conservation of photons. In the case of type Ia supernovae,  
 1456 [309] demonstrated that photons convert to chameleons in the interior of the supernova, pass  
 1457 through the surface of the supernova, and then convert back to photons in the intergalactic  
 1458 magnetic field. The net result is an observed brightening of supernovae. This scenario  
 1459 provides an explanation for the discrepancy between distance measurements of standard  
 1460 candles and standard rulers beyond  $z \sim 0.5$  [310].

1461 Another prediction of chameleon gravity is that in unscreened environments, (such as  
 1462 voids) stellar structure is modified, most notably in the red giant branch of stars. The  
 1463 authors of [311] found that chameleons affect the size and temperature of red giant stars  
 1464 where they tend to be smaller ( $\sim 10\%$ ), and hotter ( $\sim 100$ s of Kelvins). Also, observations  
 1465 of circularly polarized starlight in the wavelength range  $1 - 10^3 \text{ \AA}$  could be a strong indication  
 1466 of chameleon-photon mixing [312].

1467 Astrophysical tests of chameleons in  $f(R)$  theories may be parameterized by how effi-  
 1468 ciently bodies self-screen ( $\chi$ ) and the strength of the fifth force ( $\alpha$ ) [313]. For the case of  
 1469 chameleon  $f(R)$  gravity,  $\chi \equiv df/dR$  is measured at present time. The additional force is  
 1470 parametrized by rescaling Newton's constant  $G \rightarrow G(1 + \alpha)$  for unscreened objects and  
 1471  $G(r) \rightarrow G[1 + \alpha(1 - M(r_s)/M(r))]$  for partially screened objects. Fifth forces are screened  
 1472 at radii  $r < r_s$ , unscreened for radii  $r_s < r$ , and  $M(r)$  is the mass contained within a shell at  
 1473 radius  $r$ . For an object to be unscreened,  $\Phi_N \ll \chi$  where  $\Phi_N$  is the Newtonian potential. The  
 1474 Sun and Milky Way (coincidentally) possess a similar gravitational potential:  $\Phi_\odot \sim 2 \times 10^{-6}$   
 1475 and  $\Phi_{MW} \sim 10^{-6}$ . Stars in the tip of the red giant branch of the HR diagram and Cepheid  
 1476 variables have gravitational potentials  $\Phi_N \sim 10^{-7}$ . These stars will have their outer layers  
 1477 unscreened provided they reside in smaller galaxies in a shallow gravitational potential. For

1478 fifth forces of a strength described by  $\alpha = 1/3$ , values of  $\chi$  greater than  $5 \times 10^{-7}$  may be  
1479 ruled out at 95% confidence. This upper bound is moderately lower for fifth force strength  
1480 defined by  $\alpha = 1$ , where values of  $\chi$  greater than  $1 \times 10^{-7}$  may be ruled out at a 95%  
1481 confidence level [313] (also see Fig.(5) of [313]). These constraints on  $\chi$  and  $\alpha$  from local  
1482 Universe observations are stronger than current cosmological constraints on chameleon fifth  
1483 forces [314]-[315] which typically give an upper limit not less than  $\chi \sim 10^{-6}$ .

## 1484 5.5. Space tests of Gravity

1485 Remarkably, the original predictions of signatures in space for chameleon models would still  
1486 be the most striking [283, 284]. The proposed experiments discussed there have not yet taken  
1487 place. However, the MicroSCOPE [316] mission and STE-QUEST [317] are future satellite  
1488 experiments that hold the promise of testing these theories in a way complementary to the  
1489 terrestrial and astrophysical methods discussed here. The expected signatures are large and  
1490 for example an  $\mathcal{O}(1)$  observed difference in Newton's constant for unscreened objects would  
1491 be a smoking gun for these models.

1492 There is great potential for testing chameleon theories in the laboratory, the sky and  
1493 through astrophysics ; both at the cosmic and the intensity frontiers. The possibilities for  
1494 astrophysics are discussed further under the Novel Probes of Dark Energy and Gravity in  
1495 the Cosmic Frontier.

## 1496 6. CONCLUSIONS

1497 **Establishing the existence of a Dark Sector, and the new light weakly-coupled**  
1498 **particles it could contain, would revolutionize particle physics** at the Copernican  
1499 level: once again our simple conception of Nature would be fundamentally altered, and here  
1500 we would realize that there is much more to the world than just the SM sector. Searches  
1501 for dark-sector particles are strongly motivated by our attempts to understand the nature  
1502 of the dark matter, the strong CP problem, and puzzling astrophysical and particle physics  
1503 observations. New physics need not reside exclusively at the TeV scale and beyond; it  
1504 could well be found at the low-energy frontier and be accessible with intensity frontier tools.  
1505 Axions, invented to solve the strong CP problem, are a perfect dark matter candidate. Dark  
1506 photons, and any dark-sector particles that they couple to, can be equally compelling dark  
1507 matter candidates, could resolve outstanding puzzles in particle and astro-particle physics,  
1508 and may also explain dark matter interactions with the SM. Other dark-sector particles could

1509 account for the Dark Energy. **Discovery of any of these particles would redefine our**  
1510 **worldview.**

1511 **Existing facilities and technologies, modest experiments, and experimental**  
1512 **cleverness enable the exploration of dark sectors.** Searches for new light weakly-  
1513 coupled particles depend on the tools and techniques of the intensity frontier, i.e. intense  
1514 beams of photons and charged particles, on technological means of dealing with high in-  
1515 tensities, and on extremely sensitive, needle-in-the-haystack detection techniques. A rich,  
1516 diverse, and low-cost experimental program is already underway that has the potential for  
1517 one or more game-changing discoveries. Current ideas for extending the searches to smaller  
1518 couplings and higher masses increase this potential markedly. The US high-energy physics  
1519 program needs to include these experimental searches, especially when the investment is so  
1520 modest, the motives so clear, and the payoff so spectacular. **At present, nearly all the**  
1521 **experimental efforts world-wide have strong US contributions or significant US**  
1522 **leadership, a position that should be maintained.**

1523 Axions, ALPS, dark photons, milli-charged particles, and light dark matter are all natu-  
1524 rally connected by their dark-sector origins, and by the fact that all these particles couple  
1525 to the photon, either directly, or through couplings induced by kinetic mixing. Microwave  
1526 cavities and light-shining-through-walls experiments designed to search for axions and ALPs  
1527 have been adapted to search for dark photons. So have helioscopes looking for solar axions.  
1528 A series of beam dump experiments, originally motivated as axion searches, have been rein-  
1529 terpreted to set important limits on dark photon couplings and masses. More recently, a  
1530 new series of electron and proton beam dump experiments, the latter capitalizing on exist-  
1531 ing neutrino detectors and eventually Project X beam intensities, will hunt for signs of light  
1532 dark matter produced in the dump by dark photon decays.

1533 **Searches for new light weakly coupled particles are, compared to typical con-**  
1534 **temporary particle physics experiments, small, accessible, hands-on, and per-**  
1535 **sonal in a way that is impossible in much larger efforts.** The NLWCP environment  
1536 offers ideal educational opportunities for undergraduates, graduate students, and post docs,  
1537 and revitalizes more experienced physicists too. All must deal with the full breadth of ex-  
1538 perimental activities: theory, design, proposal writing and defense, hardware construction  
1539 and commissioning, software implementation, data taking, and analysis. These experiments  
1540 have brought theorists and experimentalists into very close collaboration, to the benefit of  
1541 both camps and the field as a whole.

1542 A great deal can be done with existing tools and techniques, in searching for QCD



1543 axions that could account for the dark matter, in extending searches for dark photons  
1544 throughout the favored parameter space, and in searching for new dark-sector particles like  
1545 light dark matter. Even more is possible with the addition of relatively modest investments  
1546 in superconducting magnets, more sensitive microwave detection, resonant optical cavities,  
1547 high rate, highly pixelated silicon detectors, and new higher energy electron accelerators,  
1548 high intensity proton facilities, and upgraded  $e^+e^-$  and  $pp$  colliding beam facilities. Modest  
1549 investments will pay great dividends.

1550 **In conclusion, the search for dark sectors and the new, light, weakly-coupled**  
1551 **particles they may contain should be vigorously pursued in the US and else-**  
1552 **where.**

- 
- 1553 [1] J. L. Hewett, H. Weerts, R. Brock, J. N. Butler, B. C. K. Casey, J. Collar, A. de Gouvea  
1554 and R. Essig *et al.*, arXiv:1205.2671 [hep-ex].
- 1555 [2] K. Baker, G. Cantatore, S. A. Cetin, M. Davenport, K. Desch, B. Döbrich, H. Gies and  
1556 I. G. Irastorza *et al.*, *Annalen Phys.* **525**, A93 (2013) [arXiv:1306.2841 [hep-ph]].
- 1557 [3] R. D. Peccei and H. R. Quinn, *Phys. Rev. Lett.* **38**, 1440 (1977).
- 1558 [4] S. Weinberg, *Phys. Rev. Lett.* **40** (1978) 223.
- 1559 [5] F. Wilczek, *Phys. Rev. Lett.* **40**, 279 (1978).
- 1560 [6] K. Nakamura *et al.* [Particle Data Group], *J. Phys. G* **37** (2010) 075021.
- 1561 [7] J. Jaeckel and A. Ringwald, *Ann. Rev. Nucl. Part. Sci.* **60**, 405 (2010) [arXiv:1002.0329  
1562 [hep-ph]].
- 1563 [8] E. Witten, *Phys. Lett. B* **149**, 351 (1984).
- 1564 [9] J. P. Conlon, *JHEP* **0605**, 078 (2006) [hep-th/0602233].
- 1565 [10] P. Svrcek and E. Witten, *JHEP* **0606**, 051 (2006) [hep-th/0605206].
- 1566 [11] A. Arvanitaki, S. Dimopoulos, S. Dubovsky, N. Kaloper and J. March-Russell, *Phys. Rev. D*  
1567 **81**, 123530 (2010) [arXiv:0905.4720 [hep-th]].
- 1568 [12] B. S. Acharya, K. Bobkov and P. Kumar, *JHEP* **1011** (2010) 105 [arXiv:1004.5138 [hep-th]].
- 1569 [13] M. Cicoli, M. Goodsell and A. Ringwald, *JHEP* **1210**, 146 (2012) [arXiv:1206.0819 [hep-th]].
- 1570 [14] S. J. Asztalos, R. Bradley, G. Carosi, J. Clarke, C. Hagmann, J. Hoskins, M. Hotz and  
1571 D. Kinion *et al.*,
- 1572 [15] R. Bähre, B. Döbrich, J. Dreyling-Eschweiler, S. Ghazaryan, R. Hodajerdi, D. Horns,  
1573 F. Januschek and E. -A. Knabbe *et al.*, *JINST* **1309**, T09001 (2013) [arXiv:1302.5647  
1574 [physics.ins-det]].

- 1575 [16] I. G. Irastorza, F. T. Avignone, S. Caspi, J. M. Carmona, T. Dafni, M. Davenport, A. Du-  
1576 darev and G. Fanourakis *et al.*, JCAP **1106** (2011) 013 [arXiv:1103.5334 [hep-ex]].
- 1577 [17] J. K. Vogel, F. T. Avignone, G. Cantatore, J. M. Carmona, S. Caspi, S. A. Cetin, F. E. Chris-  
1578 tensen and A. Dael *et al.*, arXiv:1302.3273 [physics.ins-det].
- 1579 [18] I. G. Irastorza, IAXO, Letter of Intent to the CERN SPS committee, CERN-SPSC-2013-022,  
1580 SPSC-I-242, Aug. 2013.
- 1581 [19] D. Horns, J. Jaeckel, A. Lindner, A. Lobanov, J. Redondo and A. Ringwald, JCAP **1304**,  
1582 016 (2013) [arXiv:1212.2970 [hep-ph]].
- 1583 [20] S. Hannestad, A. Mirizzi, G. G. Raffelt and Y. Y. Y. Wong, JCAP **1008**, 001 (2010)  
1584 [arXiv:1004.0695 [astro-ph.CO]].
- 1585 [21] D. Cadamuro, S. Hannestad, G. Raffelt and J. Redondo, JCAP **1102**, 003 (2011)  
1586 [arXiv:1011.3694 [hep-ph]].
- 1587 [22] P. Sikivie, Lect. Notes Phys. **741** 19 (2008) [astro-ph/0610440].
- 1588 [23] T. Hiramatsu *et al.*, Phys. Rev. D **85** 105020 (2012). [1202.5851 [hep-ph]].
- 1589 [24] O. Wantz and E. P. S. Shellard, Phys. Rev. D **82** (2010) 123508 [arXiv:0910.1066 [astro-  
1590 ph.CO]].
- 1591 [25] P. Arias, D. Cadamuro, M. Goodsell, J. Jaeckel, J. Redondo and A. Ringwald, JCAP **1206**,  
1592 013 (2012) [arXiv:1201.5902 [hep-ph]].
- 1593 [26] O. Erken, P. Sikivie, H. Tam and Q. Yang, arXiv:1111.1157 [astro-ph.CO].
- 1594 [27] W. Hu, R. Barkana and A. Gruzinov, Phys. Rev. Lett. **85**, 1158 (2000) [astro-ph/0003365].
- 1595 [28] M. Boylan-Kolchin, J. S. Bullock and M. Kaplinghat, Mon. Not. Roy. Astron. Soc. **415**, L40  
1596 (2011) [arXiv:1103.0007 [astro-ph.CO]].
- 1597 [29] L. Amendola and R. Barbieri, Phys. Lett. B **642**, 192 (2006) [hep-ph/0509257].
- 1598 [30] D. J. E. Marsh, E. Macaulay, M. Trebitsch and P. G. Ferreira, Phys. Rev. D **85**, 103514  
1599 (2012) [arXiv:1110.0502 [astro-ph.CO]].
- 1600 [31] L. Amendola *et al.* [Euclid Theory Working Group Collaboration], arXiv:1206.1225 [astro-  
1601 ph.CO].
- 1602 [32] D. J. E. Marsh, D. Grin, R. eHlozek and P. G. Ferreira, arXiv:1303.3008 [astro-ph.CO].
- 1603 [33] C. P. Burgess, M. Cicoli and F. Quevedo, arXiv:1306.3512 [hep-th].
- 1604 [34] J. Isern, E. Garcia-Berro, S. Torres and S. Catalan, Astrophys. J. **682**, L109 (2008)  
1605 [arXiv:0806.2807 [astro-ph]].
- 1606 [35] J. Isern, S. Catalan, E. Garcia-Berro and S. Torres, J. Phys. Conf. Ser. **172**, 012005 (2009)  
1607 [arXiv:0812.3043 [astro-ph]].
- 1608 [36] J. Isern, L. Althaus, S. Catalan, A. Corsico, E. Garcia-Berro, M. Salaris, S. Torres and

- 1609 L. Althaus *et al.*, arXiv:1204.3565 [astro-ph.SR].
- 1610 [37] A. H. Corsico, L. G. Althaus, M. M. M. Bertolami, A. D. Romero, E. Garcia-Berro, J. Isern  
1611 and S. O. Kepler, Monthly Notices of the Royal Astronomical Society, Volume 424, Issue 4,  
1612 pp. 2792-2799. arXiv:1205.6180 [astro-ph.SR].
- 1613 [38] A. H. Corsico, L. G. Althaus, A. D. Romero, A. S. Mukadam, E. Garcia-Berro, J. Isern,  
1614 S. O. Kepler and M. A. Corti, JCAP **1212**, 010 (2012) [arXiv:1211.3389 [astro-ph.SR]].
- 1615 [39] B. Melendez, M. M. Bertolami and L. Althaus, arXiv:1210.0263 [hep-ph].
- 1616 [40] D. Horns and M. Meyer, JCAP **1202**, 033 (2012) [arXiv:1201.4711 [astro-ph.CO]].
- 1617 [41] A. De Angelis, O. Mansutti and M. Roncadelli, Phys. Rev. D **76**, 121301 (2007)  
1618 [arXiv:0707.4312 [astro-ph]].
- 1619 [42] M. Simet, D. Hooper and P. D. Serpico, Phys. Rev. D **77**, 063001 (2008) [arXiv:0712.2825  
1620 [astro-ph]].
- 1621 [43] M. A. Sanchez-Conde, D. Paneque, E. Bloom, F. Prada and A. Dominguez, Phys. Rev. D  
1622 **79**, 123511 (2009) [arXiv:0905.3270 [astro-ph.CO]].
- 1623 [44] A. De Angelis, G. Galanti and M. Roncadelli, Phys. Rev. D **84**, 105030 (2011)  
1624 [arXiv:1106.1132 [astro-ph.HE]].
- 1625 [45] M. Meyer, D. Horns and M. Raue, Phys. Rev. D **87**, 035027 (2013) [arXiv:1302.1208 [astro-  
1626 ph.HE]].
- 1627 [46] A. V. Maccio, S. Paduroiu, D. Anderhalden, A. Schneider and B. Moore, arXiv:1202.1282  
1628 [astro-ph.CO].
- 1629 [47] D. J. E. Marsh and J. Silk, arXiv:1307.1705 [astro-ph.CO].
- 1630 [48] K. van Bibber, N.R. Dagdeviren, S.E. Koonin, A.K. Kerman and H.N. Nelson, Phys. Rev.  
1631 Lett. **59**, 759 (1987).
- 1632 [49] J. Redondo and A. Ringwald, Contemp. Phys. **52**, 211 (2011) [arXiv:1011.3741 [hep-ph]].
- 1633 [50] F. Hoogeveen and T. Ziegenhagen Nucl. Phys. B **358**, 3 (1991).
- 1634 [51] P. Sikivie, D.B. Tanner, and Karl van Bibber, Phys. Rev. Lett. **98**, 172002 (2007).
- 1635 [52] G. Mueller, P. Sikivie, D.B. Tanner and K. van Bibber, Phys. Rev. D **80**, 072004 (2009).
- 1636 [53] G. Mueller, P. Sikivie, D.B. Tanner, and K. van Bibber, AIP Conf. Proc. **1274**, 150 (2010).
- 1637 [54] G. Mueller, P. Sikivie, D. B. Tanner and K. van Bibber, Phys. Rev. D **80**, 072004 (2009)  
1638 [arXiv:0907.5387 [hep-ph]].
- 1639 P. Arias, J. Jaeckel, J. Redondo and A. Ringwald, Phys. Rev. D **82**, 115018 (2010)  
1640 [arXiv:1009.4875 [hep-ph]].
- 1641 P. Arias and A. Ringwald, arXiv:1110.2126 [hep-ph].
- 1642 [55] B. Abbott *et al.* (LIGO Scientific Collaboration), Nucl. Instrum. Methods A **517**, 154–179

- (2004); Rep. Prog. Phys. **72**, 076901/1–25 (2009).
- [56] R.J. Cruz, J.I. Thorpe, A. Preston, R. Delgadillo, M. Hartman, S. Mitryk, A. Worley, G. Boothe, S. R. Guntaka, S. Klimenko, D.B. Tanner and G. Mueller, Class. Quant. Grav. **23**, S751-S760 (2006).
- [57] P. Sikivie, Phys. Rev. Lett. **51**, 1415 (1983).
- [58] G. Raffelt and L. Stodolsky, Phys. Rev. D **37**, 1237 (1988).
- [59] G. Ruoso, R. Cameron, G. Cantatore, A. C. Melissinos, Y. Semertzidis, H. J. Halama, D. M. Lazarus, A. G. Prodell, F. Nezrick, C. Rizzo and E. Zavattini, Z. Phys. C **56**, 505 (1992).
- [60] R. Cameron, G. Cantatore, A. C. Melissinos, G. Ruoso, and Y. Semertzidis, H. J. Halama, D. M. Lazarus, and A. G. Prodell, F. Nezrick, C. Rizzo and E. Zavattini, Phys. Rev. D **47**, 3707 (1993).
- [61] C. Robilliard, R. Battesti, M. Fouché, J. Mauchain, A.-M. Sautivet, F. Amiranoff, and C. Rizzo, Phys. Rev. Lett. **99**, 190403 (2007).
- [62] A. S. Chou, W. Wester, A. Baumbaugh, H. R. Gustafson, Y. Irizarry-Valle, P. O. Mazur, J. H. Steffen, R. Tomlin, X. Yang, and J. Yoo, Phys. Rev. Lett. **100**, 080402 (2008).
- [63] A. Afanasev, O. K. Baker, K. B. Beard, G. Biallas, J. Boyce, M. Minarni, R. Ramdon, M. Shinn, and P. Slocum, Phys. Rev. Lett. **101**, 120401 (2008).
- [64] Pierre Pugnat et.al., Phys. Rev. D **78**, 092003 (2008).
- [65] K. Ehret *et al.* [ALPS Collaboration], Nucl. Instrum. Meth. A **612**, 83 (2009) [arXiv:0905.4159 [physics.ins-det]].
- [66] K. Ehret et.al., Phys. Lett. B **689**, 149 (2010) [arXiv:1004.1313 [hep-ex]].
- [67] A.E. Siegman, *Lasers* (University Science Books, Sausalito, 1984).
- [68] For example, see <http://lma.in2p3.fr/Activites/loss.htm>
- [69] R.W.P. Drever, J.L. Hall, F.V. Kowalski, J. Hough, G.M. Ford, A.J. Munley, and H. Ward, Appl. Phys. B **31**, 97 (1983); Eric D. Black, Am. J. Phys. **69**, 79 (2001).
- [70] K. Goda, D. Ottaway, B. Connelly, R. Adhikari, N. Mavalvala, and A. Gretarsson, Optics Letters **29**, 1452–1454 (2004).
- [71] K. Zioutas *et al.* (CAST collaboration), Phys. Rev. Lett. **94**, 121301 (2005); E. Arik *et al.* (CAST collaboration) J. Cosmo. Astropart. Phys. **02**, 008 (2009).
- [72] G.G. Raffelt, *Stars as Laboratories for Fundamental Physics* (UCP, Chicago, 1996).
- [73] L. B. Okun, Sov. Phys. JETP **56**, 502 (1982) [Zh. Eksp. Teor. Fiz. **83**, 892 (1982)].
- [74] M. Ahlers, H. Gies, J. Jaeckel, J. Redondo, and A. Ringwald, Phys. Rev. D **77**, 095001 (2008). [arXiv:0711.4991 [hep-ph]].
- [75] A. Afanasev et.al., Phys. Lett. B **679**, 317–320 (2009).

- 1677 [76] J. Jaeckel, J. Redondo, & A. Ringwald, Phys. Rev. Lett. **101**, 131801 (2008). [arXiv:0804.4157  
1678 [astro-ph]].
- 1679 [77] F. Hoogeveen, Phys. Lett. B **288** (1992) 195.
- 1680 [78] J. Jaeckel and A. Ringwald, Phys. Lett. B **659**, 509 (2008) [arXiv:0707.2063 [hep-ph]].
- 1681 [79] R. Povey, J. Hartnett and M. Tobar, Phys. Rev. D **82**, 052003 (2010) [arXiv:1003.0964  
1682 [hep-ex]].
- 1683 [80] A. Wagner, G. Rybka, M. Hotz, L. J. Rosenberg, S. J. Asztalos, G. Carosi, C. Hagmann and  
1684 D. Kinion *et al.*, Phys. Rev. Lett. **105**, 171801 (2010) [arXiv:1007.3766 [hep-ex]].
- 1685 [81] M. Betz and F. Caspers, Conf. Proc. C **1205201**, 3320 (2012) [arXiv:1207.3275 [physics.ins-  
1686 det]].
- 1687 [82] P. Sikivie, Phys. Rev. Lett. **51**, 1415 (1983) [Erratum-ibid. **52**, 695 (1984)].
- 1688 [83] S. De Panfilis, *et al.*, Phys. Rev. Lett. **59**, 839 (1987).
- 1689 [84] C. Hagmann, P. Sikivie, N.S. Sullivan, D.B. Tanner, Phys. Rev. D **42**, 1297 (1990).
- 1690 [85] S.J. Asztalos, *et al.*, Phys. Rev. D **69**, 011101 (2004) [astro-ph/0310042].
- 1691 [86] E.I. Gates, G. Gyuk, M.S. Turner, Astrophys. J. **449**, L123 (1995) [astro-ph/9505039].
- 1692 [87] S.J. Asztalos *et al.*, Phys. Rev. Lett. **104**, 041301 (2010).
- 1693 [88] A. Malagon *et al.*, 9th Patras Workshop on Axions, WIMPs, and WISPs, Mainz, Germany  
1694 (2013).
- 1695 [89] P. W. Graham and S. Rajendran, Phys. Rev. D **84**, 055013 (2011) [arXiv:1101.2691 [hep-ph]].
- 1696 [90] P. W. Graham and S. Rajendran, Physical Review D **88**, **035023** (2013) [arXiv:1306.6088  
1697 [hep-ph]].
- 1698 [91] D. Budker, P. W. Graham, M. Ledbetter, S. Rajendran and A. Sushkov, arXiv:1306.6089  
1699 [hep-ph].
- 1700 [92] H. Primakoff, Phys. Rev. **81**, 899 (1951).
- 1701 [93] P. Sikivie, Phys. Rev. Lett. **51**, 1415 (1983).
- 1702 [94] P. Sikivie, Phys. Rev. D **32**, 2988 (1985).
- 1703 [95] K. van Bibber, P. M. McIntyre, D. E. Morris, and G. G. Raffelt, Phys. Rev. D **39**, 2089  
1704 (1989).
- 1705 [96] D. M. Lazarus *et al.*, Phys. Rev. Lett. **69**, 2333 (1992).
- 1706 [97] S. Moriyama *et al.*, Phys. Lett. B **434**, 147 (1998).
- 1707 [98] Y. Inoue *et al.*, Phys. Lett. B **536**, 18 (2002).
- 1708 [99] Y. Inoue *et al.*, Phys. Lett. B **668**, 93 (2008).
- 1709 [100] K. Zioutas *et al.*, NIM A **425**, 480 (1999).
- 1710 [101] M. Kuster *et al.*, New Journal of Physics **9**, 169 (2007).

- 1711 [102] CAST Collaboration, K. Zioutas *et al.*, Phys. Rev. Lett. **94**, 121301 (2005).
- 1712 [103] S. Andriamonje *et al.*, Journal of Cosmology and Astroparticle Physics **2007**, 010 (2007).
- 1713 [104] E. Arik *et al.*, Journal of Cosmology and Astroparticle Physics **2009**, 008 (2009).
- 1714 [105] CAST Collaboration, M. Arik *et al.*, Phys. Rev. Lett. **107**, 261302 (2011) [arXiv:1106.3919].
- 1715 [106] CAST Collaboration, M. Arik *et al.*, publication in preparation for Phys. Rev. Lett. (2013),  
1716 [arxiv:1307.1985].
- 1717 [107] G. G. Raffelt, Lect. Notes Phys. **741**, 51 (2008).
- 1718 [108] S. Hannestad, A. Mirizzi, G. G. Raffelt, Y. Y. Y. Wong, JCAP **08** 001 (2010).
- 1719 [109] K. Barth *et al.*, "CAST constraints on the axion-electron coupling," JCAP **1305**, 010 (2013).
- 1720 [110] I. Irastorza *et al.*, Journal of Cosmology and Astroparticle Physics **2011**, 013 (2011).
- 1721 [111] P. Brax and K. Zioutas, Phys. Rev. D **82**, 043007 (2010).
- 1722 [112] O.K. Baker *et al.*, Phys. Rev. D **85**, 035018 (2012).
- 1723 [113] P. Brax, A. Lindner, K. Zioutas, Phys. Rev. D **85**, 043014 (2012).
- 1724 [114] K. Zioutas, M. Tsagri, Y. Semertzidis, T. Papaevangelou, T. Dafni, V Anastassopoulos, New  
1725 J. Phys. **11**, 105020 (2009).
- 1726 [115] The Annual Patras Workshops on Axions, WIMPs & WISPs, <http://axion-wimp.desy.de/>
- 1727 [116] R. Essig, R. Harnik, J. Kaplan and N. Toro, Phys. Rev. D **82**, 113008 (2010) [arXiv:1008.0636  
1728 [hep-ph]].
- 1729 [117] B. Holdom, Phys. Lett. B **166** (1986) 196.
- 1730 [118] P. Galison and A. Manohar, Phys. Lett. B **136** (1984) 279.
- 1731 [119] J. D. Bjorken, R. Essig, P. Schuster and N. Toro, Phys. Rev. D **80**, 075018 (2009)  
1732 [arXiv:0906.0580 [hep-ph]].
- 1733 [120] J. D. Bjorken *et al.*, Phys. Rev. D **38** (1988) 3375.
- 1734 [121] E. M. Riordan *et al.*, Phys. Rev. Lett. **59** (1987) 755.
- 1735 [122] A. Bross, M. Crisler, S. H. Pordes, J. Volk, S. Errede and J. Wrbanek, Phys. Rev. Lett. **67**  
1736 (1991) 2942.
- 1737 [123] M. Pospelov, Phys. Rev. D **80** (2009) 095002 [arXiv:0811.1030 [hep-ph]].
- 1738 [124] H. Davoudiasl, H. -S. Lee and W. J. Marciano, Phys. Rev. D **86** (2012) 095009  
1739 [arXiv:1208.2973 [hep-ph]].
- 1740 [125] M. Endo, K. Hamaguchi and G. Mishima, Phys. Rev. D **86** (2012) 095029 [arXiv:1209.2558  
1741 [hep-ph]].
- 1742 [126] D. Babusci *et al.* [KLOE-2 Collaboration], Phys. Lett. B **720**, 111 (2013) [arXiv:1210.3927  
1743 [hep-ex]].
- 1744 [127] F. Archilli, D. Babusci, D. Badoni, I. Balwierz, G. Bencivenni, C. Bini, C. Bloise and V. Bocci

- 1745 *et al.*, Phys. Lett. B **706**, 251 (2012) [arXiv:1110.0411 [hep-ex]].
- 1746 [128] S. Abrahamyan *et al.* [APEX Collaboration], Phys. Rev. Lett. **107**, 191804 (2011)
- 1747 [arXiv:1108.2750 [hep-ex]].
- 1748 [129] H. Merkel *et al.* [A1 Collaboration], Phys. Rev. Lett. **106**, 251802 (2011) [arXiv:1101.4091
- 1749 [nucl-ex]].
- 1750 [130] M. Reece and L. T. Wang, JHEP **0907** (2009) 051 [arXiv:0904.1743 [hep-ph]].
- 1751 [131] B. Aubert *et al.* [BABAR Collaboration], Phys. Rev. Lett. **103**, 081803 (2009)
- 1752 [arXiv:0905.4539 [hep-ex]].
- 1753 [132] J. B. Dent, F. Ferrer and L. M. Krauss, arXiv:1201.2683 [astro-ph.CO].
- 1754 [133] H. K. Dreiner, J.-F. Fortin, C. Hanhart and L. Ubaldi, arXiv:1310.3826 [hep-ph].
- 1755 [134] R. Essig, P. Schuster, N. Toro and B. Wojtsekhowski, JHEP **1102**, 009 (2011)
- 1756 [arXiv:1001.2557 [hep-ph]].
- 1757 [135] The Heavy Photon Search Collaboration (HPS),
- 1758 <https://confluence.slac.stanford.edu/display/hpsg/>
- 1759 [136] M. Freytsis, G. Ovanesyanyan and J. Thaler, JHEP **1001** (2010) 111 [arXiv:0909.2862 [hep-ph]].
- 1760 [137] B. Wojtsekhowski, AIP Conf. Proc. **1160** (2009) 149 [arXiv:0906.5265 [hep-ex]].
- 1761 [138] B. Wojtsekhowski, D. Nikolenko and I. Rachek, arXiv:1207.5089 [hep-ex].
- 1762 [139] T. Beranek, H. Merkel and M. Vanderhaeghen, arXiv:1303.2540 [hep-ph].
- 1763 [140] R. Essig, P. Schuster and N. Toro, Phys. Rev. D **80** (2009) 015003 [arXiv:0903.3941 [hep-ph]].
- 1764 [141] S.A. Abel, M.D. Goodsell, J. Jaeckel, V.V. Khoze, and A. Ringwald, JHEP **07**, 124 (2008).
- 1765 [142] M. Goodsell, J. Jaeckel, J. Redondo and A. Ringwald, JHEP **0911**, 027 (2009)
- 1766 [arXiv:0909.0515 [hep-ph]].
- 1767 [143] M. Cicoli, M. Goodsell, J. Jaeckel and A. Ringwald, JHEP **1107**, 114 (2011) [arXiv:1103.3705
- 1768 [hep-th]].
- 1769 [144] M. Goodsell, S. Ramos-Sanchez and A. Ringwald, JHEP **1201**, 021 (2012) [arXiv:1110.6901
- 1770 [hep-th]].
- 1771 [145] M. Goodsell and A. Ringwald, Fortsch. Phys. **58**, 716 (2010) [arXiv:1002.1840 [hep-th]].
- 1772 [146] P. Candelas, G. T. Horowitz, A. Strominger and E. Witten, Nucl. Phys. B **258**, 46 (1985).
- 1773 [147] E. Witten, Nucl. Phys. B **268**, 79 (1986).
- 1774 [148] S. Andreas, M. D. Goodsell and A. Ringwald, arXiv:1109.2869 [hep-ph].
- 1775 [149] P. Fayet, Phys. Rev. D **75** (2007) 115017 [arXiv:hep-ph/0702176].
- 1776 [150] C. Cheung, J. T. Ruderman, L. T. Wang and I. Yavin, Phys. Rev. D **80** (2009) 035008
- 1777 [arXiv:0902.3246 [hep-ph]].
- 1778 [151] N. Arkani-Hamed and N. Weiner, JHEP **0812**, 104 (2008) [arXiv:0810.0714 [hep-ph]].

- 1779 [152] D. E. Morrissey, D. Poland and K. M. Zurek, JHEP **0907** (2009) 050 [arXiv:0904.2567 [hep-  
1780 ph]].
- 1781 [153] H. Davoudiasl, H.-S. Lee and W. J. Marciano, Phys. Rev. D **85**, 115019 (2012)  
1782 [arXiv:1203.2947 [hep-ph]].
- 1783 [154] H. Davoudiasl, H.-S. Lee and W. J. Marciano, Phys. Rev. Lett. **109**, 031802 (2012)  
1784 [arXiv:1205.2709 [hep-ph]].
- 1785 [155] H. Davoudiasl, H.-S. Lee, I. Lewis and W. J. Marciano, Phys. Rev. D **88**, **015022** (2013)  
1786 [arXiv:1304.4935 [hep-ph]].
- 1787 [156] B. Batell, M. Pospelov and A. Ritz, Phys. Rev. D **80**, 095024 (2009) [arXiv:0906.5614 [hep-  
1788 ph]].
- 1789 [157] M. J. Strassler and K. M. Zurek, Phys. Lett. B **651** (2007) 374 [arXiv:hep-ph/0604261].
- 1790 [158] G. Amelino-Camelia *et al.*, Eur. Phys. J. C **68** (2010) 619 [arXiv:1003.3868 [hep-ex]].
- 1791 [159] B. Aubert *et al.* [BaBar Collaboration], arXiv:0902.2176 [hep-ex].
- 1792 [160] B. Batell, M. Pospelov and A. Ritz, Phys. Rev. D **79** (2009) 115008 [arXiv:0903.0363 [hep-  
1793 ph]].
- 1794 [161] B. Aubert *et al.* [BaBar Collaboration], arXiv:0908.2821 [hep-ex].
- 1795 [162] V. M. Abazov *et al.* [D0 Collaboration], Phys. Rev. Lett. **103**, 081802 (2009) [arXiv:0905.1478  
1796 hep-ex]].
- 1797 [163] V. M. Abazov *et al.* [D0 Collaboration], **p $\bar{p}$**  collisions at  $\sqrt{s} = 1.96$  TeV,” Phys. Rev. Lett.  
1798 **105**, 211802 (2010) [arXiv:1008.3356 [hep-ex]].
- 1799 [164] J. P. Lees and others [The BABAR Collaboration], arXiv:1202.1313 [hep-ex].
- 1800 [165] M. Baumgart, C. Cheung, J. T. Ruderman, L. T. Wang and I. Yavin, JHEP **0904**, 014  
1801 (2009) [arXiv:0901.0283 [hep-ph]].
- 1802 [166] N. Arkani-Hamed, D. P. Finkbeiner, T. R. Slatyer and N. Weiner, Phys. Rev. D **79** (2009)  
1803 015014 [arXiv:0810.0713 [hep-ph]].
- 1804 [167] M. Pospelov and A. Ritz, Phys. Lett. B **671** (2009) 391 [arXiv:0810.1502 [hep-ph]].
- 1805 [168] A. P. Lobanov, H. -S. Zechlin and D. Horns, Phys. Rev. **D** 87, Issue 6, id. 065004,  
1806 arXiv:1211.6268 [astro-ph.CO].
- 1807 [169] A. E. Nelson and J. Scholtz, Phys. Rev. D **84**, 103501 (2011) [arXiv:1105.2812 [hep-ph]].
- 1808 [170] O. Adriani *et al.* [PAMELA Collaboration], Nature **458**, 607 (2009) [arXiv:0810.4995 [astro-  
1809 ph]].
- 1810 [171] M. Ackermann *et al.* [Fermi LAT Collaboration], Phys. Rev. Lett. **108**, 011103 (2012)  
1811 [arXiv:1109.0521 [astro-ph.HE]].
- 1812 [172] M. Aguilar *et al.* [AMS Collaboration], Phys. Rev. Lett. **110**, no. 14, 141102 (2013).



- 1813 [173] K. Blum, B. Katz and E. Waxman, arXiv:1305.1324 [astro-ph.HE].
- 1814 [174] P. Blasi, Phys. Rev. Lett. **103**, 051104 (2009) [arXiv:0903.2794 [astro-ph.HE]].
- 1815 [175] R. Cowsik and B. Burch, arXiv:0905.2136 [astro-ph.CO].
- 1816 [176] A. A. Abdo *et al.* [Fermi LAT Collaboration], Phys. Rev. Lett. **102**, 181101 (2009)  
1817 [arXiv:0905.0025 [astro-ph.HE]].
- 1818 [177] I. Cholis, L. Goodenough, D. Hooper, M. Simet and N. Weiner, Phys. Rev. D **80**, 123511  
1819 (2009) [arXiv:0809.1683 [hep-ph]].
- 1820 [178] P. -F. Yin, Z. -H. Yu, Q. Yuan and X. -J. Bi, arXiv:1304.4128 [astro-ph.HE].
- 1821 [179] T. Linden and S. Profumo, arXiv:1304.1791 [astro-ph.HE].
- 1822 [180] D. P. Finkbeiner, L. Goodenough, T. R. Slatyer, M. Vogelsberger and N. Weiner, JCAP  
1823 **1105**, 002 (2011) [arXiv:1011.3082 [hep-ph]].
- 1824 [181] I. Cholis and D. Hooper, arXiv:1304.1840 [astro-ph.HE].
- 1825 [182] Q. Yuan, X. -J. Bi, G. -M. Chen, Y. -Q. Guo, S. -J. Lin and X. Zhang, arXiv:1304.1482  
1826 [astro-ph.HE].
- 1827 [183] M. Ackermann *et al.* [LAT Collaboration], Astrophys. J. **761** (2012) 91 [arXiv:1205.6474  
1828 [astro-ph.CO]].
- 1829 [184] J. Zavala, M. Vogelsberger, T. R. Slatyer, A. Loeb and V. Springel, Phys. Rev. D **83** (2011)  
1830 123513 [arXiv:1103.0776 [astro-ph.CO]].
- 1831 [185] K. N. Abazajian and J. P. Harding, JCAP **1201**, 041 (2012) [arXiv:1110.6151 [hep-ph]].
- 1832 [186] N. Padmanabhan and D. P. Finkbeiner, Phys. Rev. D **72**, 023508 (2005) [astro-ph/0503486].
- 1833 [187] M. S. Madhavacheril, N. Sehgal and T. R. Slatyer, “Current Dark Matter Annihilation Con-  
1834 straints from Cmb and Low-Redshift Data,” arXiv:1310.3815 [astro-ph.CO].
- 1835 [188] L. Lopez-Honorez, O. Mena, S. Palomares-Ruiz and A. C. Vincent, arXiv:1303.5094 [astro-  
1836 ph.CO].
- 1837 [189] S. Galli, T. R. Slatyer, M. Valdes and F. Iocco, arXiv:1306.0563 [astro-ph.CO].
- 1838 [190] T. R. Slatyer, N. Toro and N. Weiner, Phys. Rev. D **86**, 083534 (2012) [arXiv:1107.3546  
1839 [hep-ph]].
- 1840 [191] M. Ibe, S. Matsumoto, S. Shirai and T. T. Yanagida, arXiv:1305.0084 [hep-ph].
- 1841 [192] R. Agnese *et al.* [CDMS Collaboration], Submitted to: Phys.Rev.Lett. [arXiv:1304.4279 [hep-  
1842 ex]].
- 1843 [193] C. E. Aalseth *et al.* [CoGeNT Collaboration], arXiv:1208.5737 [astro-ph.CO].
- 1844 [194] D. Hooper, arXiv:1306.1790 [hep-ph].
- 1845 [195] A. Djouadi, A. Falkowski, Y. Mambrini and J. Quevillon, arXiv:1205.3169 [hep-ph].
- 1846 [196] K. -Y. Choi and O. Seto, arXiv:1305.4322 [hep-ph].

- 1847 [197] S. Andreas, M. D. Goodsell and A. Ringwald, arXiv:1306.1168 [hep-ph].
- 1848 [198] D. Hooper and T. Linden, Phys. Rev. D **84**, 123005 (2011) [arXiv:1110.0006 [astro-ph.HE]].
- 1849 [199] T. Linden, D. Hooper and F. Yusef-Zadeh, Astrophys. J. **741**, 95 (2011) [arXiv:1106.5493
- 1850 [astro-ph.HE]].
- 1851 [200] K. N. Abazajian and M. Kaplinghat, Phys. Rev. D **86**, 083511 (2012) [arXiv:1207.6047
- 1852 [astro-ph.HE]].
- 1853 [201] D. Hooper and T. R. Slatyer, arXiv:1302.6589 [astro-ph.HE].
- 1854 [202] D. Hooper, N. Weiner and W. Xue, Phys. Rev. D **86**, 056009 (2012) [arXiv:1206.2929 [hep-
- 1855 ph]].
- 1856 [203] D. N. Spergel and P. J. Steinhardt, Phys. Rev. Lett. **84**, 3760 (2000) [astro-ph/9909386].
- 1857 [204] M. Vogelsberger, J. Zavala and A. Loeb, Mon. Not. Roy. Astron. Soc. **423**, 3740 (2012)
- 1858 [arXiv:1201.5892 [astro-ph.CO]].
- 1859 [205] J. Zavala, M. Vogelsberger and M. G. Walker, arXiv:1211.6426 [astro-ph.CO].
- 1860 [206] S. Tulin, H. -B. Yu and K. M. Zurek, Phys. Rev. Lett. **110** (2013) 111301 [arXiv:1210.0900
- 1861 [hep-ph]].
- 1862 [207] H. An, M. Pospelov and J. Pradler, Phys. Lett. B **725**, 190 (2013)
- 1863 [208] J. Redondo and M. Postma, JCAP **0902**, 005 (2009) [arXiv:0811.0326 [hep-ph]].
- 1864 [209] M. Pospelov, A. Ritz and M. B. Voloshin, Phys. Rev. D **78**, 115012 (2008) [arXiv:0807.3279
- 1865 [hep-ph]].
- 1866 [210] S. Andreas, C. Niebuhr and A. Ringwald, Phys. Rev. D **86**, 095019 (2012) [arXiv:1209.6083
- 1867 [hep-ph]].
- 1868 [211] A. Konaka, K. Imai, H. Kobayashi, A. Masaike, K. Miyake, T. Nakamura, N. Nagamine and
- 1869 N. Sasao *et al.*, Phys. Rev. Lett. **57**, 659 (1986).
- 1870 [212] M. Davier and H. Nguyen Ngoc, Phys. Lett. B **229**, 150 (1989).
- 1871 [213] J. Balewski, J. Bernauer, W. Bertozzi, J. Bessuille, B. Buck, R. Cowan, K. Dow and C. Ep-
- 1872 stein *et al.*, arXiv:1307.4432 [physics.ins-det].
- 1873 [214] R. Alarcon *et al.* Phys. Rev. Lett. **111** (2013) 164801 [arXiv:1305.0199 [physics.acc-ph]].
- 1874 [215] K. Aulenbacher, M. Dehn, H. -J. Kreidel, R. Heine and R. Eichhorn, ICFA Beam Dyn.
- 1875 Newslett. **58**, 145 (2012).
- 1876 [216] C. Athanassopoulos *et al.* [LSND Collaboration], Phys. Rev. C **58**, 2489 (1998) [nucl-
- 1877 ex/9706006].
- 1878 [217] J. Blumlein and J. Brunner, Phys. Lett. B **701**, 155 (2011) [arXiv:1104.2747 [hep-ex]].
- 1879 [218] J. Blumlein, J. Brunner, H. J. Grabosch, P. Lanius, S. Nowak, C. Rethfeldt, H. E. Ryseck
- 1880 and M. Walter *et al.*, Z. Phys. C **51**, 341 (1991).

- 1881 [219] J. Blumlein, J. Brunner, H. J. Grabosch, P. Lanius, S. Nowak, C. Rethfeldt, H. E. Ryseck  
1882 and M. Walter *et al.*, *Int. J. Mod. Phys. A* **7**, 3835 (1992).
- 1883 [220] S. N. Gninenko, *Phys. Rev. D* **85**, 055027 (2012) [arXiv:1112.5438 [hep-ph]].
- 1884 [221] P. Astier *et al.* [NOMAD Collaboration], *Phys. Lett. B* **506**, 27 (2001) [hep-ex/0101041].
- 1885 [222] G. Bernardi, G. Carugno, J. Chauveau, F. Dicarolo, M. Dris, J. Dumarchez, M. Ferro-Luzzi  
1886 and J. M. Levy *et al.*, *Phys. Lett. B* **166**, 479 (1986).
- 1887 [223] S. N. Gninenko, *Phys. Lett. B* **713**, 244 (2012) [arXiv:1204.3583 [hep-ph]].
- 1888 [224] F. Bergsma *et al.* [CHARM Collaboration], *Phys. Lett. B* **166**, 473 (1986).
- 1889 [225] R. Dharmapalan *et al.* [MiniBooNE Collaboration], arXiv:1211.2258 [hep-ex].
- 1890 [226] M. Ablikim *et al.* [BESIII Collaboration], *Phys. Rev. D* **87**, 012009 (2013) [arXiv:1209.2469  
1891 [hep-ex]].
- 1892 [227] B. Aubert *et al.* [BABAR Collaboration], arXiv:0908.2821 [hep-ex].
- 1893 [228] B. Batell, M. Pospelov and A. Ritz, *Phys. Rev. D* **83**, 054005 (2011)
- 1894 [229] J. Jaeckel, M. Jankowiak and M. Spannowsky, *Phys. Dark Univ.* **2** (2013) 111  
1895 [arXiv:1212.3620 [hep-ph]].
- 1896 [230] J. T. Ruderman and T. Volansky, *JHEP* **1002**, 024 (2010) [arXiv:0908.1570 [hep-ph]].
- 1897 [231] C. Cheung, J. T. Ruderman, L. -T. Wang and I. Yavin, *JHEP* **1004**, 116 (2010)  
1898 [arXiv:0909.0290 [hep-ph]].
- 1899 [232] [CDF Collaboration], with a  $W$  or  $Z$  Boson and Additional Leptons,”  
1900 CDF/ANAL/EXOTIC/PUBLIC/10526.
- 1901 [233] [ATLAS Collaboration], ATLAS-CONF-2011-076.
- 1902 [234] S. Chatrchyan *et al.* [CMS Collaboration], *JHEP* **1107**, 098 (2011) [arXiv:1106.2375 [hep-ex]].
- 1903 [235] S. Chatrchyan *et al.* [CMS Collaboration], arXiv:1210.7619 [hep-ex].
- 1904 [236] G. Aad *et al.* [ATLAS Collaboration], *Phys. Lett. B* **719**, 299 (2013) [arXiv:1212.5409].
- 1905 [237] G. Aad *et al.* [ATLAS Collaboration], *New J. Phys.* **15**, 043009 (2013) [arXiv:1302.4403  
1906 [hep-ex]].
- 1907 [238] G. Aad *et al.* [ATLAS Collaboration], *Phys. Lett. B* **721**, 32 (2013) [arXiv:1210.0435 [hep-  
1908 ex]].
- 1909 [239] J. Redondo, *JCAP* **0807**, 008 (2008) [arXiv:0801.1527 [hep-ph]].
- 1910 [240] J. Redondo and G. Raffelt, *JCAP* **1308**, 034 (2013) [arXiv:1305.2920 [hep-ph]].
- 1911 [241] H. An, M. Pospelov and J. Pradler, *Phys. Rev. Lett.* **111** 041302 (2013) [arXiv:1304.3461  
1912 [hep-ph]].
- 1913 [242] M. Schwarz, A. Lindner, J. Redondo, A. Ringwald, G. Wiedemann, A. Lindner, J. Redondo  
1914 and A. Ringwald *et al.*, Proceedings of the 7th Patras Workshop on Axions, WIMPs and

- 1915 WISPs. PATRAS 2011, Mykonos, Greece, June 27-July 1, 2011, arXiv:1111.5797 [astro-  
1916 ph.IM].
- 1917 [243] P. L. Slocum, O. K. Baker, J. L. Hirshfield, Y. Jiang, G. Kazakevitch, S. Kazakov, M. A. La-  
1918 Pointe and A. T. Malagon *et al.*, arXiv:1301.6184 [astro-ph.CO].
- 1919 [244] J. Jaeckel and J. Redondo, arXiv:1307.7181 [hep-ph].
- 1920 [245] J. Jaeckel and J. Redondo, arXiv:1308.1103 [hep-ph].
- 1921 [246] M. Graham at Snowmass 2013,  
1922 <https://indico.fnal.gov/getFile.py/access?contribId=423&sessionId=43&resId=0&materialId=slides&confId=6890>
- 1923 [247] T. Nelson at Snowmass 2013,  
1924 <https://indico.fnal.gov/getFile.py/access?contribId=422&sessionId=43&resId=0&materialId=slides&confId=6890>
- 1925 [248] R. Bernabei *et al.* [DAMA Collaboration], Eur. Phys. J. C **56**, 333 (2008) [arXiv:0804.2741  
1926 [astro-ph]];
- 1927 [249] C. E. Aalseth *et al.* [CoGeNT Collaboration], Phys. Rev. Lett. **106**, 131301 (2011)  
1928 [arXiv:1002.4703 [astro-ph.CO]].
- 1929 [250] See e.g. D. H. Weinberg, J. S. Bullock, F. Governato, R. K. de Naray and A. H. G. Peter,  
1930 arXiv:1306.0913 [astro-ph.CO].
- 1931 [251] C. Boehm and P. Fayet, Nucl. Phys. B **683**, 219 (2004) [hep-ph/0305261].
- 1932 [252] R. Essig, J. Mardon and T. Volansky, Phys. Rev. D **85**, 076007 (2012) [arXiv:1108.5383  
1933 [hep-ph]].
- 1934 [253] R. Essig, A. Manalaysay, J. Mardon, P. Sorensen and T. Volansky, Phys. Rev. Lett. **109**,  
1935 021301 (2012) [arXiv:1206.2644 [astro-ph.CO]].
- 1936 [254] B. Batell and T. Gherghetta, Phys. Rev. D **73** (2006) 045016 [hep-ph/0512356].
- 1937 [255] F. Brummer and J. Jaeckel, Phys. Lett. B **675** (2009) 360 [arXiv:0902.3615 [hep-ph]].
- 1938 [256] F. Brummer, J. Jaeckel and V. V. Khoze, JHEP **0906** (2009) 037 [arXiv:0905.0633 [hep-ph]].
- 1939 [257] H. Goldberg and L. J. Hall, Phys. Lett. B **174** (1986) 151.
- 1940 [258] K. Cheung and T. -C. Yuan, JHEP **0703** (2007) 120 [hep-ph/0701107].
- 1941 [259] D. Feldman, Z. Liu and P. Nath, Phys. Rev. D **75** (2007) 115001 [hep-ph/0702123 [HEP-PH]].
- 1942 [260] A. V. Artamonov *et al.* [BNL-E949 Collaboration], Phys. Rev. D **79**, 092004 (2009)  
1943 [arXiv:0903.0030 [hep-ex]].
- 1944 [261] B. Aubert *et al.* [BABAR Collaboration], arXiv:0808.0017 [hep-ex].
- 1945 [262] R. Essig, J. Mardon, M. Papucci, T. Volansky and Y. -M. Zhong, arXiv:1309.5084 [hep-ph].
- 1946 [263] E. Izaguirre, G. Krnjaic, P. Schuster and N. Toro, arXiv:1307.6554 [hep-ph].
- 1947 [264] P. deNiverville, M. Pospelov and A. Ritz, Phys. Rev. D **84**, 075020 (2011) [arXiv:1107.4580  
1948 [hep-ph]].

- 1949 [265] Y. Kahn and J. Thaler, Phys. Rev. D **86**, 115012 (2012) [arXiv:1209.0777 [hep-ph]].
- 1950 [266] A. Hook, E. Izaguirre and J. G. Wacker, Adv. High Energy Phys. **2011**, 859762 (2011)
- 1951 [arXiv:1006.0973 [hep-ph]].
- 1952 [267] L. B. Auerbach *et al.* [LSND Collaboration], Phys. Rev. D **63**, 112001 (2001) [hep-
- 1953 ex/0101039].
- 1954 [268] A. A. Prinz, R. Baggs, J. Ballam, S. Ecklund, C. Fertig, J. A. Jaros, K. Kase and A. Kulikov
- 1955 *et al.*, Phys. Rev. Lett. **81**, 1175 (1998) [hep-ex/9804008].
- 1956 [269] M. D. Diamond and P. Schuster, arXiv:1307.6861 [hep-ph].
- 1957 [270] B. Batell, R. Essig, and Z. Surujon, to appear.
- 1958 [271] T. Lin, H. -B. Yu & K. M. Zurek, Phys. Rev. D **85**, 063503 (2012) [arXiv:1111.0293 [hep-ph]].
- 1959 [272] S. Davidson, S. Hannestad and G. Raffelt, JHEP **0005**, 003 (2000) [hep-ph/0001179].
- 1960 [273] S. Davidson and M. E. Peskin, Phys. Rev. D **49**, 2114 (1994) [hep-ph/9310288].
- 1961 [274] E. Golowich and R. W. Robinett, Phys. Rev. D **35**, 391 (1987).
- 1962 [275] T. Mitsui, R. Fujimoto, Y. Ishisaki, Y. Ueda, Y. Yamazaki, S. Asai and S. Orito, Phys. Rev.
- 1963 Lett. **70**, 2265 (1993).
- 1964 [276] M. I. Dobroliubov and A. Y. Ignatiev, Phys. Rev. Lett. **65**, 679 (1990).
- 1965 [277] B. Dobrich, H. Gies, N. Neitz and F. Karbstein, Phys. Rev. Lett. **109**, 131802 (2012)
- 1966 [arXiv:1203.2533 [hep-ph]].
- 1967 [278] B. Dobrich, H. Gies, N. Neitz and F. Karbstein, Phys. Rev. D **87**, 025022 (2013)
- 1968 [arXiv:1203.4986 [hep-ph]].
- 1969 [279] P. deNiverville, D. McKeen and A. Ritz, Phys. Rev. D **86**, 035022 (2012) [arXiv:1205.3499
- 1970 [hep-ph]].
- 1971 [280] C. Adams *et al.* [LBNE Collaboration], arXiv:1307.7335 [hep-ex].
- 1972 [281] A. S. Kronfeld, R. S. Tschirhart, U. Al-Binni, W. Altmannshofer, C. Ankenbrandt, K. Babu,
- 1973 S. Banerjee and M. Bass *et al.*, arXiv:1306.5009 [hep-ex].
- 1974 [282] N. Borodatchenkova, D. Choudhury and M. Drees, Phys. Rev. Lett. **96** (2006) 141802 [hep-
- 1975 ph/0510147].
- 1976 [283] J. Khoury and A. Weltman. *Phys. Rev. Lett.*, 93, 2004. 171104.
- 1977 [284] J. Khoury and A. Weltman. *Phys. Rev. D*, 69, 2004. 044026.
- 1978 [285] P Brax, C. van de Bruck , A. C. Davis, J. Khoury, A. Weltman, Aug 2004. 31pp. Published
- 1979 in Phys.Rev.D70:123518,2004. e-Print: astro-ph/0408415
- 1980 [286] P. J. E. Peebles and B. Ratra. *Ap. J. Lett.*, 325:17, 1988.
- 1981 [287] B. Ratra and P. J. E. Peebles. *Phys. Rev. D*, 37(12):3406, 1988.
- 1982 [288] L. Hui and A. Nicolis. *Phys. Rev. Lett.*, 105, 2010. 231101.

1983 [289] K. Hinterbichler, J. Khoury, and H. Nastase. *JHEP*, 1103(61), 2011.

1984 [290] K. Hinterbichler, J. Khoury, H. Nastase and R. Rosenfeld [arXiv:1301:6756 [hep-th]].

1985 [291] H. Nastase and A. Weltman [arXiv:1301:7120[hep-th]].

1986 [292] H. Nastase and A. Weltman [arXiv:1302:1748 [hep-th]].

1987 [293] P. Brax, C. Burrage, A.-C. Davis, D. Seery, and A. Weltman. *Phys. Rev. D*, 81:103524, 2010.

1988 e-Print arXiv:0911.1267.

1989 [294] L. Hui, A. Nicolis and C. Stubbs, *Phys. Rev. D* **80** (2009) 104002 [arXiv:0905.2966 [astro-  
1990 ph.CO]].

1991 [295] D. Kapner et al. *Phys. Rev. Lett.*, 98:021101, 2007. e-Print arXiv:hep-ph/0611184.

1992 [296] P. Brax and G. Pignol. *Phys. Rev. Lett.*, 107:111301, 2011.

1993 [297] J. H. Steffen et al. *Phys. Rev. Lett.*, 105:261803, 2010. ePrint: arXiv:1010.0988.

1994 [298] A. Upadhye, J. H. Steffen, and A. Weltman. *Phys. Rev. D*, 81:015013, 2010.

1995 [299] A. Upadhye, J. H. Steffen, and A. S. Chou. *Phys. Rev. D*, 86:035006, 2012.

1996 [300] P. Brax, C. Burrage, A.-C. Davis, D. Seery, and A. Weltman. *JHEP*, 0909:128, 2009. e-print  
1997 arXiv:0904.3002.

1998 [301] A. Upadhye, W. Hu, and J. Khoury. *Phys. Rev. Lett*, 109:041301, 2012.

1999 [302] A. Upadhye. *Phys. Rev. D*, 86:102003, 2012. e-Print: arXiv:1209.0211.

2000 [303] P. Brax, C. van de Bruck, A. C. Davis, D. F. Mota, and D. J. Shaw. *Phys. Rev. D*, 76:124034,  
2001 2007. e-Print arXiv:0709.2075.

2002 [304] P. Brax, A. Lindner and K. Zioutas, *Phys. Rev. D* **85** (2012) 043014 [arXiv:1110.2583 [hep-  
2003 ph]].

2004 [305] B. Bertotti, L. Iess and P. Tortora, *Nature* **425** (2003) 374.

2005 [306] P. Brax, C. van de Bruck, A. -C. Davis and A. M. Green, *Phys. Lett. B* **633** (2006) 441  
2006 [astro-ph/0509878].

2007 [307] P. .Brax, R. Rosenfeld and D. A. Steer, *JCAP* **1008** (2010) 033 [arXiv:1005.2051 [astro-  
2008 ph.CO]].

2009 [308] R. Pourhasan, N. Afshordi, R. B. Mann and A. C. Davis, *JCAP* **1112** (2011) 005  
2010 [arXiv:1109.0538 [astro-ph.CO]].

2011 [309] C. Burrage, *Phys. Rev. D* **77** (2008) 043009 [arXiv:0711.2966 [astro-ph]].

2012 [310] B. A. Bassett and M. Kunz, *Phys. Rev. D* **69** (2004) 101305 [astro-ph/0312443].

2013 [304]

2014 [311] P. Chang and L. Hui, *Astrophys. J.* **732** (2011) 25 [arXiv:1011.4107 [astro-ph.CO]].

2015 [312] C. Burrage, A. -C. Davis and D. J. Shaw, *Phys. Rev. D* **79** (2009) 044028 [arXiv:0809.1763  
2016 [astro-ph]].

- 2017 [313] B. Jain, V. Vikram and J. Sakstein, arXiv:1204.6044 [astro-ph.CO].
- 2018 [314] F. Schmidt, A. Vikhlinin and W. Hu, Phys. Rev. D **80** (2009) 083505 [arXiv:0908.2457  
2019 [astro-ph.CO]].
- 2020 [315] L. Lombriser, K. Koyama, G. -B. Zhao and B. Li, Phys. Rev. D **85** (2012) 124054  
2021 [arXiv:1203.5125 [astro-ph.CO]].
- 2022 [316] <http://microscope.onera.fr/>
- 2023 [317] <http://sci.esa.int/science-e/www/area/index/cfm?fareaid=127>
- 2024 [318] **THE REMAINING CITATIONS ARE NEVER REFERED TO.**
- 2025 [319] A. Loeb and M. Zaldarriaga, Phys. Rev. D **71**, 103520 (2005).
- 2026 [320] J. Dunkley *et al.*, Astrophys. J. **739**, 52 (2011) [arXiv:1009.0866 [astro-ph.CO]].
- 2027 [321] V. Spevak, N. Auerbach, V. V. Flambaum, Phys. Rev. **C56**, 1357-1369 (1997). [nucl-  
2028 th/9612044].
- 2029 [322] J. Albert, S. Bettarini, M. Biagini, G. Bonneaud, Y. Cai, G. Calderini, M. Ciuchini and  
2030 G. P. Dubois-Felsmann *et al.*, physics/0512235.
- 2031 [323] C. W. Leemann, D. R. Douglas and G. A. Krafft, Laboratory,” Ann. Rev. Nucl. Part. Sci.  
2032 **51**, 413 (2001).
- 2033 [324] P. Brax, A. Lindner, and K. Zioutas. 2011. ePrint arXiv:1110.2583.
- 2034 [325] C. Athanassopoulos *et al.* [LSND Collaboration], Nucl. Instrum. Meth. A **388**, 149 (1997)  
2035 [nucl-ex/9605002].
- 2036 [326] F. Bergsma *et al.* [CHARM Collaboration], Phys. Lett. B **157**, 458 (1985).
- 2037 [327] R. Cameron, G. Cantatore, A. C. Melissinos, G. Ruoso, Y. Semertzidis, H. J. Halama,  
2038 D. M. Lazarus and A. G. Prodell *et al.*, Phys. Rev. D **47**, 3707 (1993).
- 2039 [328] M. Ablikim *et al.* [BES Collaboration], Phys. Rev. Lett. **100**, 192001 (2008) [arXiv:0710.0039  
2040 [hep-ex]].
- 2041 [329] M. Kaplinghat, A. Peter and K. Sigurdson, to appear.
- 2042 [330] M. Davier, A. Hoecker, B. Malaescu and Z. Zhang, Eur. Phys. J. C **71**, 1515 (2011)  
2043 [arXiv:1010.4180 [hep-ph]].
- 2044 [331] B. Osmanov [on behalf of MINERvA Collaboration], arXiv:1109.2855 [physics.ins-det].
- 2045 [332] D. G. E. Walker, D. Finkbeiner, L. Moustakas and K. Sigurdson, to appear.
- 2046 [333] R. Balest *et al.* *Phys. Rev. D*, 51:2053, 1995.
- 2047 [334] E. Komatsu *et al.* [WMAP Collaboration], Astrophys. J. Suppl. **192**, 18 (2011)  
2048 [arXiv:1001.4538 [astro-ph.CO]].
- 2049 [335] S. V. Benson, D. Douglas, G. R. Neil and M. D. Shinn, J. Phys. Conf. Ser. **299**, 012014  
2050 (2011).

- 2051 [336] V. V. Nesvizhevsky et al. *Nature*, 415:297, 2002.
- 2052 [337] M. Kleban and R. Rabadan. 2005. ePrint arXiv:hep-ph/0510183.
- 2053 [338] I. Ambats *et al.* [MINOS Collaboration], NUMI-L-337.
- 2054 [339] A. S. Chou et.al. *Phys. Rev. Lett.*, 102, 2009. 030402.
- 2055 [340] G. Venanzoni, Nucl. Phys. Proc. Suppl. **162**, 339 (2006).
- 2056 [341] E. Zavattini *et al.* [PVLAS Collaboration], Phys. Rev. Lett. **96**, 110406 (2006) [arXiv:hep-  
2057 ex/0507107]; Phys. Rev. D **77**, 032006 (2008) [arXiv:0706.3419 [hep-ex]].
- 2058 [342] A. S. Chou et.al. [GammeV (T-969) Collaboration]. *Phys. Rev. Lett.*, 100, 2008. 080402  
2059 [arXiv:0710.3783 [hep-ex]].
- 2060 [343] A. A. Anselm, Yad. Fiz. **42**, 1480 (1985).
- 2061 [344] M. Kreuz et al. 2009. ePrint arXiv:0902.0156.
- 2062 [345] P. Brax and K. Zioutas. *Phys. Rev. D*, 82:043007, 2010.
- 2063 [346] A. Afanasev et al. *AIP Conf. Proc.*, 1274:163, 2010.
- 2064 [347] K. Abe *et al.* [T2K Collaboration], Nucl. Instrum. Meth. A **659**, 106 (2011) [arXiv:1106.1238].
- 2065 [348] C. Burrage, A.-C. Davis, and D. J. Shaw. *Phys. Rev. D*, 79:044028, 2009.
- 2066 [349] L. Lombriser, A. Slosar, U. Seljak and W. Hu, Phys. Rev. D **85** (2012) 124038  
2067 [arXiv:1003.3009 [astro-ph.CO]].
- 2068 [350] A. E. Nelson and J. Walsh, Phys. Rev. D **77**, 033001 (2008) [arXiv:0711.1363 [hep-ph]].
- 2069 [351] N. Auerbach, V. V. Flambaum, V. Spevak, Phys. Rev. Lett. **76**, 4316-4319 (1996). [nucl-  
2070 th/9601046].
- 2071 [352] K. Hinterbichler, J. Khoury, and H. Nastase. *JHEP*, 1103(61), 2011.
- 2072 [353] E. Bertschinger, Phys. Rev. D **74**, 063509 (2006).
- 2073 [354] T. Kageyama, AIP Conf. Proc. **842**, 1064 (2006).
- 2074 [355] P. Brax and C. Burrage. *Phys. Rev. D*, 83:035020, 2011.
- 2075 [356] C. Burrage, A.-C. Davis, and D. J. Shaw. *Phys. Rev. Lett.*, 102:201101, 2009.
- 2076 [357] M. Fouche *et al.* [BMV Collaboration], Phys. Rev. D **78**, 032013 (2008) [arXiv:0808.2800  
2077 [hep-ex]].
- 2078 A. S. Chou *et al.* [GammeV Collaboration], Phys. Rev. Lett. **100**, 080402 (2008)  
2079 [arXiv:0710.3783 [hep-ex]].
- 2080 A. Afanasev *et al.* [LIPSS Collaboration], Phys. Rev. Lett. **101**, 120401 (2008)  
2081 [arXiv:0806.2631 [hep-ex]].
- 2082 P. Pugnati *et al.* [OSQAR Collaboration], Phys. Rev. D **78**, 092003 (2008) [arXiv:0712.3362  
2083 [hep-ex]].
- 2084 K. Ehret *et al.* [ALPS Collaboration], Phys. Lett. B **689**, 149 (2010).



- 2085 [358] N. D. Scielzo, I. Ahmad, K. Bailey *et al.*, AIP Conf. Proc. **842**, 787-789 (2006).
- 2086 [359] L. D. Carr, D. DeMille *et al.*, [arXiv:0904.3175 [quant-ph]].
- 2087 [360] A. A. Aguilar-Arevalo *et al.* [MiniBooNE Collaboration], Phys. Rev. D **79**, 072002 (2009)
- 2088 [arXiv:0806.1449 [hep-ex]].
- 2089 [361] K. Van Bibber, N. R. Dagdeviren, S. E. Koonin, A. Kerman and H. N. Nelson, Phys. Rev.
- 2090 Lett. **59**, 759 (1987).
- 2091 [362] R. Keisler, C. L. Reichardt, K. A. Aird, B. A. Benson, L. E. Bleem, J. E. Carlstrom,
- 2092 C. L. Chang and H. M. Cho *et al.*, Astrophys. J. **743**, 28 (2011) [arXiv:1105.3182 [astro-
- 2093 ph.CO]].
- 2094 [363] L. AMoustakas, A. J. Bolton, J. T. Booth, J. SBullock, E. Cheng, D. Coe, C. D. Fassnacht
- 2095 and V. Gorjian *et al.*, arXiv:0806.1884 [astro-ph].
- 2096 [364] R. Poltis and A. Weltman
- 2097 [365] S. D. Holmes [Project X Collaboration], Conf. Proc. C **100523**, TUYRA01 (2010).
- 2098 [366] E. G. Adelberger *et al.* *Phys. Rev. Lett.*, 98:131104, 2007. e-Print arXiv:hep-ph/0611223.
- 2099 [367] M. Ahlers, H. Gies, J. Jaeckel, J. Redondo and A. Ringwald, Phys. Rev. D **77**, 095001 (2008)
- 2100 [arXiv:0711.4991 [hep-ph]].
- 2101 [368] J. Hamann, S. Hannestad, G. G. Raffelt and Y. Y. Y. Wong, JCAP **0906** (2009) 022
- 2102 [arXiv:0904.0647 [hep-ph]].
- 2103 [369] M. Dehn, K. Aulenbacher, R. Heine, H. J. Kreidel, U. Ludwig-Mertin and A. Jankowiak,
- 2104 recirculators,” Eur. Phys. J. ST **198**, 19 (2011).